IOWA STATE UNIVERSITY
Digital Repository

Retrospective Theses and Dissertations

Iowa State University Capstones, Theses and Dissertations

1990

Laser excited fluorescence spectroscopic studies of cellular macromolecular damage from chemical carcinogens

Peiqi Lu
Iowa State University

Follow this and additional works at: https://lib.dr.iastate.edu/rtd

 Part of the Physical Chemistry Commons

Recommended Citation
Lu, Peiqi, "Laser excited fluorescence spectroscopic studies of cellular macromolecular damage from chemical carcinogens " (1990). *Retrospective Theses and Dissertations*. 9399.
https://lib.dr.iastate.edu/rtd/9399

This Dissertation is brought to you for free and open access by the Iowa State University Capstones, Theses and Dissertations at Iowa State University Digital Repository. It has been accepted for inclusion in Retrospective Theses and Dissertations by an authorized administrator of Iowa State University Digital Repository. For more information, please contact digirep@iastate.edu.

www.manaraa.com

3

91

00487

U·M·I

MICROFILMED 1990

INFORMATION TO USERS

The most advanced technology has been used to photograph and reproduce this manuscript from the microfilm master. UMI films the text directly from the original or copy submitted. Thus, some thesis and dissertation copies are in typewriter face, while others may be from any type of computer printer.

The quality of this reproduction is dependent upon the quality of the copy submitted. Broken or indistinct print, colored or poor quality illustrations and photographs, print bleedthrough, substandard margins, and improper alignment can adversely affect reproduction.

In the unlikely event that the author did not send UMI a complete manuscript and there are missing pages, these will be noted. Also, if unauthorized copyright material had to be removed, a note will indicate the deletion.

Oversize materials (e.g., maps, drawings, charts) are reproduced by sectioning the original, beginning at the upper left-hand corner and continuing from left to right in equal sections with small overlaps. Each original is also photographed in one exposure and is included in reduced form at the back of the book.

Photographs included in the original manuscript have been reproduced xerographically in this copy. Higher quality 6" x 9" black and white photographic prints are available for any photographs or illustrations appearing in this copy for an additional charge. Contact UMI directly to order.

U·M·I

University Microfilms International
A Bell & Howell Information Company
300 North Zeeb Road, Ann Arbor, MI 48106-1346 USA
313/761-4700 800/521-0600

Order Number 9100487

Laser-excited fluorescence spectroscopic studies of cellular macromolecular damage from chemical carcinogens

Lu, Peiqi, Ph.D.

Iowa State University, 1990

U·M·I
300 N. Zeeb Rd.
Ann Arbor, MI 48106

Laser excited fluorescence spectroscopic studies of cellular macromolecular damage from chemical carcinogens

by

Peiqi Lu

A Dissertation Submitted to the

Graduate Faculty in Partial Fulfillment of the

Requirements for the Degree of

DOCTOR OF PHILOSOPHY

Department: Chemistry

Major: Physical Chemistry

Approved:

Signature was redacted for privacy.

In Charge of Major Work

Signature was redacted for privacy.

For the Major Department

Signature was redacted for privacy.

For the Graduate College

Iowa State University
Ames, Iowa

1990

TABLE OF CONTENTS

TO MY FATHER AND MOTHER
WHO HAVE DEDICATED THEIR LIVES
TO ME !

献给辛勤哺育我多年的父亲和母亲!

——— Peiqi Lu

I. INTRODUCTION

Worldwide cancer epidemiology indicates that some 80% of all human tumors probably have their origin in dietary and environmental factors of a chemical nature (1-3). The widespread environmental pollutants, polycyclic aromatic hydrocarbons (PAHs), constitute one of the largest and most potent classes of chemical carcinogens. PAHs are found in various petroleum and combustion products derived from heat and power generation, motor vehicle exhausts (4), and pyrolysis of organic matters such as tobacco smoking and certain procedures of food preparation. In the United States, estimates of the total annual emission of benzo[a]pyrene (BaP) (Figure 1), one of the most widely studied potent carcinogenic PAHs, range from 900 tons (4) to about 1300 tons (5). In addition to their widespread environmental prevalence, the important role that PAHs potentially play in human cancer is also implicated by their relatively high tumorigenic potency and their capability of selectively inducing diverse tumors in animal tissues, including mammary carcinoma, leukemia, sarcoma, etc. (6). Studies on several typical PAH compounds, and in particular BaP, have contributed largely to our present knowledge of the molecular mechanisms underlying PAH-induced carcinogenesis (1, 7).

A. Mechanistic Studies of Chemical Carcinogenesis

Chemical carcinogenesis is generally considered a multi-step process emanating from a single somatic cell. One of the key events in the initiation of chemical carcinogenesis involves a genetic damage — the formation of DNA-

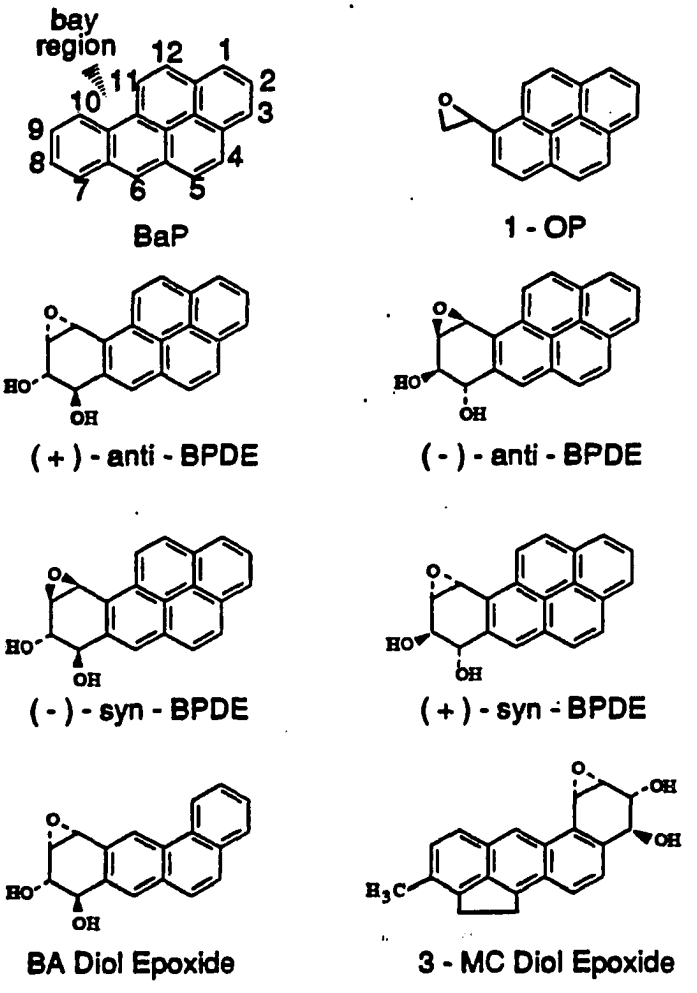

Figure 1. Structures of benzo[a]pyrene, 1-oxiranylpyrene (1-OP), (+)- and (-)-anti-BaP diol epoxides (BPDE), (+)-, and (-)-syn-BPDE, benz[a]anthracene anti-diol epoxide, and 3-methylchol-benz[a]anthracene (3-MC) anti-diol epoxide

carcinogen adducts. The damage is permanently fixed as a mutation following cell replication. In the case where the formation of the adducts at one or more particular sites in DNA triggers proto-oncogene's[1] expression (oncogenes), the damaged cell will be transformed into a tumor cell (8). Under the proper set of circumstances, the transformed cell may escape the normal cellular controls, proliferate, and eventually lead to cancer. This mechanism is supported by a variety of experiments which found that the initiation event of carcinogenesis induced by PAHs involved specific modification of proto-oncogenes to active oncogenes (9). For example, the experiments found that anti-BPDE (Figure 1), the ultimate carcinogenic metabolite of BaP, could induce a series of point mutations, predominantly GC → TA and AT → TA base substitutions, in codons 61 and 12 (corresponding to glycine (Gly(CGC)) of the *Ha-ras* proto-oncogene (10). Modification *in vitro* of a plasmid containing the *c-Ha-ras* proto-oncogene with anti-BPDE and subsequent transfection of the plasmid into NIH 3T3 cells generates a transforming oncogene (11). In a recent study, exposure of diploid human fibroblasts in culture to racemic anti-BPDE induces a mutation in codon 12 of the *Ha-ras* proto-oncogene yielding a GC → TA transition (12). The *Ha-ras* oncogene and an as yet unidentified oncogene were shown to transform the fibroblasts.

Polycyclic aromatic hydrocarbons are chemically stable, water insoluble compounds and, as such, are inactive as tumor initiators. Therefore, conversion of PAHs to reactive metabolites is a necessary condition in the initiation of cancer

---

[1] Proto-oncogenes are normal and highly conserved genes controlling essential cellular functions like proliferation and differentiation.

(13-15). The metabolism of PAHs in a single somatic cell occurs primarily through monooxygenation pathways and is catalyzed by the mixed-function oxygenase enzymes, like cytochrome P450s (16). The major metabolites are relatively unstable arene oxide intermediates which rearrange spontaneously to phenols. The more stable arene oxide metabolites survive sufficiently long to undergo hydration catalyzed by epoxide hydrase to yield *trans*-dihydrodiols or to add glutathione catalyzed by glutathione-S-transferase. Further oxidative metabolism of the phenols and dihydrodiols yields quinones, diol epoxides, and other products (17). Extensive studies on the tumorigenic activity in animals have led to the conclusion that the bay region diol epoxides are the most reactive and biologically active of all of the given PAH metabolites (14, 15, 18-20).

The prototype of a "bay region" in a PAH is the sterically-hindered region between C-4 and C-5 of phenanthrene, and additional aromatic rings may be fused to the aromatic nucleus. The bay region epoxides on tetrahydrobenzo rings of PAH are characterized by this structural feature. Perturbational molecular orbital calculations were applied to the opening of the epoxide to form a resonance-stabilized carbocation in the bay region (21). In the case of BaP, this corresponds to carbocation formation at position 10 (Figure 1). The relative ease of this ring opening is characterized by a parameter, $\Delta E/\beta$, describing the energy stabilization of the carbocation relative to its precursor. It was found that the bay region epoxides of a given parent PAH had greater stabilization of the carbocation than an epoxide at a non-bay region position. Furthermore, a correlation was established between high $\Delta E/\beta$ values at bay region positions and strong carcinogenic potency of various PAH (21, 22). The bay region theory is supported by a lot of

experimental evidence that whatever situations favor the formation of more bay region diol epoxides, the carcinogenicity of the PAHs will be greatly enhanced. A good example is based on co-existing carcinogen effects. When rat liver nuclei were incubated with BaP in the presence of a NADPH-generating system, the major metabolites were 9,10-, 4,5-, and 7,8-dihydrodiols, the 3,6- and 1,6-quinones, as well as 3- and 9-phenols. By prior administration of 3-methycholanthracene (3-MC) to the rat, the total nuclear mutagenicity could be stimulated 11-fold. The major metabolites yielded were characterized as bay region diol epoxides of benzo[a]pyrene (BPDE) (23). As a matter of fact, the binding of BPDE to cellular DNA is believed to be a critical event in the initiation of tumorigenesis and mutagenesis (23-26), which has lead to great effects to elucidate the mechanism of interaction of BPDE with DNA.

Stopped flow kinetic measurements indicate that the reaction of BPDE with DNA are consistent with a mechanism involving initial rapid intercalation (complete in < 5 ms) of the diol epoxide between the base pairs of DNA (27). The experimentally-observed pseudo first-order rate constant increases in the presence of DNA (28, 29). This enhanced reactivity is also a result of the formation of physical BPDE-DNA complexes. The intercalated complex was observed to undergo rate-determining protonation (~500 sec) to yield an intercalated triol carbonium ion intermediate in light that the process is catalyzed by specific and general acid (30, 31). Ninety percent of the intermediate is then hydrolyzed to yield tetraols which are also physically associated with DNA. The minor part forms covalently bounded adducts. The whole process can be illustrated by the following reaction scheme (32):

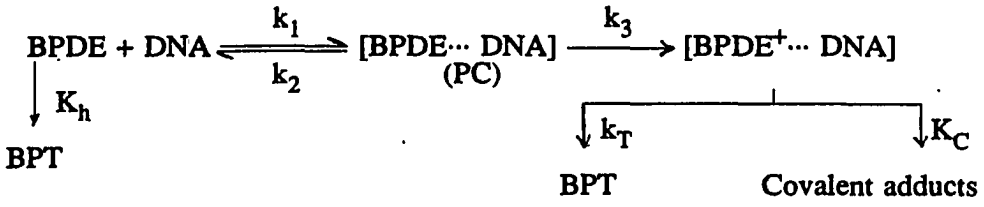

Here, two important parameters are directly related to carcinogenicity and mutagenicity of a given PAH. The first is the equilibrium association constant, $K=k_1/k_2$, which is used to measure the extent of the intercalative diol epoxides with DNA. Another parameter is f_{cov}, which represents the percentage of PAH molecules that bind covalently to DNA. A close relationship between the carcinogenicity of PAHs and their facility of reaction with DNA can be revealed by several model systems (33). A typical example is 3-MC anti-diol epoxide (Figure 1). Studies of the reaction of 3-MC-anti-diol epoxide with DNA show that both the mechanism of reaction and the structures of the adducts formed closely resemble those of anti-BPDE (34), but the reactivity of these two diol epoxides is quite different. K and the overall rate constant for the reaction (k_3) are both about one-fourth those of anti-BPDE, whereas the extent of covalent binding (f_{cov}) is almost triple that of BPDE. Since 3-MC is a more potent carcinogen than BP, these observations suggest that f_{cov} relates more to carcinogenicity than either K or k_3. However, some abnormal phenomena are also observed. The carcinogenicity of some PAHs exhibits a significant difference although they have a similar extent of covalent binding, for example, the synthetic BPDE analogue 1-OP (Figure 1) has similar values of K and f_{cov}, while it is a weak carcinogen (35). Another example is the BA diol epoxide (Figure 1). The BA diol epoxide reacts with DNA by a similar mechanistic pathway to anti-BPDE. The values of K and k_3 are also very

similar, but its f_{cov} value is much higher. Unexpectedly, BA is a weak carcinogen. These observations implicate that in addition to the extent of covalent binding of the diol epoxide, other factors are also able to make a significant contribution to the mutagenicity and carcinogenicity of a given PAH. A variety of experiments and reasons have led to speculation that the spatial orientation of the aromatic moiety at the covalent binding sites (36), and the structure and the conformation of the PAH-DNA adducts are crucial for the carcinogenic effects (17, 32, 33, 37). Spectroscopic studies of structures and conformation of BPDE-DNA adducts provide a key to understanding these mysterious factors.

Extensive spectroscopic studies have shown that the structures of the covalent adducts formed by anti-BPDE with DNA are of two types, designated "site I" and "site II." Site I adducts are characterized by a 10 nm red shift in the ultraviolet absorption spectrum and a negative linear dichroism spectrum (LD). Therefore, site I appears to involve intercalation or partial intercalation of the pyrenyl chromophore between base pairs of the DNA. The site II adducts exhibit a positive LD and a small 2-3 nm red shift in the UV region, and therefore, have an externally bound conformation with the aromatic moiety residing in the minor groove with its long axis inclined at an angle of ~35^{0} to the DNA helix (17). (-)-anti-BPDE-DNA adducts are heterogeneous and consist of about 2/3 site I and 1/3 site II adducts (38); in contrast, the majority of (+)-ani-BPDE-DNA adducts (90%) are of the site II type. Since (+)-anti-BPDE-DNA adducts are potent carcinogens, type II adducts are assumed to be mainly responsible for their potent carcinogenicity. This mechanism can explain why 1-OP and BA diol epoxide are weak carcinogens since both of them were found to form predominantly type I adducts.

The studies of the interaction of BPDE with DNA have contributed largely to our present knowledge of the molecular mechanisms underlying PAH-induced carcinogenesis. However, several problems still remain unclear. 1) The LD experiment is not able to distinguish the physically intercalated BP tetraols and covalently intercalated adducts. In addition, UV absorption cannot determine if a small amount of free BPT exists, since its absorption peak is almost overlapped with that of site II adducts. 2) The absorption and LD spectrometries do not have sufficient sensitivity to study *in vivo* systems when the adduct level is very low. 3) Earlier studies with the mutagenic and carcinogenic alkyl-nitrosoureas have shown that minor products of DNA reactions are largely responsible for the biological effects of these molecules, and similar situations may apply to the PAHs (24). This argument is further supported by the results of the carcinogenic studies of 7,12-dimethylbenz[a]anthracene (DMBA) (39, 40). In addition, recent experiments found that the binding of anti-BPDE to dA might be an important factor to initiate a tumor in mouse skin (41). Previous studies using digested adducts have found that (+)-anti-BPDE is almost exclusively bound to the N^2-dG position (94%) (36), while the covalent (-)-anti-BPDE-DNA adducts formed *in vitro* consists of 58% N^2-dG-BPDE, 21% O^6-dG-BPDE, and 18% N^6-dA-BPDE (24, 36). These different adducts are expected to manifest themselves by their different spectra. But the UV absorption and LD spectra of (-)-anti-BPDE-DNA cannot discern these adducts and only show a broad band with a maximum around 343 nm for all type II adducts. Fluorescence decay experiments did not exhibit much difference either, and even worse, they could not reveal if the adducts detected correspond to site I or II (38). Therefore, in carcinogenic studies it is important to develop highly selective and

sensitive bioassay methods to determine how many types of site I and site II adducts exist, and to assign the chemical origin of the adducts detected. Solutions to these problems will shed light on the understanding PAH interactions with DNA.

B. Studies of Carcinogenesis in Environmental Monitoring Using Fish Exposed to Chemical Carcinogens

The concern over contamination of the estuarine and coastal environments in the world has led to great efforts to evaluate the relationships between contaminant exposure and observed biological effects in aquatic organisms. For example, two tributaries of the Great Lakes, Buffalo River and Detroit River, are extensively used for drinking water. Field assays found that both of them were heavily contaminated by PAHs. In several PAH-contaminated areas of the Buffalo River, levels of 15 individual priority pollutant PAHs ranged from 0.5 to 17 mg/kg in sediments, with BaP being 3.1 mg/kg (42). In the Detroit River, levels of individual PAHs ranged from 0.1 to 38.8 mg/kg, with BaP levels ranging from 0.1 to 17.6 mg/kg in different samples (43). The concern was further underscored when spontaneous tumors were found in a variety of fish species from both freshwater and marine environments. For example, English sole and rock sole exhibit a high frequency of liver cancer when sampled from chemically-polluted estuaries in Puget Sound, WA (44, 45). Winter flounder in Boston Harbor, MA and brown bullhead in Niagara River, NY also show a high incidence of liver neoplasia (42). The freshwater drum captured from areas in eastern Lake Erie and the Niagara River had developed dermal neoplasms on their flanks (42). Moreover, in laboratory studies brown bullhead painted with river sediment extract were found to undergo a series of

localized skin changes and eventually to develop multiple skin papillomas, which indicate that PAHs are responsible for cancer found in the fish (42). As early as 1964, Dawe et al. hypothesized that bottom-dwelling fish species exhibit increased frequencies of neoplasms and thus, may serve as early warning indicators of carcinogenic hazards to man (46). This argument is further supported by the study which found that the repair mechanism of some fish is relatively inefficient (47, 48), and thus, an evaluation of the fish DNA-adducts may reflect the genuine initiation processes of chemical carcinogenesis. However, some bottom fish species do not show a high prevalence of cancer. Starry flounder, from Puget Sound, WA, exhibits only a low frequency of liver cancer (49). The dissection of thousands of carp from several contaminated areas did not find any obvious propensity for neoplasm development (50). In addition, laboratory studies with salmonid fish have demonstrated that the Mount Shasta strain of rainbow trout is susceptible to both BaP and aflatoxin B_1 induced cancers, whereas coho salmon is relatively resistant to these carcinogens (51, 52). As many xenobiotics exert their carcinogenic effects only after metabolic activation, detailed studies on the activation and detoxication of carcinogens in various fish may provide valuable insights into whether there is a biochemical basis for the differences among fish species in their susceptibility to chemical carcinogens.

Our research focused on the study of the metabolic activation of PAH in the liver tissues of English sole because this species exhibits a high prevalence of liver neoplasms in several PAH-contaminated areas (44, 45, 53). The significance of this study is further emphasized by the finding that long-term exposure of English sole to BaP results in a spectrum of toxicopathic lesions similar to those observed in

fish captured from contaminated areas (54). Enzymatic hydrolysis and analysis by reversed-phase HPLC of hepatic DNA isolated from English sole exposed to radiolabeled BaP, however, did not show the presence of detectable levels of BPDE-DNA adducts (55). A recent study (56) using English sole hepatocytes exposed to ^{3}H-BP showed no detectable BPDE-dG adducts. The adduct level in this *in vivo* fish sample is apparently very low, and highly sensitive bioanalytical techniques are imperative in this study. The second fish sample we investigated is carp captured from a heavily PAH-contaminated area of the Buffalo River. Since carp are not found to develop neoplasia when exposed to heavily PAH-contaminated areas, the study of this project attempts to determine what kind of adducts can be formed in fish, and the detailed features of the adducts (e.g., conformation and stereochemical structures, etc.). Apparently, it is significant to characterize the adducts, to reveal the chemical origins of exposure. But the determination of the conformations and stereochemistry of the DNA adducts is also of particular importance, since in the case where the DNA adducts are detected in the carp and English sole, the specific features of the adducts could explain why these two fishes exhibit quite different carcinogenicity.

C. Studies of Chemical Carcinogenesis in Human System

Since PAHs are widely distributed throughout the atmosphere and water sources in the world, it is almost impossible to avoid exposure to nanogram quantities of these substances on a daily basis (1-3). Chemical carcinogens and co-carcinogens are considered to be responsible for many human cancers (57). Therefore, it is very significant to study the biological effect of man's exposure to

the numerous chemical compounds, the mechanism by which these compounds exert their deleterious effects in exposed subjects, and the overall consequences of such exposure. The placental tissue is a potentially important source of material for molecular epidemiological studies in light of several experimental observations (58). For example, cigarette smoking and exposure to cooking oil contaminated with polychlorinated biphenyl and their thermal degradation products are known to strongly induce cytochrome P-450-related monooxygenase activity in human placenta. This suggests that this tissue is able to activate metabolically a variety of chemical carcinogens and is highly responsive to effects of environmental exposures (59-61). Studies in experimental animals showed that transplacental exposure to several classes of known carcinogens can cause cancer in adult animals (62, 63). Consideration of the extraordinary difficulties implicit in using traditional epidemiologic approaches to study prenatal determinants of disease in adult life suggests a need for developing new approaches to the identification of potential human transplacental carcinogens (58). Moreover, a large quantity of tissue available facilitated replicate analyses of each specimen by several assays for DNA adducts and could potentially be used for additional assays studying the relationships between levels of adducts and such factors as metabolic activity or differences in DNA repair.

Previous experiments using ^{32}P-postlabeling assay detected the presence of a DNA adduct in the human placenta which was strongly associated with maternal smoking during pregnancy (64). This adduct was also found to be related with maternal smoking for a larger study population (58). Recently, both ^{32}P-postlabeling assay and ELISA (using antibodies to chemically-modified DNA in

enzyme-linked immunosorbent assay) have been successfully used to detect carcinogen adducts in women's placental DNA samples (65). A total of seven different adducts were detected in 53 subjects, and three of these adducts were found almost exclusively in smokers. Among smokers, there were positive dose-response relationships between levels of the smoking-related adducts and biochemical estimates of doses of maternal exposure to cigarette smoke during pregnancy. In addition, levels of smoking-related adducts were inversely associated with the birth weight of offspring. Everson and co-workers (65) observed by ELISA that the antibodies modified by anti-BPDE have a positive response to the placenta adducts regardless of whether the person smoked. Since other adducts formed from anti-benz[a]anthracene diol epoxide and anti-chrysene diol epoxide also reacted with the antibodies (64, 66, 67), they could not verify that the placenta DNA contained anti-BPDE-DNA adducts. To date, neither the chemical origin of the adducts nor their precise structures have been determined, and the exposure or susceptibility factors that are most closely associated with biochemical or molecular damage to human tissues are still a mystery (65). Besides, characterization of the DNA adducts formed from the specific stereoisomer of a chemical carcinogen in human tissues is also of particular significance, since different stereoisomers of a chemical carcinogen can have quite different mutagenicities and tumorigenicities (17, 33). Hence, further studies of carcinogenesis in humans require highly selective and sensitive assay techniques which not only detect very low adduct levels (pmol to fmol), but also characterize the chemical origins and specific stereochemistry of the adducts as well.

II. FLUORESCENCE LINE NARROWING SPECTROSCOPY (FLNS)

A. Principles of FLNS

Prior to the following discussion, we point out that some experimental conditions are met. First, the concentration of the molecules of interest is low enough (usually < 10^{-3} M) to neglect all interaction between them; second, the temperature is also sufficiently low (< 30 K) to minimize the effects of the thermal broadening; and third, the electronic excitations of the solvent lie at higher energies than the lowest excited singlet state (S_1) of the analyte molecules so that the selective excitation of the molecule is possible. Since the theory of FLNS has previously been discussed in great detail (68, 69), only a brief discussion will be given here.

In an amorphous host matrix such as a glass, the inherent structural disorder leads to energetic inequivalence of different analyte sites. As a result of the differing local electrostatic fields, a distribution of narrow homogeneous absorption bands due to the individual sites are formed. The broad absorption profile created is known as a site inhomogeneously-broadened absorption profile, and it is in the case of inhomogeneous broadening that the FLN phenomenon is possible. Figure 2A shows a site inhomogeneously-broadened absorption profile which is actually an ensemble of a very large number of individual site absorptions possessing a homogeneous linewidth Γ_{hom}. At liquid helium temperature (T = 4.2 K), $\Gamma_{hom} \leq$ 0.1 cm^{-1} for the 0-0 transition, while for the broadened absorption profile, the bandwidth $\Gamma_{Inh} \geq 100$ cm^{-1}. FLNS is a member of the class of spectral line narrowing spectroscopies and, as such, has the ability to eliminate or greatly

diminish the contribution of inhomogeneous-broadening to the fluorescence vibronic bandwidth. By exciting into the inhomogeneously broadened absorption band with a narrow line excitation source, only those sites with absorption profiles that overlap the excitation line will be excited. Provided that intersite conversion processes (e.g., due to intermolecular energy transfer) do not occur in the time scale of the fluorescence, only the initially excited sites (isochromats) will fluorescence. The resultant spectrum consists of a series of greatly narrowed bands (called zero-phonon lines, or abbreviated as ZPL) corresponding to the fluorescence emitted from the initially excited isochromat. The width of a vibronic ZPL is ~ 2 cm^{-1}. The effect of the inhomogeneous broadening is thereby reduced, and the narrow-line fluorescence serves as the basis for a qualitative and quantitative methodology for fluorescing molecules (68, 69).

An interesting complication to the above picture is provided by the coupling between the vibronic states of the analyte molecule and the phonons of the host medium (electron-phonon coupling). This coupling manifests itself by the appearance of a phonon sideband (PSB) which builds on the ZPL. For the fluorescence spectrum, the PSB is located on the lower energy side of the ZPL (Figure 2B). In glasses, the PSB due to one-phonon creation is typically broad (~ 30 cm^{-1}). The ratio of the integrated intensities of ZPL (I_{ZPL}) and PSB (I_{PSB}) is given by the Debye-Waller factor α (68),

$$\alpha = I_{ZPL}/(I_{ZPL} + I_{PSB}) \qquad (1)$$

Taking into account the absorption process which leads to fluorescence, it can be shown that the observed Debye-Waller factor in fluorescence, α', is

approximately equal to the product of the α_{abs} and α_{fl} (68), for example,

$$\alpha' = \alpha_{abs}\alpha_{fl}$$
$$\approx \alpha^2 \qquad (2)$$

Since to a first approximation, $\alpha_{abs} = \alpha_{fl} \equiv \alpha$.

Under the linear approximation for electron-phonon coupling, the Debye-Waller factor can be expressed by a simplified equation which takes into account the temperature dependence (68):

$$\alpha(T) = \exp\left[- \int_0^\infty f_0(\nu)[2(e^{\nu/kT}-1)^{-1}+1]d\nu \right] \qquad (3)$$

Here, $f_0(\nu)$ is the weighted density of phonon states given by equation (4):

$$f_0(\nu) = 6N\xi^2(\nu)\rho(\nu) \qquad (4)$$

Where, $\rho(\nu)$ is the phonon density of states of the host, N is the number of impurity molecules, and $\xi(\nu)$ is the linear electron-phonon coupling constant.

The approximate relations (1-4) indicate that the general appearance of the fluorescence spectra upon selective excitation significantly depends upon the quantity α, and the host medium plays an important part in the solid state spectroscopy of a molecule. If the coupling between the vibronic states of the molecule and the phonon state of the host medium is very strong, the value of α will be greatly reduced. Under this circumstance, the fluorescence of non-resonantly-excited centers which absorb via their PSB will dominate and the ZPL intensities will be diminished. That is, the PSB will dominate the fluorescence spectrum. For example, for a Debye-Waller factor $\alpha = 0.05$, and $\alpha' = 0.0025$, it would be difficult to detect the ZPL in the spectrum (68). In addition, temperature has a pronounced effect on the relative intensities of the ZPL and PSB.

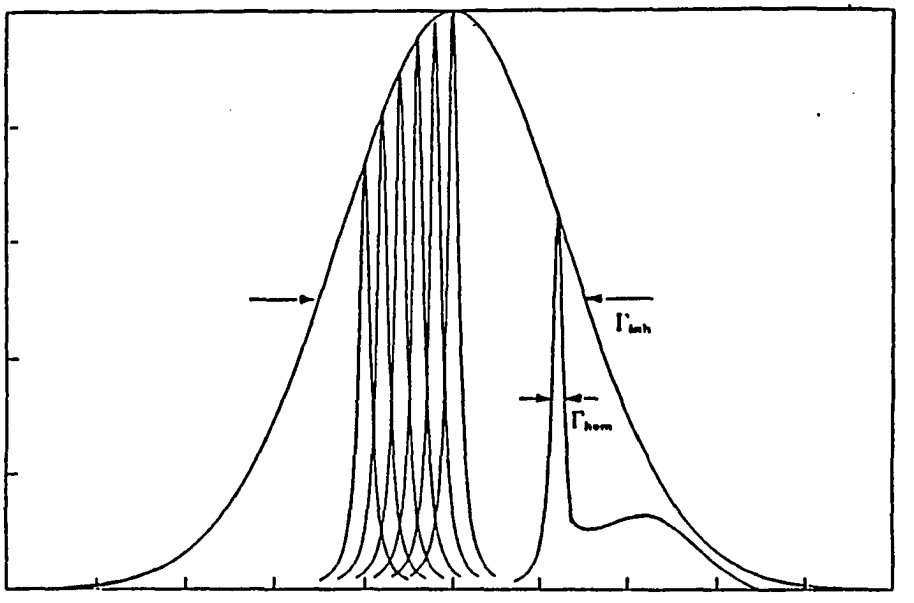

Figure 2. A. Inhomogeneous broadening of an absorption profile in a glassy matrix at low temperature (<20 K). The homogeneous (Γ_{hom}) and inhomogeneous (Γ_{Inh}) linewidths are indicated. B. The general nature of the spectral band of an impurity center

According to equation (3) and for a fixed coupling, an increase in temperature will lead to a decrease in ZPL intensity and to the "transfer" of the lost intensity to the PSB. A good example of this effect has been provided by fluorescence studies of perylene dissolved in both polar and non-polar solvents (70). At 4.2 K, the spectrum of perylene is dominated by strong ZPL. A marked decrease in ZPL intensity accompanies an increase in temperature. Between 40 and 50 K, the ZPL practically disappears.

The features and appearance of a spectrum are also dependent upon the excitation wavelength. The narrow excitation region must be situated within the inhomogeneously-broadened absorption profile so as to excite only one or a few isochromats belonging to different vibrational states. For high energy vibronic excitation of the S_1 state (e.g., exceeding the (0,0) transition frequency by ≥ 3000 cm^{-1}), high vibronic levels and corresponding ZPL are considerably broader than the purely electronic ones. Furthermore, in this region there is a significant increase in the density of states, which results in high congestion of "isochromats" belonging to many vibrations. As a result, the laser excites practically all types of centers. The pertinent fluorescence spectrum is virtually broad-band. The greatest degree of line narrowing will take place, therefore, if excitation is into either the origin or low lying vibronic bands of the lowest excited singlet state (S_1). For origin excitation, the ZPL are generated by the transitions originating from the zero-point vibronic level of S_1 and terminating at the zero-point and vibronic levels of S_0. The resonance 0-0 transition line is not a reliable analytical line because its frequency coincides with that of the laser line. Therefore, the vibronic transitions only provide the ground vibrational frequencies. One of the features of origin

excitation is that the variation of the laser frequency within the limits of the inhomogeneous broadening (100 to 300 cm^{-1}) in the 0-0 region causes a corresponding displacement of the FLN spectrum along the frequency scale without changing its nature.

Utilization of vibronic excitation has several advantages over the origin band excitation from the standpoints of characterization and selectivity. The improved selectivity with vibronic excitation is based upon the fact that the vibronic features in $S_1 \leftarrow S_0$ absorption spectrum are often more sensitive to structure perturbations than the $S_1 \leftarrow S_0$ fluorescence spectrum (71, 72). Figure 3 is presented here to describe a vibronic excitation scheme. An absorption spectrum in Figure 3A includes two overlapping vibronic levels, 1_α and 1_β, and a narrow line laser excites the two overlapping one-quantum vibronic transitions, $(1_\alpha,0)$ and $(1_\beta,0)$. Taking the molecule population distribution in each vibronic level into consideration, ω_L excites an isochromat associated with 1_β that lies close to the most probable position (or central position) of its distribution, while that associated with 1_α lies near the top of its distribution. Subsequently, the excited molecules relax within picoseconds to the zero-point vibronic level of S_1. Fluorescence then occurs. Vibrational relaxation is indicated by the downward wiggly arrows which show that fluorescence is due to two different isochromats linked to the two vibronic levels initially excited. The fluorescence from the two isochromats results in a doubling of the origin as well as the (0,1) vibronic transitions. The resulting fluorescence has the appearance of Figure 3B in which the intensity of the β mode transition is much higher than that of the α mode transition.

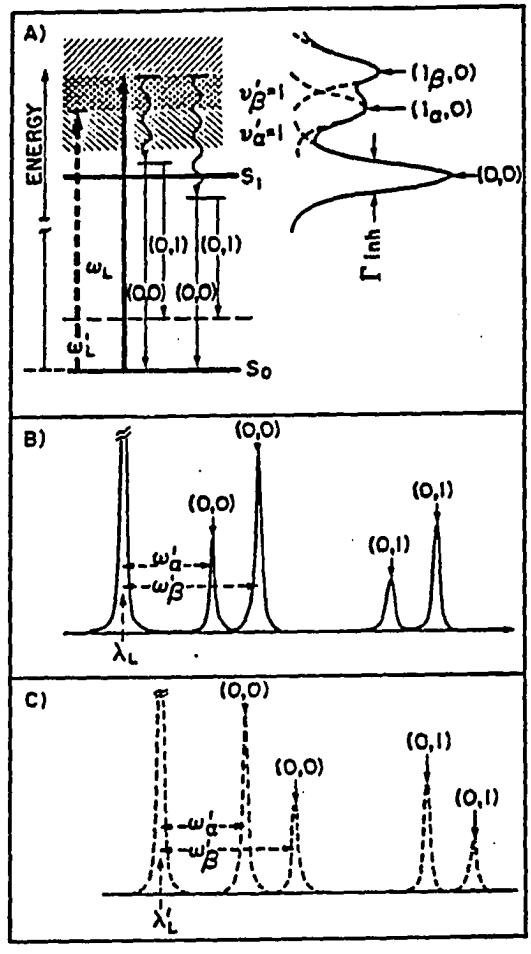

Figure 3. Schematic representation of laser site selection for vibronic (1,0) excitation, and the resulting line-narrowed fluorescence spectrum. See text for detail discussion

An important point is that the energy differences from the laser line to the (0,0) bands are equal to the vibrational frequencies of the molecule in the S_1 state, while the displacements between the (0,0) and (0,1) bands yield ground state frequencies. A slight variation of the laser frequency in the overlapping region of 1_α and 1_β will result in the change of relative intensity distribution of ZPL that originates from the α and β modes. For instance, if a frequency ω'_L selects an isochromat associated with 1_α that lies close to the most probable position of its distribution, the appearance of the fluorescence spectrum will look like Figure 3C when α-ZPL are the more intense. By varying ω_L throughout the vibronic absorption region, it is possible to explore a wide range (~ 400-1600 cm^{-1}) of active S_1 vibrational frequencies. Thus, a great degree of characterization and minimization of spectral interferences is possible.

With the notion of isochromat selection established by FLN, photochemical hole burning (PHB) followed logically. It is apparent that if the species giving rise to the absorption is photoreactive, isochromats can be photobleached selective (73).

"Non-photochemical hole burning (NPHB) does not require photoreactivity of the absorbing species. What is required is a host with a 'faulty memory' for its pre-excitation configuration around the absorber. That is upon completion of the ground state → excited state → ground state cycle, the host configuration must have changed and, more or less, permanently if persistent holes are to be produced". (74). Because hole burning processes result in a loss of absorbers at the excitation energy, it is important for high sensitivity measurements not only to be aware of their possibility but also to be able to minimize such processes where they do occur. For example, it has been shown recently that one can minimize the

deleterious effects of NPHB by synchronous scanning of excitation and detection wavelength, (thus, continuously changing the isochromat excited), by use of a slightly higher temperature (10-20 K, which can increase the bleaching time of the hole-burning) and by restoring the original inhomogeneous distribution through broad band excitation (e.g., using white light to refill the hole) (72).

Under some circumstances, broad band fluorescence, strong phonon wings, and laser and other scattering backgrounds degrade the FLN spectrum so badly that it is hard to analyze the spectrum. In such cases, a recently developed methodology called double selection FLN-NPHB spectrometry (DSFLNS) can be used to circumvent these problems (72). This method takes advantage of the NPHB effect and is based on the following three procedures. First, obtain a normal spectrum. Second, increase the laser power to burn a large majority of molecules on that site and then take a second spectrum. Finally, substract both spectra to produce a very nice spectrum with improved detection limits.

B. Applicability of FLNS to the Study of Chemical Carcinogenesis

Formation of an adduct between the genetic material DNA and a chemical agent is thought to be a crucial step in the initiation of carcinogenesis and tumorigenesis (13-15). Since typical DNA damage levels are low ($< 1{:}10^8$ adduct:base pairs), there has recently been considerable interest in the development of highly sensitive bioanalytical techniques for damage analysis. Equally important as high sensitivity is the requirement of high selectivity of the type which allows for the distinction between structurally similar DNA adducts. Advantages also exist for a technique which is applicable to the intact DNA adduct rather than only to the

ideal method for the study of DNA damage should be applicable to small samples of DNA with low adduction levels found in real samples (75, 76). Several fluorescence-based techniques have been utilized (75, 77-79). In particular, FLNS has become an effective technique for the identification and determination of DNA adducts and the study of various metabolic pathways leading to tumor formation (72, 80-86).

The inherent advantage of FLNS is its high selectivity, which is a direct consequence of the presence of many narrow lines in the FLN spectra of a given molecule (68, 69). Since both the ground and excited state vibrational frequencies can be probed utilizing origin (0,0) and vibronic (1,0) excitation, a unique spectral characterization is generally possible. FLNS has previously been shown to have sufficient selectivity to directly distinguish substitutional isomers of a given PAH, polar PAH metabolites, and their corresponding DNA-bound adducts (82, 83, 87); for example, BP tetraol and the covalently bound BPDE-DNA adduct, and different DNA adducts possessing the same fluorescent chromophore (82, 87). FLNS also exhibits sufficient selectivity to analyze the complex mixtures of PAH metabolites and PAH-DNA adducts which are likely to be found in real samples (87). Using selective excitation and temporal discrimination, FLNS has been shown to be capable of directly resolving all the components in a laboratory mixture of five DNA adducts, three of which possessed the same fluorescent chromophore, phenanthrene (82), and all the components in a mixture of six PAH metabolites and two DNA adducts (82, 87). In addition, FLNS was successfully applied to the study of the one electron oxidation pathway involved in the metabolic activation of BaP *in vitro* (83, 88). FLNS could distinguish between five BaP-nucleoside

adducts synthesized by one electron oxidation of BaP in the presence of guanosine, deoxyguanosine, and deoxyadenosine. When FLNS was used to study the horseradish peroxidase catalyzed reaction of BaP with DNA, the major adduct identified in this *in vitro* system was found to be 8-(BaP-6-yl)guanine, a typical mono-electron oxidation product.

It is noted that only a small fraction (~ 10 µl DNA sample (1mg/ml)) of the sample molecules is sufficient, hence, the sensitivity of FLNS is quite impressive. For moderately strong absorbing and fluorescing molecules such as anthracene and 1-methylpyrene, detection limits of 0.2 pg can be achieved (72). For (+)-anti-BPDE-DNA when using double selection of FLNS-non-photochemical hole burning technique, a detection limit of ~ 3 adducts in 10^8 DNA bases was reported for a 20 µg DNA sample (72).

Perhaps the most valuable attribute of FLNS is the ability to characterize intact (i.e., macromolecular) DNA samples. There is no need to chemically or enzymatically digest the DNA to nucleotides and isolate the damaged (adducted) nucleotides or derivatize the adducts prior to the analysis. The fact that DNA digestion can be avoided is important in the sense that less manipulation of the DNA is required and, therefore, there is a smaller chance of altering the profile of adducts; all adducts formed, including the unstable adducts which can depurinate and be lost from the DNA, can, in principle, be detected. Moreover, the fact that extensive sample preparation is not required makes FLNS a rapid method of analysis.

III. EXPERIMENTAL

A. Materials and Methods

The solvents and chemicals used were from different commercial sources. Electrophoresis purity reagent acrylamide, the fluorescence quencher used, was from Bio-Rad Laboratories and was > 99.9% purity. 7,8,9,10-tetrahydro-7,8,9,10-tetrahydroxy-benzo[a]pyrene (BPT) was obtained from the Midwest Research Institute, Kansas City, Missouri, through the NCI depository. Reagent grade glycerol (Fisher Scientific Company) and absolute ethanol (100%) (Ames Lab storeroom) were used without further purification. The water used to dissolve samples was deionized distilled water. A mixture consisting of 5:1 glycerol:ethanol (by volume) was used as a glass-forming solvent for the majority of the samples analyzed. Calf thymus DNA was obtained from the Sigma Chemical Company and repurified by phenol extraction and ethanol precipitation prior to use. DNA samples were mixed to form a glass with 50% glycerol, 10% ethanol and 40% water, which is optically clear at 4.2 K. DNA samples were dissolved in water to a concentration of ~ 1 mg/ml. These samples were mixed 60:40 with the glycerol:ethanol solvent prior to analysis or were analyzed as dissolved. At 4.2 K, the DNA-in-water samples were not optically clear, but were FLN-functional. However, if the sample contains an extra amount of salt (e.g., from buffer solutions), a snowing glass will form at the low temperature. The formation of this kind of snowing glass could significantly affect the efficiency of the detection, since most of the laser beam is scattered without penetrating the sample. In such a case, the sample must be desalted to get rid of the majority of the salts in the DNA

sample by the following procedure. First, redissolve a dried DNA sample into 100 µl distilled water; then, add 2 volumes of ice cold ethanol (- 20 °C) to precipitate DNA; leave the sample in the freezer overnight to make sure most of the DNA has been precipitated, then put the precipitated DNA sample in a microcentrifuge (Fisher 235B) and spin for 10 minutes at 4 °C; finally, remove the supernatant and ethanol.

Quartz tubing, 3-mm O.D. x 2-mm I.D. x 1 cm, sealed at one end, was used as the sample container (30 µl total volume). The smaller sample volume was desirable to achieve lower detection limits, and quartz tubes were necessary for the ultraviolet excitation and emission wavelengths typically encountered with the species investigated. For most of the experiments performed, anaerobic sample conditions were needed. The degas procedures were accomplished by a series of freeze/pump/thaw cycles prior to completely sealing the tube under anaerobic conditions. The sample tubes were held vertically in an aluminum sample holder designed to occlude laser scatter from the sample tube edges and were lowered into a liquid helium dewar (2 min total immersion time) for analysis. Two different liquid helium dewars were employed: a double-nested 3 L glass liquid helium dewar (Pope Scientific) having quartz windows and designed to have no liquid nitrogen in the optical pathways and a 5 L glass liquid helium dewar. All FLN spectra presented in this dissertation were obtained with the samples at liquid helium temperature, 4.2 K. The laser-excited conventional fluorescence spectra were obtained at liquid nitrogen temperature, 77 K.

Room temperature absorption spectra were obtained using a Varian DMS 100 UV/vis spectrophotometer, and fluorescence spectra were obtained using a Spex

Fluorolog-2 spectrometer.

B. Samples and Preparation

All of the model compounds, standards, and the DNA samples were supplied by our collaborators: Dr. N. E. Geacintov (Department of Chemistry, New York University, NY); Dr. U. Varanasi (National Marine Fisheries, Seattle, WA); Dr. A. Maccubbin (Grace Cancer Drug Center, Roswell Park Memorial Institute, New York State Department of Health, NY); and Dr. A. Jeffrey (Institute for Cancer Research, Columbia University, New York, NY). I would like to express my sincere gratitude to them for their great support and assistance here.

The DNA, synthetic alternating (dG-dC) and (dA-dT) polynucleotides, single strand dG and dG-dC polynucleotides, d(ATATGTATA) oligomer adducts of (+)- and (-)-anti-BPDE were provided by Dr. N. E. Geacintov (Department of Chemistry, New York University, NY). The synthesis of the two enantiomers of (+)- and (-)-anti-BPDE was accomplished by a method described previously (89, 90). The high molecular weight calf thymus DNA (Worthington Biochemicals, Freehold, NJ) was dissolved in 5 mM sodium cacodylate buffer, 0.1 M NaCl, and 3 mM ethylene diamine tetraacetate and extensively dialyzed against 5 mM sodium cacodylate buffer. The hyperchromicity of this DNA (comparison of absorbance at 260 nm at 25 °C and at 90 °C, 1.1 M NaCl, pH 7.0) was in the range of 38-40%. The reaction mixture containing either one of the enantiomers of anti-BPDE (3.5×10^{-6} M) and DNA (7.6×10^{-4} M, nucleotide concentration) in a buffer solution was incubated at 25 °C, pH 7.0 for 12 hrs. After reaction was complete, the physically-bound tetraols were removed by extracting the aqueous phase twelve

times with ether, followed by a precipitation of the modified DNA by a 2.5-fold excess of cold ethanol. The DNA was then resuspended in the buffer solution. This procedure was repeated with mixtures of tetraol and unreacted DNA; all of the physically-bound tetraols can be removed by this technique, thus verifying that this method is adequate for isolating only the covalently bound reaction products. The similar procedures were used to make the synthetic polynucleotides and oligomer adducts. The adduct level measured for (+)-anti-BPDE-DNA is about 0.5% modification; for (-)-anti-BPDE-DNA, 1.5%; for single strand poly dG adducts of (+)-anti-BPDE, 0.37%; for single strand poly dG adducts of (-)-anti-BPDE, 0.22%.

The syn-BPDE-DNA and English sole liver DNA samples were obtained from Dr. U. Varanasi (National Marine Fisheries, Seattle, WA). [^{3}H]-Syn-BPDE was obtained from the National Cancer Institute Chemical repository. Unlabeled BaP (B-1760), salmon sperm DNA (D-1626), NADPH (N-1630), RNase (R-4875), and sodium dodecyl sulfate (L4509), were obtained from Sigma Chemical Co., St. Louis, MO. Phenol (24232-2) was purchased from Aldrich Chemical Co., Milwaukee, WI. T4 polynucleotide kinase (#70031) was purchased from the United States Biochemical Corporation, Cleveland, OH. All other chemicals used were of analytical grade and were used without further purification.

The BaP was purified by the method of Varanasi and Gmur (91). The DNA adduct standards of syn-BPDE were prepared by the addition of 66 nmoles of [^{3}H]-syn-BPDE in tetrahydrofuran:triethylamine (19:1, v/v) to a solution of 2 mg of salmon sperm DNA in 1 ml of distilled water. The solution was incubated at 25 °C for 1 hr while being gently stirred and then extracted with nitrogen-sparged ethyl acetate (3 x 1 ml) to remove hydrolysis products of BPDE. The modified DNA

was isolated by precipitation with cold ethanol (- 20 °C), dissolved in 0.05 M Tris, pH 7.5, to a concentration of 1 mg DNA/ml; and then stored at - 20 °C. The level of modification of [^{3}H]-syn-BPDE-DNA, as determined radiometrically, was approximately 1 adduct in 10^7 bases.

English sole were collected by otter trawl from a non-industrialized area of Puget Sound, WA and were held in flowing seawater (28‰) for up to two weeks for acclimation. Fish were fed with a 1:1 mixture of ground clams and krill containing gelatin as a binder. Neither PAHs or PCBs were present at detectable concentrations in the food. English sole (47±11 g) were injected parenterally in a sinus near the fin ray with either 50 mg or 100 mg BaP/kg (by weight (b.w.)); the BaP was dissolved in Emulphor 620:acetone (1:1) and administered at 1 ml/kg b.w. The second batch of English sole were exposed under controlled laboratory conditions to water contaminated with a mixture of dibenz[a,h]anthracene, benzo[b]fluoranthene, and BaP. The control fish were given an injection of solvent vehicle only. The fish were not fed during the 24 hr period preceding sampling to insure that bile would be present in the gall bladder when the English sole were sampled. The liver was sampled from English sole from all dose groups at one day post-exposure. The liver samples were immediately frozen in liquid nitrogen and then stored at - 80 °C.

Hepatic DNA was isolated using the method of Bender et al. (92) with slight modifications. A sample of liver (50-100 mg) was homogenized in 1 ml of grinding buffer (100 mM Tris-HCl, 100 mM sodium chloride, 50 mM EDTA, 200 mM sucrose, 0.5% SDS, pH 8.0-8.2) using a Dounce homogenizer. The homogenate was transferred to a 1.5 ml Eppendorf micro-centrifuge tube and incubated at room

temperature for 5 min, followed by the addition of 250 µl of 5 M potassium acetate. The sample was then gently vortexed and incubated on ice for 30 min. Precipitated protein was pelleted by centrifugation for 5 min at 16,000 x g in an Eppendorf centrifuge (Model 5412). The clear supernatant was extracted sequentially with phenol (containing 0.1% 8-hydroxyquinoline) and chloroform:iso-amyl alcohol (24:1, v/v). DNA was precipitated with 100% ethanol and washed once with 70% ethanol. After drying for 1 hr, the DNA was dissolved in 300 µl TE buffer (10 mM Tris-HCl, 1 mM EDTA, pH 7.5) and 10 µg of RNase A was added. The solution was incubated at 37 °C for 30 min, after which 175 µl of 7.5 M ammonium acetate were added. DNA was precipitated with 100% ethanol and incubated on ice for 10 minutes. The purified DNA was washed with 70% ethanol and subsequently dissolved in 75 µl of TE buffer. The concentration of DNA in solution was determined from A_{260} using an extinction coefficient of 22.9 ml/mg-cm.

The modification of salmon sperm DNA by BaP *in vitro* was done using hepatic microsomes from control English sole prepared according to Schnell et al. (93). The reaction mixture consisted of microsomes (0.2 mg/ml), DNA (2 mg/ml), 2.5 µM BaP, 1 mM NADPH, 50 mM Tris buffer, pH 7.5, in a total volume of 2 ml. The reaction was initiated with the NADPH and was run at 25 °C for 30 min. DNA was isolated from the reaction mixture by two extractions with chloroform:iso-amyl alcohol (24:1, v/v), followed by precipitation with two volumes of cold ethanol.

The liver DNA samples of fish from polluted areas were prepared by Dr. Alexander Maccubbin (Grace Cancer Drug Center, Roswell Park Memorial

Institute, New York State Department of Health, NY). The carp were collected from one of the polluted Great Lakes tributaries, Buffalo River, by electroshocking. The carp were obtained from a point approximately 1 km from the mouth of the river. They were compared with aquarium-raised fish of a similar or slightly lower age which had been captured from a shallow non-industrialized land locked pond and then maintained in clean aquarium at the Roswell Park Memorial Institute. Aquarium fish were fed a commercial trout diet and had been in the aquarium for a minimum of 6 months before sampling. Livers were removed from the fish, and the small (approximately 0.5 g) pieces were frozen in dry ice and were maintained in dry ice or at - 70 °C until the DNA was extracted. Pieces of liver, 100-200 mg, were diced with scissors into pieces 1 to 2 mm large, and were digested for 3 hr at 37 °C in 0.7 ml SET buffer containing 0.5% sodium dodecyl sulfate and 1 mg/ml proteinase K. Samples were then deproteinized by successive extractions with an equal volume of phenol:chloroform:isoamyl alcohol (25:24:1) and chloroform:isoamyl alcohol (24:1). Nucleic acids and a copious white precipitate of glycogen from the liver were recovered by precipitation with 2 volumes of ethanol at - 20 °C. After washing the pellets with 70% ethanol, they were redissolved on 0.5 ml SET buffer containing 200 μg hog pancreas α-amylase/ml and incubated for 1 hr at 37 °C. Samples containing dissolved glycogen initially had a slightly opalescent or milky appearance but were rendered clear by hydrolysis of the glycogen with α-amylase. Nucleic acids were precipitated with ethanol, then redissolved in 0.7 ml SET buffer containing 0.1 mg/ml heat-treated pancreatic RNase A. After a 1 hr incubation at 37 °C, 70 μg proteinase K in 10 μl water was added to the tubes, which were incubated another hour. Samples were diproteinized

with phenol and phenol:chloroform:isoamyl alcohol. The DNA was recovered and purified by two consecutive precipitations with ethanol. Purified DNA was redissolved in Tris (10 mM) EDTA (0.1 mM) buffer, and quantitated by its UV absorption at 260 nm, using the relationship of 1 absorbance unit = 50 μg/ml. The liver sample of the carp contained a total of 200 μg of DNA.

The women's placental DNA samples and (+)-anti-BPDE-DNA sample with low modification level of $8:10^7$ (adducts:base pairs) were provided by Dr. A. Jeffrey (Institute for Cancer Research, Columbia University, New York, NY). Twenty placental samples were collected from term, uncomplicated pregnant women who either were or were not smoking. The placental DNA was extracted in the similar way as Everson et al. (58, 65). (+)-anti-BPDE-DNA sample was obtained from 10T1/2 cell cultures treated with [^{3}H]-benzo-[a]pyrene (0.004 mg/mL) for 24 hrs. [^{3}H]-benzo[a]pyrene was obtained from Amersham Searle, Arlington Heights, IL. Other chemicals were commercially available from standard sources. The cells were grown as previously described in Ref. 94. After treatment with the [^{3}H]-benzo[a]pyrene, the cells were washed with PBS and scraped from the plates. The DNA was extracted using methods similar to those described in Ref. 94. The nuclei, isolated disruption of the cytoplasmic membrane by Triton X-100, were solubilized with a 1% SDS solution at pH 6.9, containing 15 mM NaCl and 1.5 mM citrate. This solution was then extracted several times with water-saturated phenol before the DNA was precipitated from the aqueous phase with two volumes of ethanol. The DNA was redissolved and treated with RNase before re-extraction with phenol and two ethanol precipitations. The modification levels of these adducts were also determined by the Randerath procedure.

C. Instrumentation

The instrumentation used for low temperature fluorescence experiments can be divided into four major components: a spectrally narrow excitation source, a low temperature dewar as a sample chamber, a monochromator for dispersing the fluorescence, and a detection system. Figure 4 presents a block diagram of the FLNS apparatus that uses a Tracor-Northern TN-6134 photodiode array as the detector. Since this set-up has been described in detail recently (87), only a brief discussion will be given here.

The excitation source used in this laboratory is a dye laser (Lambda Physik FL-2002) pumped by an XeCl (Ne buffer gas) excimer laser (Lambda Physik EMG 102 MSC). It can provide high energy (165 mJ/pulse) pulses at a repetition rate of 30 Hz at 308 nm. The firing of the laser is triggered by a synchronized electronic output pulse. Since the trigger pulse slowly drifts with time and thyratron temperature, a Lambda Physik EMG-97 Zero Drift Controller (ZDC) is used to correct for this long-term temporal drift, and provides a new "truly" synchronized output trigger pulse which occurs ~ 10 μsec before the laser pulse. The output from the excimer laser is used to pump the dye laser system. The dye laser uses a grazing incidence grating in a Littrow geometry for wavelength selection. The excitation wavelength from 340 to 410 nm was selected for the present work by use of various dyes, p-Terphenyl, DMQ, PBD, BBQ, and PBBO. The conversion efficiency of the dye lasers is typically from ~ 4% to 8%, and thus, the excitation powers range from 2 to 13 mJ/pulse. The output beam of the dye laser has a spectral linewidth of 0.22 cm^{-1} and a temporal width of ~ 10 ns. It has a symmetrical trapezoid shape with approximate dimension of 2 mm by 3 mm. This

output is then shaped using a quartz biconvex lens and a quartz plano-convex cylindrical lens combination into 10 mm x 2 mm beam to insure complete irradiation of the sample. The excitation power density at the sample can be adjusted from 5 to 500 mW/cm^2. Fluorescence is collected at right angles to the excitation and is focused into a 1-meter McPherson 2061 scanning monochromator (F 7.0) using two 50-mm diameter quartz lenses. The first lens is used to collect and collimate the fluorescence, and the second is used to match the f-number of the monochromator. The monochromator is equipped with a 2400 grooves/mm grating and is able to provide a reciprocal linear dispersion of 0.416 nm/mm. The resolving power of the monochromator ($\lambda/\Delta\lambda$) can be optimized to above 60000 at 5 μm slit width. However, considering that the slit width is often set at 300 μm when the concentration of the samples is very low, the monochromator usually has a bandpass of 0.12 nm (~ 10 cm^{-1}). Therefore, the widths of the zero-phonon lines in the FLN spectra are monochromator-limited.

Two kinds of fluorescence detector systems were used for the present work. The first utilized a photodiode array (PDA), and the second utilized a photomultiplier tube (PMT). There were two different photodiode array systems used in this study. Figure 4 presents the arrangement for Tracor-Northern TN-6134 blue-enhanced gateable photodiode array. The diode array consists of 1024 diodes (25 μ x 2.5 mm) with 700 diodes intensified. These intensified photodiodes cover

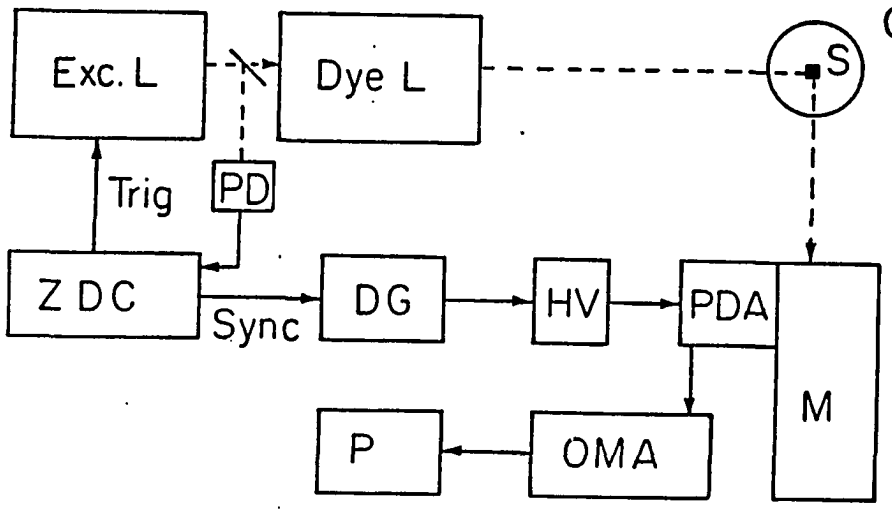

Figure 4. Block diagram of the FLNS instrumentation using Tracor-Northern TN-6134 photodiode array as the detector: excimer laser (Exc. L), dye laser (Dye L), cryostat (C), sample (S), photodiode array (PDA), monochromator (M), optical multichannel analyzer (OMA), and printer (P). See text for discussion

the spectral window of ~ 6 nm for the monochromator used. The resolution of the diode array is 4 channels FWHM and was calibrated as described by Zamzow (88). The uncertainty for the measured vibrational frequencies of the FLN peaks can be reduced to ± 3 cm^{-1}. The PDA can be gated to discriminate between scattered laser light and low levels of fluorescence. Gated detection of the fluorescence is accomplished by use of the synchronous output pulse of ZDC to trigger a pulse generator (Berkeley Nucleonic Corporation (model 8010)) acting as a delay generator (DG). The delay generator can set delay from 0 to 1 seconds between the laser pulse and the temporal window of the detector. The gate width of the temporal window can be set from 5 to 120 nsec by use of an Avtech high voltage switch (model AVL-TN-1). All data acquisition and processing, including automatic background subtraction and magnetic disk data storage, were performed by use of an optical multichannel analyzer (OMA) manufactured by Tracor-Northern Corporation (model TN-6500).

The PMT system is mainly utilized to perform the broad fluorescence experiments at 77 K and fluorescence narrowing excitation experiments (*cf.* Figure 5). The Amperex XP-2232 photomultiplier tube is specially wired for fast signal response (95). The fluorescence signal from the PMT is sent to a SRS Model SR250 boxcar averager (BXC. I). The SR250 boxcar consists of a gate generator, a fast gated integrator, and exponential averaging circuitry. The synchronous output pulse of ZDC triggers the gate generator, which provides both an adjustable delay from a few nanoseconds to 0.1 seconds and a continuously adjustable gate from 2 nanoseconds to 15 milliseconds. The fast gated integrator integrates the

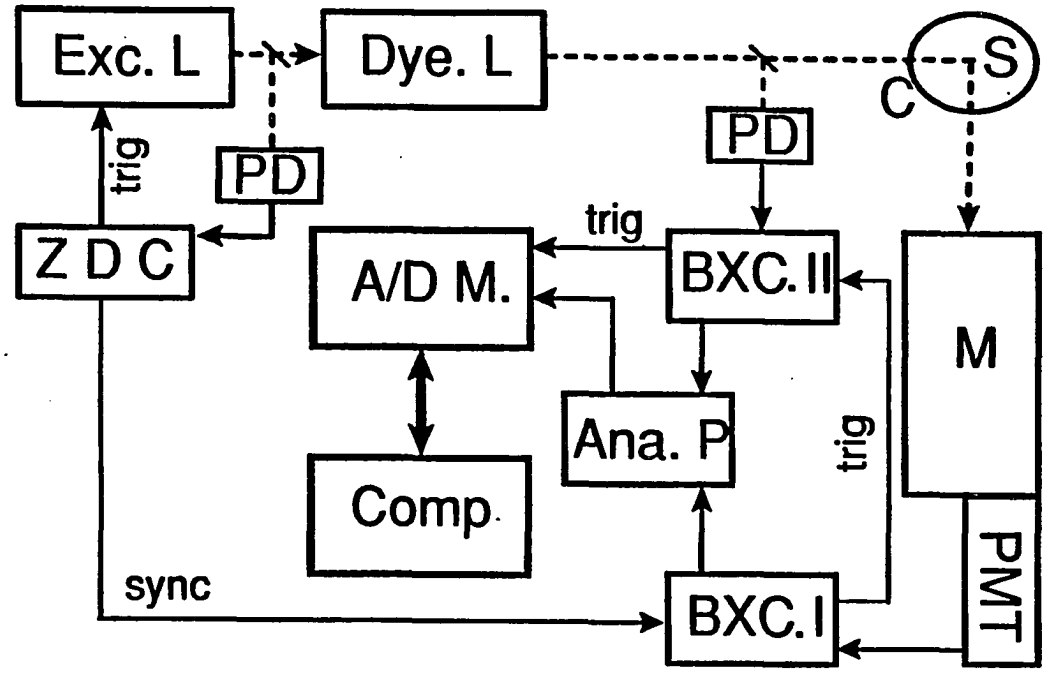

Figure 5. Block diagram of the fluorescence instrumentation using Amperex XP-2232 photomultiplier tube as the detector: excimer laser (Exc. L), dye laser (Dye L), cryostat (C), sample (S), photomultiplier tube (PMT), monochromator (M), SRS Model SR250 boxcar averager (BXC I or II), SRS Model SR235 analog processor (Ana. P), SRS model SR245 computer interfacing module (A/D M.), and computer (Comp). See text for discussion

input signal acquired during the gate. The output from the integrator is then normalized by the gate width to provide a voltage which is proportional to the average of the input signal during the sampling gate. The averager circuitry makes a moving exponential average over 1 to 10,000 samples available to pull small signals from noisy backgrounds. The laser beam intensity is monitored by a reference photodiode, and the signal is input to the second channel of the boxcar averager. The signals from the PMT and reference photodiode are input to a SRS Model SR235 analog processor, where they are ratioed in order to compensate for pulse-to-pulse jitter from the laser. The analog signal from the analog processor is then converted into a digital signal through the SRS model SR245 computer interfacing module, and the data acquisition is accomplished by a accompanied computer program SR267. All spectra obtained from PDA and PMT systems can be transformed into files of "Spectra Calc" and "MASS11-DRAW," commercial computer graphic programs which greatly facilitate spectral processing.

The second PDA detector system used a PI Inc. Spectrometric Multichannel Analyzer system (OSMA). The Model IRY-1024 detector for this study consisted of 1024 photodiodes optically interfaced to a microchannel plate (MCP) image intensifier through an optical-fiber coupler. The combined high gain (more than 10^6 electron multiplier) of the MCP image intensifier and the low readout noise of the diode array resulted in a very sensitive detector capable of responding to a single photoelectron. Moreover, the detector is able to detect, measure, and manipulate spectra at high acquisition rates (33 msec) with an excellent dynamic range, high resolution, and excellent overall accuracy and performance. A block diagram of the OSMA system is illustrated in Figure 6. The system comprises the

computer console, ST-120 Detector Controller, FG-100 Gate Pulse Generator, and an IRY-1024 Detector. The synchronous output pulse from ZDC is used to trigger the Model FG-100 Gate Pulse Generator. The FG-100 pulser is primarily designed to provide high speed gating with pulse delay control. Low voltage pulse (200 V) is used to gate on/off the detector. Combined with PI's high conductivity photocathodes, it is possible to obtain gating times as short as 5 nsec. The time interval between the trigger pulse and the output pulse is continuously adjustable from 20 to 1700 nsec. Considering that the synchronous output pulse of ZDC precedes laser light pulse, the actual delay time from 0 to 1500 ns can be set by FG-100. The detector controller (Model ST-120) provides power, thermostat, and timing signals to the detector head, coordinates data gathering with experiments, sets exposure time, digitizes and averages data, temporarily stores data and transmits it to an IBM/AT computer. A combination of a ST-120 controller with a FG-100 pulser provides versatile trigger modes which can meet a variety of experimental requirements. The mode illustrated in Figure 6 is used to monitor a free-running pulsing laser which operates asynchronously with the ST-120. The timing of this mode can be described as following: the ST-120 can be set for a few delays. No scan ensures no read during the FG-100 gating period. At the end of the exposure time, the spectra are summed and the spectral data are sent to the computer. In this mode since the laser is the MASTER and thus directly controls the FG-100, the temporal-jitter from the laser pulse can be greatly eliminated.

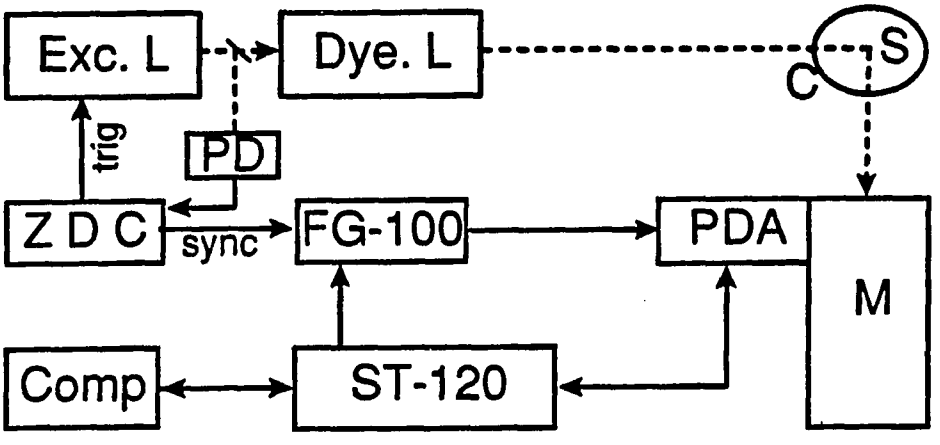

Figure 6. Block diagram of present FLNS instrumentation: excimer laser (Exc. L), dye laser (Dye L), cryostat (C), sample (S), photodiode array (PDA), monochromator (M), spectrometric optical multichannel analyzer (OSMA), gate pulse generator (FG-100), detector controller (ST-120), and computer (Comp). See text for discussion

IV. RESULTS AND DISCUSSION

A. Laser Spectroscopic Studies of DNA Adducts Structure Types from Enantiomeric Diol Epoxides of Benzo[a]pyrene[2]

A methodology based on 77 K laser-excited fluorescence spectroscopy, fluorescence quenching and fluorescence line narrowing is shown to be a highly selective and sensitive approach for the study of polycyclic aromatic carcinogen-DNA complexes. Three and five different DNA adducts derived from (+)-trans-7,8-dihydroxy-anti-9,10-epoxy-7,8,9,10-tetrahydro-benzo[a]pyrene and its (-)-enantiomer are identified, respectively. Two different methods are used to classify the adducts as type I (interior) or type II (exterior), and both yield consistent results. The first high resolution fluorescence excitation spectra are reported for DNA adducts. These spectra are suggested to be useful for characterizing the strength of the interaction between the fluorescent chromophores and the DNA bases. The above methodology has the potential for monitoring the fates of different adducts as a function of time in repair-competent cells.

---

[2] Detailed results and discussion for this topic are described in Paper I which is located in Appendix A.

B. A Comparative Laser Spectroscopic Study of DNA and Polynucleotide Adducts from the (+)-anti-diol Epoxide of Benzo[a]pyrene

Fluorescence line narrowing spectroscopy in combination with fluorescence quenching and 77 K laser-excited fluorescence spectroscopy is shown to be a powerful approach for characterization of chemically and/or structurally different adducts of (+)-anti-BPDE formed from DNA and the synthetic polynucleotides. Three polynucleotide duplexes ((poly(dG-dC)·poly(dG-dC), poly(dG)·poly(dC), poly(dA-dT)·poly(dA-dT)) and single strand poly(dG) were used in this study, and the spectral characteristics and the quenchability of each corresponding adduct were elucidated. The alternating poly(dG-dC)·poly(dG-dC) yields (+)-1 and -2 adducts which are most similar to the *trans* N^2-dG adducts of DNA. Fluorescence experiments with *trans* and *cis* standards of N^2-dG from (+)-anti-BPDE and guanine monophosphate were the bases for this stereochemical assignment. The model (+)-anti-BPDE adducts of the oligonucleotide d(ATATGTATA) were studied spectroscopically. The results further confirm our previous conformation assignment of (+)-1 as a type II adduct and (+)-2 as a quasi-intercalated adduct, and indirectly supports (+)-3 as an intercalated adduct. In addition, the FLN spectra of (+)-anti-BPDE-DNA reveal a new minor adduct, (+)-4, which is assigned as N^6-dA on the base of the spectra of standard (+)-anti-BPDE-poly(dA-dT)·poly(dA-dT)

---

[2] Detailed results and discussion for this topic are described in Paper II which is located in Appendix B.

Finally, the 77 K fluorescence spectroscopy revealed three different species of racemic anti-BP tetraol which have been physically mixed with DNA and poly(dG). Their spectral characteristics and quenchability are also presented, which will be greatly conducive to the spectral analysis of "real adducts".

C. FLNS Identification of the DNA Adducts from Different BPDE stereoisomers *in vitro* and *in vivo*

1. FLNS identification of DNA adducts formed from different BPDE stereoisomers *in vitro*

Two central dogmas underlie modern research in chemical carcinogenesis. The first is Miller's (13) hypothesis that the active forms of most carcinogens are electrophilic intermediates formed metabolically. The second is the assumption that the initial step in the induction of tumors is the covalent binding of the active carcinogen species to a cellular macromolecule, generally presumed to be DNA (1, 7, 13, 24). Most chemicals require some type of metabolic activation to produce the reactive species capable of covalently binding to cellular macromolecules. Polycyclic aromatic hydrocarbons (PAH) can be activated by two main pathways: monooxygenation to produce bay-region diol-epoxides (21, 22) and one-electron oxidation to yield reactive intermediate radical cations (83, 96, 97).

In the monooxygenation pathway, cytochrome P450 and aryl hydrocarbon hydroxylase catalyze conversion of PAHs to more water-soluble oxygenated derivatives (13-16). Among these PAH derivatives, bay-region diol epoxides are the most reactive and biologically active. BaP has a bay-region structure (*cf.*

Figure 1) and can be metabolized into bay-region diol epoxides, which are believed to be the ultimate carcinogenic species (14, 15, 18-20). The metabolism of BaP into BPDE through a monooxygenation pathway usually occurs in a three-step process. First, BaP loses an electron and is oxidized to the 7,8-oxide. The 7,8-oxide is then hydrolysed to 7,8-dihydro-7,8-dihydroxy BaP. In the third step, the dihydroxy BaP loses the second electron to form 7,8-dihydroxy-9,10-epoxy-7,8,9,10-tetrahydro-benzo[a]pyrene (BPDE).

There are four stereoisomers of BPDE, designated as (±)-anti-BPDE and (±)-syn-BPDE. The structures of these stereoisomers are illustrated in Figure 1. In syn-BPDE, the benzylic hydroxyl group and the epoxide oxygen atom are on the same side, and in the anti-isomers, they are on the opposite sides. All four stereoisomers of BPDE have been tested as carcinogens. (+)-anti-BPDE is the most potent carcinogen in mammalian cells, while (-)-anti- and syn-isomers are at best only weakly active (36, 98-100). Therefore in carcinogenic research, it is important to develop highly selective bioanalytical techniques which have sufficient resolution to distinguish these adducts with very similar structures but quite different biological activities. The ideal technique should also be very sensitive and applicable to small samples of DNA (~ 100 μg) with low adduct levels since typical DNA damage levels in *in vivo* systems are very low (~1 adduct in 10^8 base pairs).

DNA adducts formed from (+)-anti, (-)-anti, and syn-BPDE *in vitro* were determined by FLNS. The pertinent FLN spectra, obtained with λ_{ex} = 369.6 nm and T = 4.2 K, are presented in Figure 7. These DNA adducts are readily

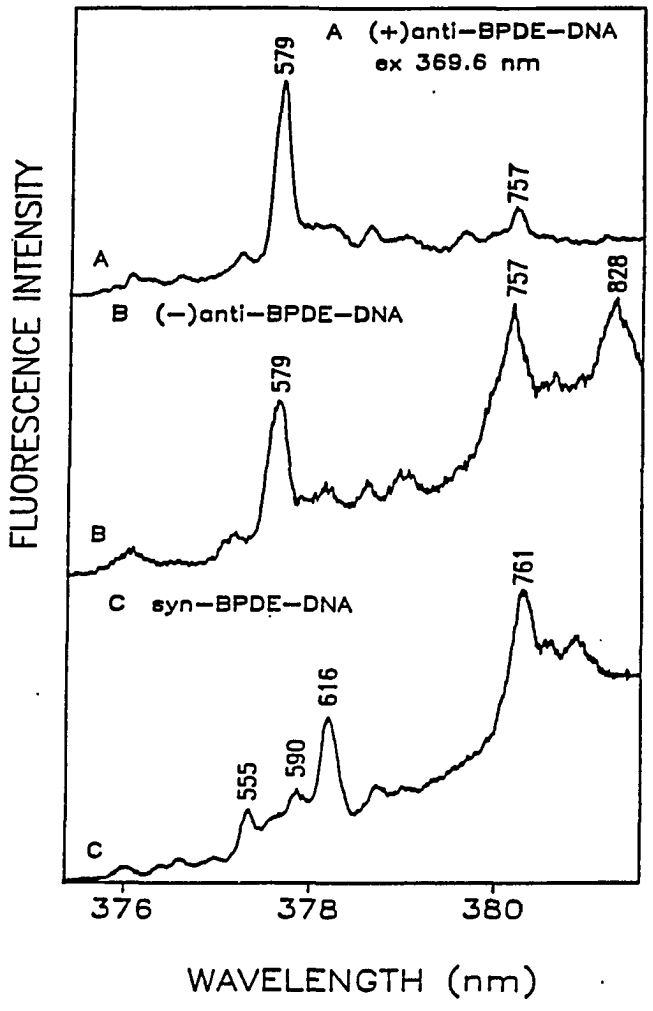

Figure 7. Comparison of the FLN spectra of three different DNA adducts from different BPDE stereoisomers. All spectra obtained in the standard gly/H_2O glass at T = 4.2 K. λ_{ex} = 369.6 nm.

A: (+)anti-BPDE-DNA; 0.5% bases modified,
B: (-)anti-BPDE-DNA; 1.5% bases modified,
C: syn-BPDE-DNA; ~ 1 adduct in 10^7 bases

The FLN peaks are labeled with their corresponding excited state vibrational frequencies (cm^{-1})

distinguished from each other primarily on the basis of differing vibronic intensity distributions. The spectrum of (+)-anti-BPDE-DNA (Figure 7A) is characterized by its major ZPL with the vibronic frequency of 579 cm^{-1} and a second ZPL with the vibronic frequency of 757 cm^{-1}. The intensity of the 757 cm^{-1} band varies with the adduct level and will be discussed later. The spectrum of (-)-anti-BPDE-DNA (Figure 7B) seems more complicated. The 579 cm^{-1} band is still a major band, but the 757 cm^{-1} band becomes almost as strong as the band 579 cm^{-1}. Underneath the 757 cm^{-1} band is an intense broad fluorescence band which contains contributions from intercalated adducts and tetrols, *vide supra*. The most characteristic band in the spectrum of the (-) adduct has the vibronic frequency of 828 cm^{-1}. It is a very strong band in the spectrum of (-)-anti-BPDE-DNA, but too weak to be noticeable in the spectra of (+)-anti- and syn-BPDE-DNA adducts. With the major 579 cm^{-1} band, the strong doublet bands 757 and 828 cm^{-1} in Figure 7B are very characteristic and can be used to test for the existence of (-)-anti-BPDE-DNA. The spectrum of syn-BPDE-DNA (Figure 7C) is readily distinguished from the spectra of (±)-anti-BPDE-DNA on the basis that the strongest vibronic mode in the spectrum of the syn-adducts has a vibronic frequency of 616 cm^{-1}, rather than 579 cm^{-1}, as in the spectra of the anti-adducts. In addition, the spectrum 7C contains another strong FLN band with the vibronic frequency of 761 cm^{-1}, which is superimposed on a strong broad fluorescence feature. The triplet structure in the FLN spectrum C, comprised of the 555, 590 and 616 cm^{-1} bands, may be viewed as characteristic of the syn-adducts.

In the study of BaP carcinogenesis, particular significance is placed on identifying the existence of (+)-anti-BPDE-DNA, since it is believed to be

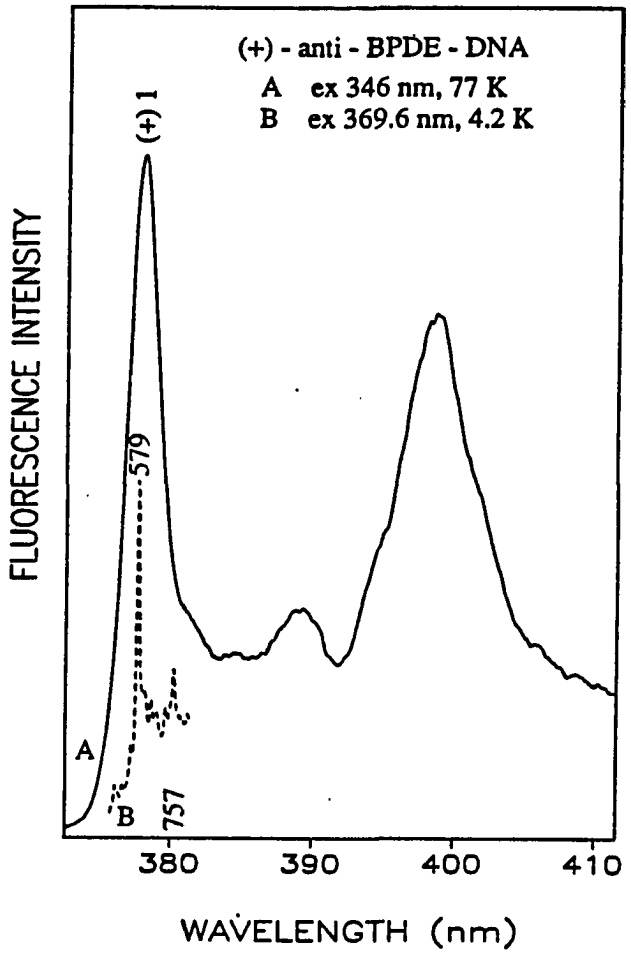

Figure 8. Laser excited fluorescence spectra of (+)anti-BPDE-DNA, 0.5% bases modified.

A: T = 77 K, λ_{ex} = 346 nm, broad fluorescence spectrum,
B: T = 4.2 K, λ_{ex} = 369.6 nm, FLN spectrum

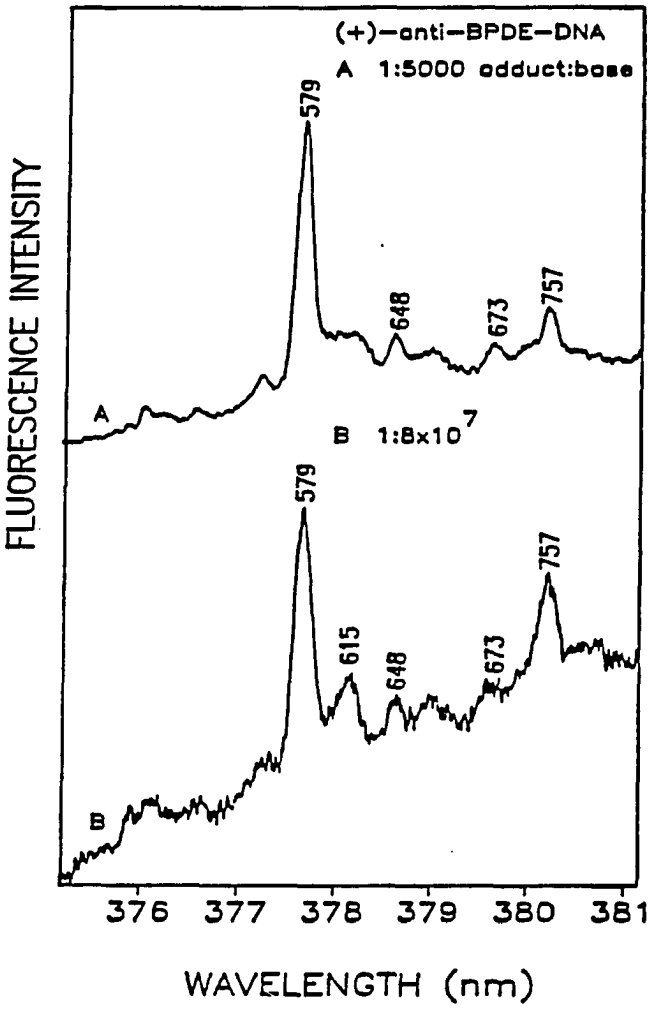

Figure 9. Comparison of the FLN spectra of (+)anti-BPDE-DNA at different concentrations, T = 4.2 K, λ_{ex} = 369.6 nm.

A: ~ 1 adduct in 5000 bases,
B: ~ 1 adduct in $8x10^7$ bases

the most potent carcinogen of all possible species. The 77K fluorescence spectrum of (+)anti-BPDE-DNA is the simplest spectrum, and exhibits a major band (denoted as (+)1) located at 378.0 nm (*cf.* Figure 8A). Since it is subject to significant quenching by ACR and has a great R-value, this band has been identified as being from covalently bound adduct which lies toward the exterior of the DNA double helix (*cf.* Appendix A: Paper I). Based upon the fact that 90% of (+)-anti-BPDE binds to N^2 of deoxyguanine (38), the 378 nm band contains significant contribution from N^2-dG-BPDE adduct. Since the laser with λ_{ex} = 369.6 nm selectively excites the vibronic bands of S_1 of the BPDE adducts, the pertinent FLN spectra will exhibit ZPL peaks derived from fluorescence origin. To (+)-anti-BPDE-DNA, the laser frequency is located about 600 cm^{-1} higher in energy than the origin band for (+)1 or N^2-dG-BPDE adduct. Therefore, the vibronic mode from the origin band of the FLN spectrum is characterized with the vibronic frequencies in the vicinity of 600 cm^{-1}. According to this analysis, the major band 579 cm^{-1} in the spectrum 8B (or 7A) is primarily originated from origin band of (+)1 and contains significant contribution from N^2- dG-BPDE adduct, too.

Figure 9 shows the FLN spectra of (+)-anti-BPDE-DNA with high (1:5000) and low ($1:8x10^7$) BPDE adduct modifications. The relative intensity of the broad underlying fluorescence in spectrum 9B is much greater, which shows that the relative level of the intercalated adducts and possible tetraols produced by degradation in the low modification sample is higher. Another difference between the two spectra is the relative intensity of the 757 cm^{-1} ZPL. It is a moderately strong in the spectrum of the low modification sample, but weak in the spectrum of the high modification sample. On the basis of the 757 cm^{-1} band's location and its

quenching behavior, we conclude that it contains a significant contribution from (+)2 (*cf.* Appendix A. Paper I). The relative increase in intensity of the 757 cm^{-1} band with addition of the quencher indicates an increase in the relative concentration of the quasi-intercalated (+)2 adduct in the low modification sample. From this study, an argument can be made that the relative amount of exterior and interior (quasi-intercalated or intercalated) depends upon the total modification level. Therefore, it is important for *in vitro* studies that a low modification level, comparable to those of *in vivo* samples, be employed.

2. FLNS identification of the liver DNA adducts of English sole exposed to BaP *in vivo*

Spontaneous tumors have occurred in a wide variety of fish species from both freshwater and marine environments (101). Although some studies have suggested that increased frequencies of some kinds of fish neoplasms may be the result of exposure to carcinogenic pollutants occurring in aquatic environments (102, 103), there has been no direct proof of this hypothesis until recently (42, 44, 45). It has also been suggested by Dawe et al. (46) that bottom-feeding fish species exhibit increased frequencies of neoplasms and thus may serve as early warning indicators of carcinogenic hazards to man. Our research focused on the study of the metabolic activation of PAH in the liver tissues of English sole, because this fish species exhibits a high prevalence of liver neoplasms in several PAH-contaminated areas (44, 45). The significance of this study is further emphasized by the finding that long-term exposure of English sole to BaP results in a spectrum of toxicopathic lesions similar to those observed in fish captured from contaminated areas (54).

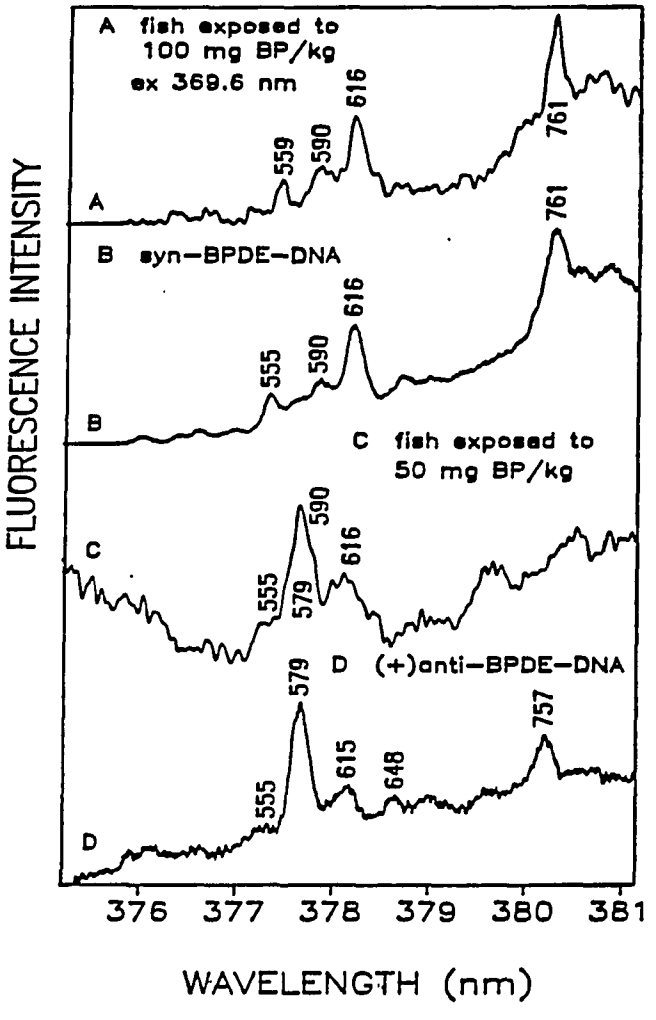

Figure 10. Comparison of the FLN spectra of the liver DNA samples of English sole exposed to BaP *in vivo* with standard BPDE-DNA adducts formed *in vitro*, T = 4.2 K, λ_{ex} = 369.6 nm.

A: The liver DNA of English sole exposed to 100 mg BaP/kg of fish,
B: Syn-BPDE-DNA, ~ 1 adduct in 10^7 bases,
C: The liver DNA of English sole exposed to 50 mg BaP/kg of fish,
D: (+)anti-BPDE-DNA, ~ 1 adduct in $8x10^7$ bases

Enzymatic hydrolysis and analysis by reversed-phase HPLC of hepatic DNA isolated from English sole exposed to radiolabeled BaP, however, did not show the presence of detectable levels of BPDE-DNA adducts (55). A recent study (56) using English sole hepatocytes exposed to ^{3}H-BP showed no detectable BPDE-dG adducts. The adduct level in this *in vivo* fish samples apparently very low, and a highly sensitive bioanalytical technique is imperative in this study.

The first *in vivo* sample tested was liver DNA of English sole exposed to a high dose of BaP (100 mg/kg. b.w.). The pertinent FLN spectrum obtained with λ_{ex} = 369.6 nm, is shown in Figure 10A. Even though the adduct level is very low (~ 1 adduct in 10^{7} bases as determined by ^{32}P-postlabeling (55)), the FLN spectrum exhibits an acceptable signal to noise ratio. Spectral analysis of the fish DNA spectrum reveals a characteristic triplet structure with the major ZPL band having the vibronic frequency of 616 cm^{-1}. Another strong ZPL has a vibronic frequency of 761 cm^{-1}, and is superimposed on a broad fluorescence feature. For comparison, the standard spectra of syn-BPDE-DNA and (+)-anti-BPDE-DNA are also presented in Figures 10B and 10D, respectively, which were obtained during the same run with the fish DNA spectrum. Based upon the analysis of the vibronic frequencies and the intensity distribution of the vibronic modes, the major adduct formed in the fish liver DNA can be identified as syn-BPDE-DNA.

Although anti- and syn-BPDE are both strongly mutagenic in bacterial and mammalian cells, anti-BPDE shows generally greater activity than syn-BPDE in most tests (15, 26). Therefore, in this study, particular emphasis was placed on determining whether or not (+)-anti-BPDE-DNA adduct is formed in English sole. In fact, even for highly PAH-contaminated areas like the Buffalo River and Detroit

River, the levels of individual PAH detected in the water ranged from 0.1 to 38.8 μg PAH/g water (42, 43). Therefore, fish exposed to lower doses of BaP are expected to provide a more realistic profile of adducts formed in nature. The second sample tested was the liver DNA of English sole exposed to a lower dose of BaP (50 mg/kg b.w.), the resulting FLN spectrum is shown in Figure 10C. Comparison of this spectrum with spectrum A reveals that the two are very different, *i.e.* the FLN spectrum depends on dosage level. The most intense ZPL in spectrum 10C is not 616 cm^{-1}, but rather 579 cm^{-1}. It is characteristic of anti-BPDE-DNA. Since the strong doublet bands 757 and 828 cm^{-1} are not observed, the major DNA adduct in the liver of English sole exposed to the lower dose of BaP is identified as (+)-anti-BPDE-DNA.

Further analysis reveals that the spectrum 10C is not quite identical to the corresponding spectrum of (+)-anti-BPDE-DNA, *cf.* spectrum 10D. The major 579 cm^{-1} band in 10C is broader and has a small shoulder with the vibronic frequency of ~ 590 cm^{-1}. Another band to the right of the 579 cm^{-1} band has a vibronic frequency of ~ 616 cm^{-1}, and a third band is also noticeable to the left with the frequency of ~ 555 cm^{-1}. Although the signal to noise ratio is rather poor, a triplet structure in spectrum 10C is discernible with the 616 cm^{-1} band being the strongest. Consequently, even though the major DNA adduct of the fish exposed to the lower dose of BaP is derived from (+)-anti-BPDE-DNA, a weak contribution from syn-BPDE-DNA cannot be excluded. Moreover, at ~ 381 nm there exists a broad fluorescence band, which adds further evidence for this argument. Similar results were also obtained by Varanasi *et al.* (53), by the use of the ^{32}P-postlabeling method. They showed that when English sole were exposed to 100 mg BaP/kg

b.w., 70 percent of liver DNA adducts formed were syn-BPDE-DNA, with the rest being anti-BPDE-DNA; however, for lower doses of BaP (2-15 mg/kg b.w.), only anti-BPDE-DNA adducts were detected in the fish liver DNA. They did not determine if the anti-BPDE-DNA arose from (+)-anti or (-)-anti-BPDE.

It has been found that in the cytochrome P450 enzyme family, different forms of P450 preferably catalyze conversion of BaP to either syn- or anti-BPDE or both (104). Since each animal cell or tissue contains different enzyme systems, different proportions of anti- and syn-BPDE-DNA can form in different animal cells or tissues. Large quantities of syn-BPDE-DNA adducts were detected in hamster epidermal cells, while in rabbit dermal fibroblast (+)-anti-BPDE-dG accounted for ~91% of the adducts (105). In the rat dermal fibroblast syn-BPDE-dG represented more than 40% of the adducts (105), while in the rabbit cell it only accounted for ~ 5% (105). However, our experiment reveals another phenomenon—that different adduct developed *in vivo* is dependent upon the BaP exposure level. This result poses an interesting problem for the study of the metabolic activation of BaP.

Kano's experiment (106) may give some clue to explain this phenomenon. Kano et al. (106) found that the interaction of BaP with a protein receptor molecule could induce the production of cytochrome P450c, which was 25-180 times as active as other forms of cytochrome P450. It is possible that the high dose of BaP promotes the production of cytochrome P450c, which then catalyzes the metabolic reaction to yield syn-BPDE.

The results from this study provide direct evidence for the formation of the suspected ultimate carcinogen through the monooxygenation pathway, BPDE, in liver of English sole exposed to BaP *in vivo*, and thus further support the

hypothesis that exposure to PAH is an important factor in the etiology of hepatic neoplasms in English sole from contaminated sites.

3. Conclusions

Despite their very similar structures, (+)-anti- , (-)-anti-, and syn-BPDE have quite different biological activities. This study shows that FLNS has sufficient resolution to distinguish the DNA adducts formed from these different BPDE stereoisomers *in vitro*. The vibronic modes from the fluorescence origins with the frequencies from 550 to 850 cm^{-1} provide the best "finger print" for identification of these different BPDE-DNA adducts. The spectra obtained can be used as standards for the study of other *in vitro* and *in vivo* systems. FLNS is also successfully applied to identify DNA adducts in the liver of English sole exposed to different doses of BaP *in vivo*. The fish species selected exhibits a high prevalence of liver neoplasms in several PAH-contaminated areas. When the fish is exposed to the lower dose of BaP (50 mg BP/kg b.w.), the major DNA adduct developed in the fish liver is identified as (+)-anti-BPDE-DNA, one of the most potent carcinogen species. However, at a high exposure (100 mg/kg b.w.), the major adduct developed in the fish liver DNA is syn-BPDE-DNA. The observation that the major adducts formed varied with exposure to different doses of BaP may pose an interesting problem in the study of metabolic activation. The results from this study provide the direct evidence for the formation of the suspected ultimate carcinogen through the monooxygenation pathway, BPDE, in liver of English sole exposed to BaP *in vivo*, and thus further support the hypothesis that exposure to PAH is an important factor in the etiology of hepatic neoplasms in English sole

from contaminated sites.

D. Laser-Excited Fluorescence Spectroscopy Study of DNA Damage to Women's Placenta and Fish Exposed to Widespread Environmental Pollutants

1. Characterization of DNA-adducts in women's placenta samples

In recent years, research in chemical carcinogenesis has been directed to human systems. The ^{32}P-postlabeling assay and the immunologic technique ELISA (using antibodies to chemically modified DNA in enzyme-linked immunosorbent assay) have been successfully used to detect carcinogen adducts from women's placental DNA samples (58, 64, 65). A total of seven different adducts were detected in the 53 subjects, and three of these adducts were found almost exclusively in smokers. Everson and co-workers (65) observed by ELISA that the antibodies modified by anti-BPDE have a positive response to the placenta DNA adducts. Since other adducts formed from anti-benz[a]anthracene diol epoxide and anti-chrysene diol epoxide also reacted with the developed antibodies (66, 67), they could not verify that the placenta DNA contained anti-BPDE-DNA adducts. The problem is that neither the chemical origin of the adducts nor their precise structures have been determined to date. The exposure or susceptibility factors that are most closely associated with biochemical or molecular damage to human tissues are still a mystery (65). Furthermore, identification of the DNA adducts formed from the different stereoisomers of a chemical carcinogen in human tissues is also of particular significance, since different stereoisomers of a chemical carcinogen

can have quite different mutagenicities and tumorigenicities (17, 33, 98, 107-109). Hence, further studies of carcinogenesis in humans require highly selective and sensitive assay techniques which not only can detect very low adduct levels (pmol to fmol), but also characterize the chemical origins and specific stereochemistry of the adducts as well.

Placental DNA samples were dissolved in the standard glycerol/ethanol/water glass, and all the samples were degassed to eliminate the oxidation and quenching effect from oxygen. FLN spectra of the placental DNA samples were obtained for all the standard vibronic excitation wavelengths used to characterize BPDE-DNA adducts. The first FLN spectrum from human placental DNA samples was obtained at excitation λ_{ex} = 369.6 nm, shown in Figure 11A. Spectrum 11A is characterized by three major peaks with vibronic frequencies of 535, 558, and 588 cm^{-1}. FLNS first exhibits a high sensitivity in detection of the low concentration of the DNA adducts from the human tissues. Seven out of twenty placental samples analyzed exhibit FLN spectra similar to that in Figure 11A, four of these seven DNA samples are from smokers, and three are from non-smokers. The spectra of (+)-anti- and syn-BPDE-DNA adducts are presented in Figures 11B and 11C for comparison. Careful analysis of the placenta DNA spectrum finds that its major band 588 cm^{-1} has a small peak on the left side, with vibrational frequency of 579 cm^{-1}. This is a typical vibronic mode for anti-BPDE-DNA adducts. Another small band in the placenta DNA spectrum can be noticed with the vibrational frequency of 757 cm^{-1}, which is also a typical peak for anti-BPDE-DNA adducts. Since there is no 828 cm^{-1} band with the proper intensity observed, the adduct can be identified as (+)-anti-BPDE-DNA. Other vibronic modes of (+)-anti-BPDE-DNA can be observed

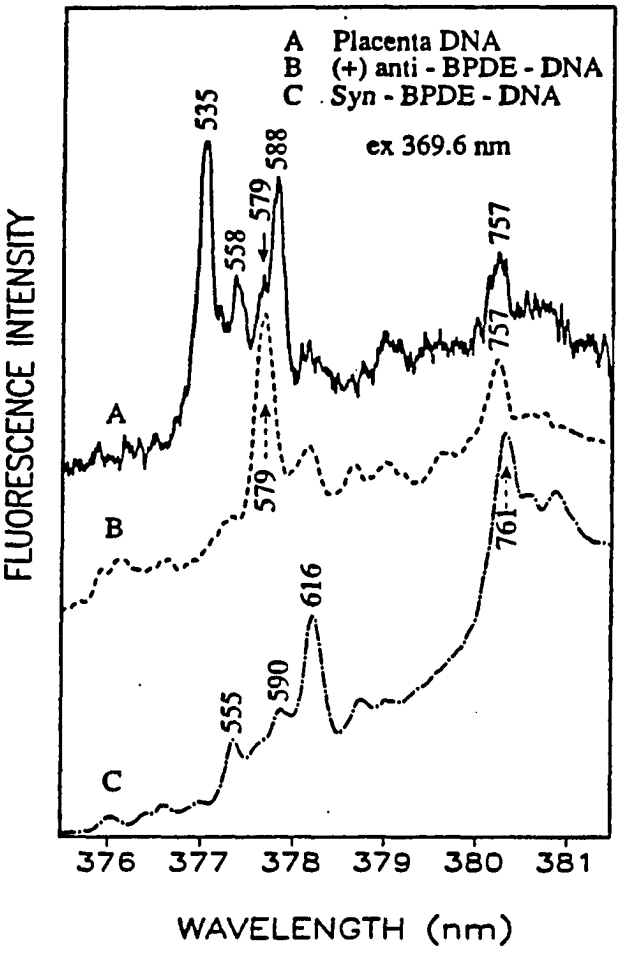

Figure 11. Comparison of the FLN spectra of the placental DNA adducts (A) with standard (+)- and syn-BPDE-DNA (B, C). All spectra obtained in the standard gly/H_2O glass at T = 4.2 K. λ_{ex} = 369.6 nm.

A: Placental DNA adducts; the samples were degased,
B: (+)anti-BPDE-DNA; ~ 1 adduct in $8x10^7$ bases,
C: Syn-BPDE-DNA; ~ 1 adduct in 10^7 bases

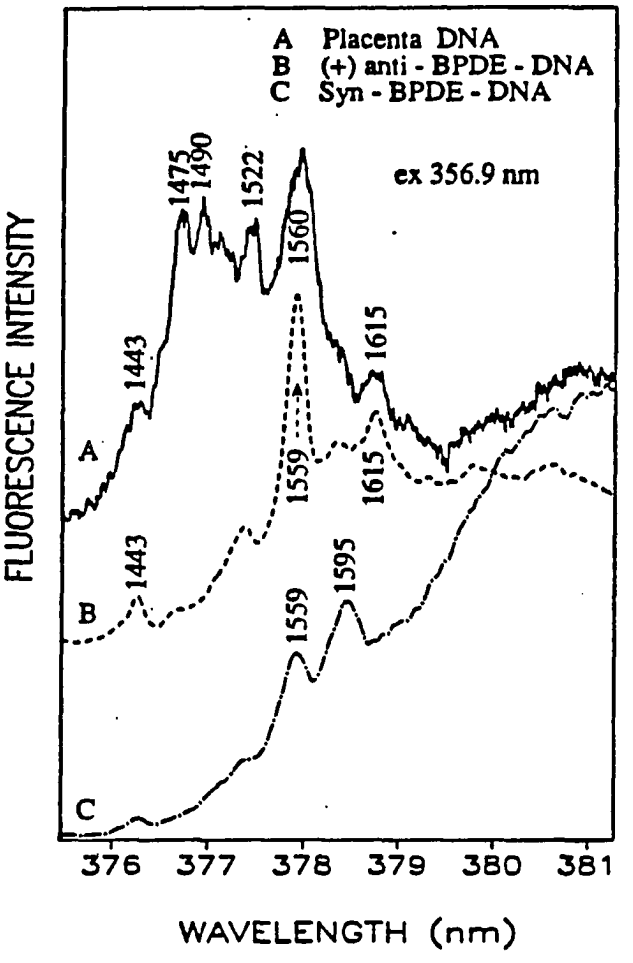

Figure 12. Comparison of the FLN spectra of the placental DNA adducts (A) with standard (+)- and syn-BPDE-DNA (B, C). All spectra obtained in the standard gly/H_2O glass at T = 4.2 K. λ_{ex} = 356.9 nm.

A: Placental DNA adducts; the samples were degased,
B: (+)anti-BPDE-DNA; ~ 1 adduct in $8x10^7$ bases,
C: Syn-BPDE-DNA; ~ 1 adduct in 10^7 bases

in the FLN spectra of the placenta samples obtained with different excitation wavelengths. Figure 12 shows the FLN spectra of the placenta sample and the standard BPDE-DNA samples obtained for λ_{ex} = 356.9 nm. The FLN spectra of BPDE adducts usually display strong vibronic modes under such an excitation, since their absorption extinction coefficients are large there. The typical bands (1559 cm^{-1} and 1615 cm^{-1}) of (+)-anti-BPDE-DNA can be readily recognized from the spectrum 12A. Analysis of the relative intensities and vibronic frequencies of the spectral bands of syn-BPDE-DNA shows that the placenta samples do not contain any notable amount of syn-BPDE-DNA adducts. Since the major vibronic modes of the placenta DNA adducts and (+)-anti-BPDE-DNA have very similar vibrational frequencies, they may contain the same kind of fluorescence chromophore. In this study, FLNS also exhibits high selectivity, since it directly identifies (+)-anti-BPDE-DNA adducts in the human placenta samples. In addition, FLNS has sufficient resolution to distinguish these structurally closely-related DNA adducts. Careful analysis of spectrum 12A can find a small band with the vibronic frequency of 1443 cm^{-1}. Since a typical vibronic mode of free BP tetraols has the same frequency, the sample may contain small amount of free BP tetraols. This assumption has been confirmed by our broad fluorescence experiments and will be discussed later.

Fluorescence spectra were also acquired at 77K to characterize the fluorescent chromophores of the placental DNA adducts. Figure 13A displays the fluorescence spectrum of the placental sample obtained with λ_{ex} = 346.0 nm. Since the excitation selected lies close to the absorption maximum of the covalently-bound BPDE adducts and free BP tetraols, the laser selectively excites these

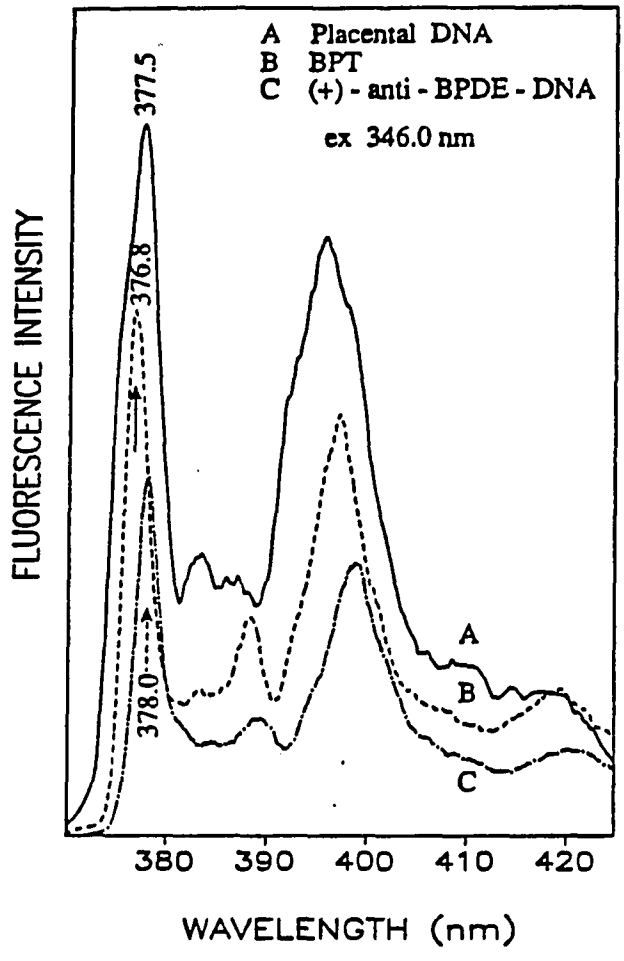

Figure 13. Laser-excited fluorescence spectra. Placental DNA adducts (A), BP tetraols (B) and (+)anti-BPDE-DNA (C). Gate delay (GD) = 30 nsec, T = 77 K, and λ_{ex} = 346 nm

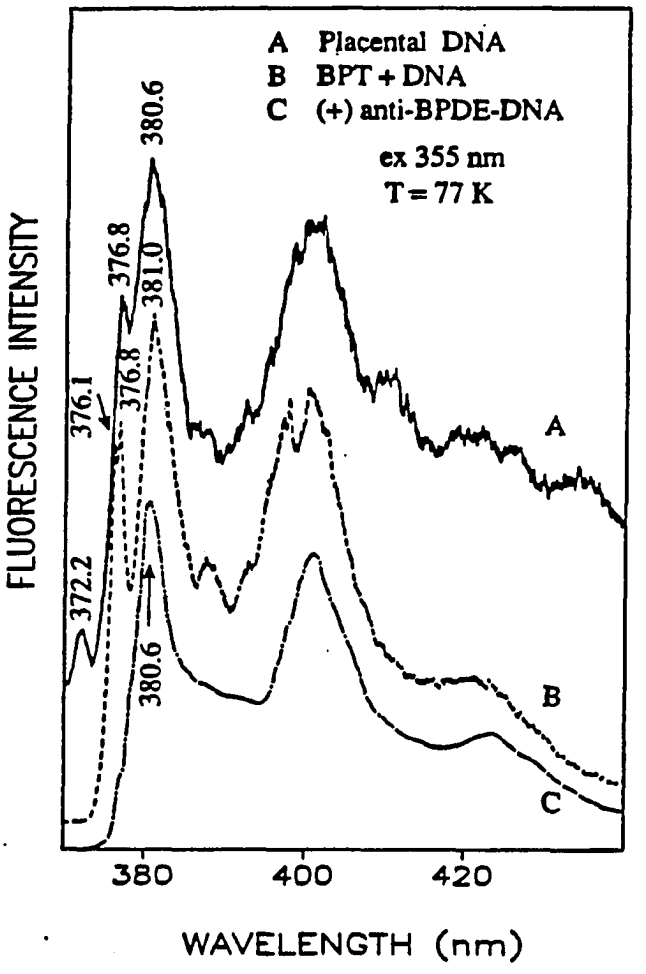

Figure 14. Laser-excited fluorescence spectra. Placental DNA adducts (A), (BP tetraol + DNA) mixture (B) and (+)anti-BPDE-DNA (C). Gate delay (GD) = 30 nsec, T = 77 K, and λ_{ex} = 355 nm

chromophores. The broad, irregular shape of the fluorescence origin band implies that the placental DNA contains more than one kind of adduct. The fluorescence origin of the placenta DNA adducts is located at ~ 377.5 nm, and the spectral shape is similar to those of BP tetraols and (+)-anti-BPDE-DNA (shown in Figures 13B and 13C). These spectral characteristics suggest that the major adduct of placental DNA contain a pyrene chromophore which is derived from the metabolism of BaP through the monooxygenation pathway. The R-value calculated for this adduct is ~1.6, which shows that the major placental DNA adduct arises from a covalently-bound adduct. This argument is consistent with the results of HPLC/SFS and GC/MS, in which BPDE adduct has been detected in the placental DNA samples at an adduct level amounting to 580 pg (110). Percentage of samples found to have the adducts by these different techniques is also very similar.

Laser excitation at 355.0 nm selectively excites intercalated BPDE adducts. The pertinent spectrum of the placental DNA is shown in Figure 14A, and the spectra of a (BPT + DNA) mixture and (+)-anti-BPDE-DNA are shown in Figure 14B and 14C, respectively. The spectrum of (BPT + DNA) mixture displays two small peaks appearing at 376.1 and 376.8 nm, respectively, which have recently been proved to arise from free *trans*- and *cis*- BP tetraols (111). The broad peak (at ~381-nm) of the (BPT + DNA) mixture arises from "quasi-intercalated" tetraols and which are subject to severe quenching by acrylamide. The R-value calculated from this band is 1.36. One small peak of the placental spectrum appears at 376.8-nm. The placenta DNA apparently contains a small amount of free BP tetraols which is consisted with the result obtained from the FLN experiment. The major origin band of the placenta DNA spectrum is located at ~380.6 nm, which is very

close to that of the intercalated adducts (+)3. The R-value calculated for the (+)3 adduct is ~ 1.15, whereas for the placenta adduct it is ~ 1.25. Since the fluorescence origin band of the placenta DNA spectrum is broader than that of (+)3 and its R-value is higher, the placenta DNA also contains a certain amount of intercalated BP tetraols and possible BPT photoproducts (*cf.* Appendix B). This argument can be further confirmed by performing fluorescence quenching experiment, for example, using acrylamide. Besides, the existence of a narrowing band 757 cm^{-1} in the FLN spectrum 11A of the placental sample provides additional evidence that placenta DNA contains a certain amount of (+)2 adducts.

The broad fluorescence spectrum 14A of the placenta DNA contains a small peak at ~372.2 nm. Since neither BaP nor BPDE metabolites were found to have a fluorescence origin band in this region, different type of adduct is present in the placenta DNA sample. For ease of discussion, this adduct will be designated as adduct A. The FLN spectra obtained for adduct A are presented in Figure 15. The vibronic frequencies of adduct A do not correlate with those of the BPDE adduct, which also shows that they do not arise from the same fluorescence chromophore. In addition, even though the broad fluorescence origin band of adduct A is a small peak in spectrum 14A, its corresponding ZPL bands are much stronger than those of the BPDE-DNA adducts. This means that the adduct A has either a small electron-phonon coupling efficiency or a great molar absorption extinction coefficient in the excitation region. Adduct A may arise from metabolites of BF and DBA. This will be discussed in detail later.

As a result, using laser-excited fluorescence spectroscopy, four kinds of BaP metabolites can be detected in the women's placental DNA samples, and three of

these can be characterized. They are (1) (+)-anti-BPDE-DNA adducts, (2) BP tetraols, and (3) intercalated BPDE adducts. The major adduct can be identified as a covalently-bound adduct having a pyrene chromophore, but it is neither anti- nor syn-BPDE-DNA formed *in vitro*. From the above analysis, we may conclude that the metabolic activation of BaP in human tissue (placenta) occurs primarily through the monooxygenation pathway.

2. Carcinogenesis study in fish exposed to several widespread environmental carcinogens *in vivo*

Searching for the chemical origins of the placenta DNA adducts leads to the fish DNA sample (English sole). The characterization of the fish DNA adducts may reveal the initial metabolic processes of the chemical carcinogens, since fish may be relatively inefficient at repairing DNA adducts (47, 48). English sole were exposed to benzo[a]pyrene, benzo[b]fluoranthene (BF), and dibenz[a,h]anthracene (DBA). BF is a chemical carcinogen and a widespread environmental pollutant, which has been detected in gasoline engine exhaust, urban air, cigarette smoke condensate, coal tar, soil, drinking water, and various foods (112). The levels of BF in the environment sometimes exceed those of BaP (112). Dibenz[a,h] anthracene is one of the major PAHs present in cigarette smoke and is also a significant environmental pollutant (113). DBA is a potent chemical carcinogen which was found able to induce a variety of neoplasms. Therefore, selection of these three widespread environmental carcinogens has a general significance in the carcinogenesis research of humans and animals exposed to the contaminants.

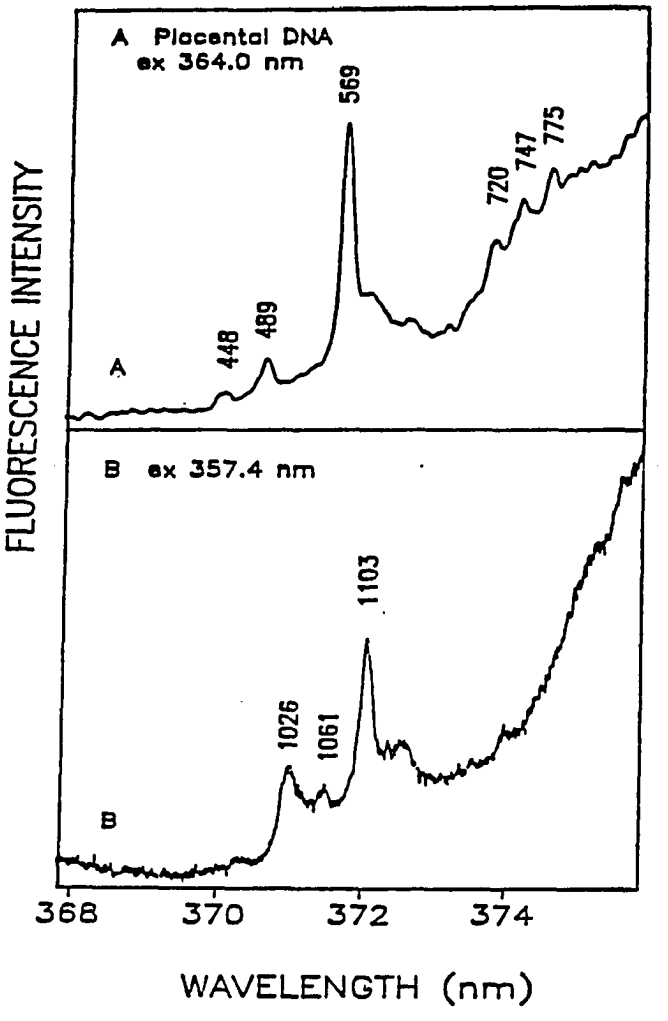

Figure 15. The FLN spectra of the placental DNA adducts under excitation of λ_{ex} = 364.0 nm (A), and λ_{ex} = 357.4 nm (B)

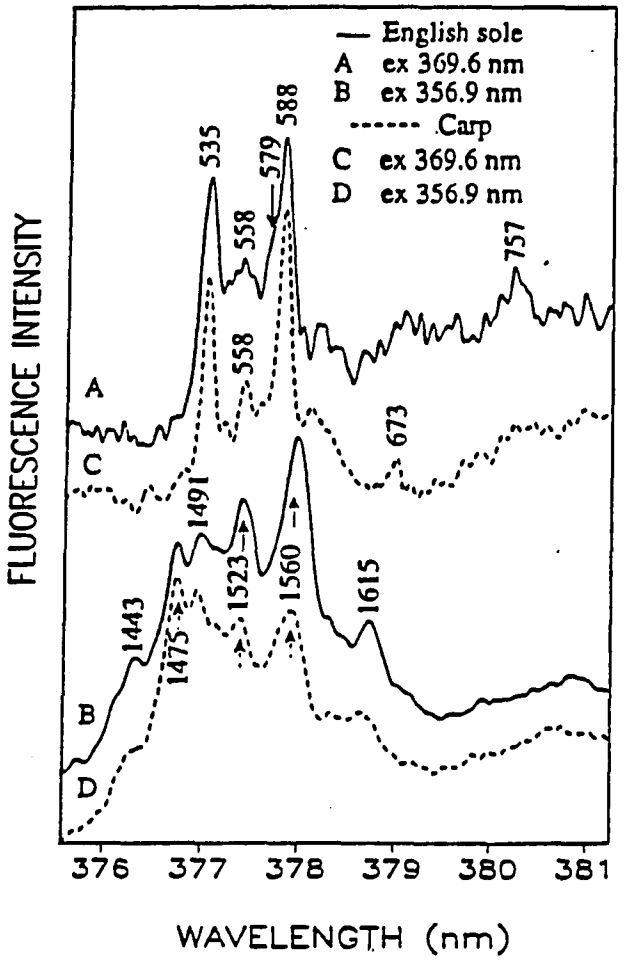

Figure 16. The FLN spectra of the fish DNA adducts with two different excitation wavelengths at T = 4.2 K.

English sole exposed to BaP, BF, and DBA;
A: λ_{ex} = 369.6 nm,
B: λ_{ex} = 356.9 nm,

Carp from the Buffalo River;
C: λ_{ex} = 369.6 nm,
D: λ_{ex} = 356.9 nm

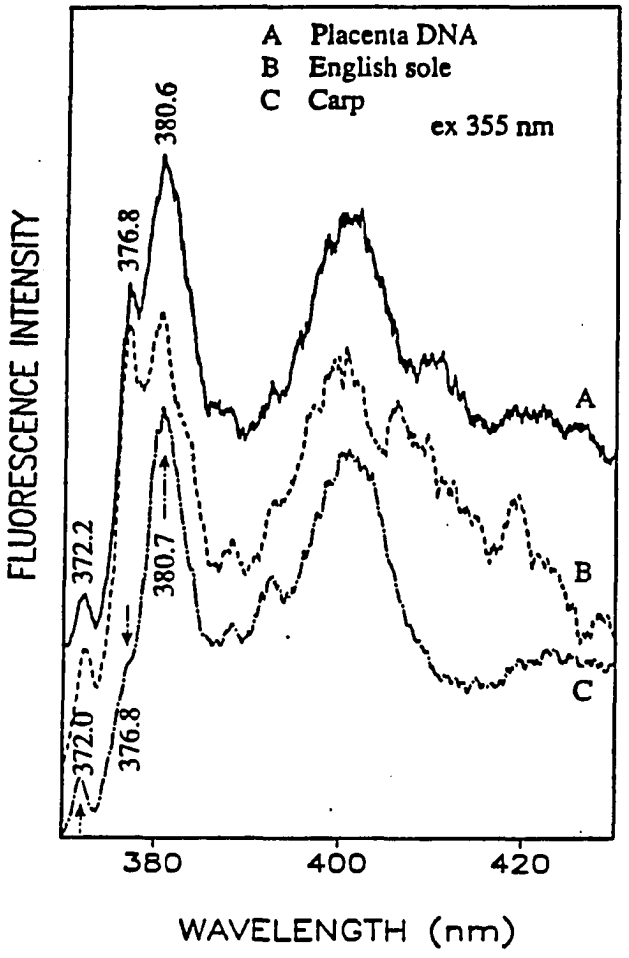

Figure 17. 77 K laser-excited fluorescence spectra at λ_{ex} = 355 nm. Placental DNA adducts (A), the DNA adducts of the English sole exposed to BaP, BF, and DBA *in vivo* (B), and the DNA adducts of the carp from Buffalo River (C). GD = 30 nsec

The FLN spectra of English sole obtained using two different excitation wavelengths are shown in Figures 16A and 16B. The ZPL characteristic of the (+)-anti-BPDE-DNA can be readily identified in the FLN spectra obtained for the English sole DNA sample with the vibrational frequencies of 579, 757, 1559, and 1615 cm^{-1}, but none is a major band. Therefore, (+)-anti-BPDE-DNA constitutes only a minor portion of the adducts present in the English sole sample. Surprisingly, the FLN spectra of the English sole DNA sample are very similar to those of the placenta DNA. The adducts in the fish DNA have the same chemical structures and conformations as those found in the human placenta DNA. This indicates that the carcinogens experience the same metabolic pathways in fish as in humans. The major adduct in fish is neither anti- nor syn-BPDE-DNA formed *in vitro*, but can be identified as containing a pyrene chromophore, as is the case for the placental DNA adduct. The major adduct which forms in English sole exposed to a mixture of carcinogens was found by FLNS to be different from that when the fish is exposed to BaP only. The results of this study show that co-existing substance effects play a very important role in metabolic activations of BaP in human and animal systems.

Figure 17B presents one of the 77K fluorescence spectra of the English sole DNA sample obtained for λ_{ex} = 355.0 nm. The fish DNA spectrum is very similar to the corresponding placental DNA spectrum (Figure 17A). The broad peak at ~380.5 nm shows that the fish DNA contains a certain amount of intercalated BPDE adducts, tetraols, and/or possible photoproducts. A small peak from free BP tetraols is located at ~ 376.8 nm. Note that the English sole DNA spectrum also contains a small peak at ~ 372.2 nm, so does the carp spectrum. The pertinent

FLN spectra of the English sole DNA sample are presented in Figure 18, which shows that the major vibronic modes have the same vibrational frequencies observed in the placenta DNA spectra (Figure 15), with a similar intensity distribution. The adduct A can be identified in the fish sample. Based on the knowledge of the chemical carcinogens which the fish were exposed to, the adduct A is presumed to arise from metabolites of either DBA or BF. Further experiments involving the analysis of DNA samples exposed to BF and DBA *in vitro* or *in vivo* are necessary to characterize the chemical structure of adduct A.

This study has shown that fish exposed to three different chemical carcinogens developed the same DNA adducts as those present in human placenta DNA, and thus we propose that the metabolic activations of BaP with the co-existing carcinogens in the fish are the same as in the human placenta. The placenta DNA adducts identified by our fluorescence experiments are originated from three widespread environmental pollutants BaP, BF, and DBA. The results of this study may support the hypothesis that bottom-feeding fish species exhibit increased frequencies of neoplasms, and thus, may serve as early warning indicators of carcinogenic hazards to man. Finally, this study points out the significance of using a mixture of widespread environmental carcinogens in carcinogenesis research.

3. Characterization of the DNA adducts of the fish from contaminated areas

Several fish species from different contaminated areas were collected, and the fish liver DNA was extracted and subsequently analyzed by FLNS. Figures 16C and 16D show two of the FLN spectra of the DNA sample of carp captured from

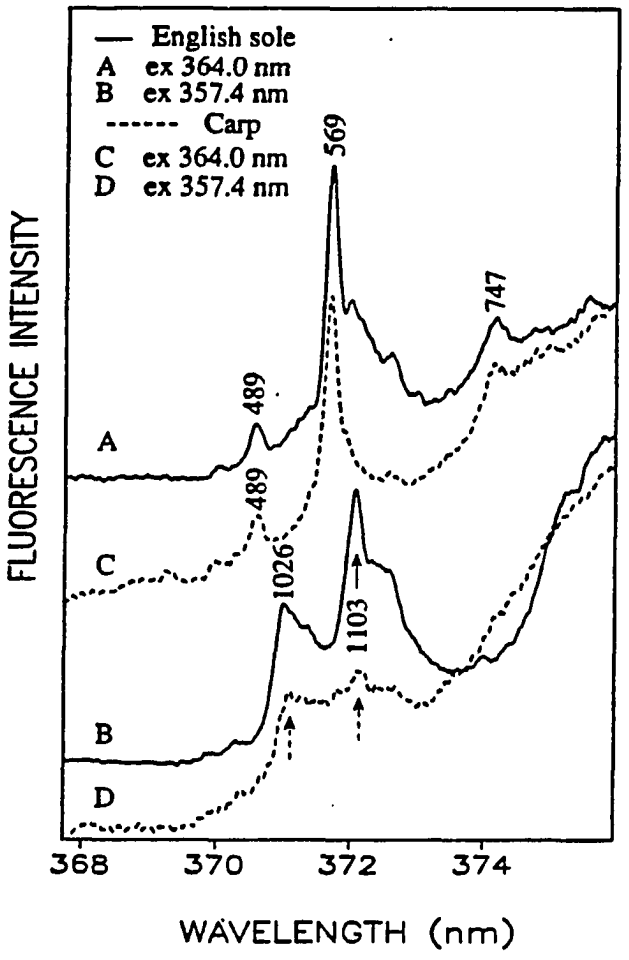

Figure 18. The FLN spectra of the fish DNA adducts with two different excitation wavelengths at T = 4.2 K.

English sole exposed to BaP, BF, and DBA *in vivo*;
A: λ_{ex} = 364.0 nm,
B: λ_{ex} = 357.4 nm,

Carp from the Buffalo River;
C: λ_{ex} = 364.0 nm,
D: λ_{ex} = 357.4 nm

the Buffalo River. The spectra of carp DNA are very similar to those of placental DNA by comparison of Figure 16C and 16D with Figure 11A and 12A, which show that the major DNA adducts in carp DNA sample are the same as those found in the placental DNA and the English sole DNA samples. Since the carp spectra do not show any noticeable ZPL with vibrational frequencies of 579, 757, and 1615 cm^{-1}, the carp DNA sample contains much less (+)-anti-BPDE-DNA adduct. In such cases, the amount of free tetraols in the carp DNA sample is also expected to decrease. The FLN spectrum 16D of the carp DNA sample shows that the free tetraol band 1443 cm^{-1} is very weak. The broad fluorescence spectrum of the carp DNA sample was obtained with λ_{ex} = 355 nm and is shown in Figure 17C. In this spectrum, the free tetraol peak (~ 376.8 nm) is apparently much lower than that in the corresponding spectra of the placenta DNA and the English sole DNA. The pertinent broad fluorescence origin band (~ 380.5 nm) in the spectrum shown in Figure 17C is also narrower, which means that carp DNA contains less intercalated tetraols. The observation that the carp liver DNA contains much less of potent carcinogenic species, (+)-anti-BPDE-DNA, than does English sole is very interesting, since English sole exhibit a high prevalence of liver neoplasms, while carp rarely develop cancer.

The origin band of adduct A can also be recognized in the fluorescence spectrum of the carp DNA sample shown in Figure 17D, and the pertinent FLN spectra of carp DNA are presented in Figures 18C and 18D, which provide additional evidence to confirm the presence of adduct A in the carp DNA sample.

This study, using different fish species, has shown that fish (carp) from a contaminated area develop the same major DNA adducts as those found in human

tissues. Also, the chemical carcinogens in carp undergo similar metabolic pathway as in the human systems. Therefore, the research using fish species is very important in the study of environmental exposure of chemical carcinogens to human beings. The use of a mixture of several widespread carcinogens may have a general significance in carcinogenesis research of *in vitro* and *in vivo* systems. BaP, BF, and DBA are very important environmental pollutants, worthy to be further investigated.

4. Conclusions

For the first time, (+)-anti-BPDE-DNA adduct has been directly detected by FLNS in the DNA from women's placental samples. Laser-excited fluorescence spectroscopy has also identified intercalated BPDE adducts and a small amount of free tetraols in the placental DNA. The major adduct of the placental DNA can be identified as a covalently bound adduct having a pyrene chromophore, but it is neither anti- nor syn-BPDE-DNA formed *in vitro*. The fact that the major adduct in placental DNA has a BPDE chromophore is consistent with the results of HPLC/SFS and GC/MS, in which the BPDE adduct has been detected in the placental samples at an adduct level amounting to 580 pg. Moreover, laser fluorescence spectroscopy has revealed another adduct having fluorescence origin at 372.2 nm. Further experiments are needed to characterize its specific chemical structure. The chemical origins of these adducts can be determined arising from three widespread environmental carcinogens: benzo[a]pyrene, benzo[b]fluoranthene, and dibenz[a,h]anthracene. The metabolic activations of BaP in the human body are mainly through the monooxygenation pathway.

This study determines that two different fish species (English sole and carp), when exposed to the three carcinogens *in vivo* and in a contaminated area, respectively, develop the same major DNA adducts as those which form in human tissue. However, the carp DNA contains much less of the potent carcinogenic species, (+)-anti-BPDE-DNA than do English sole DNA. This observation is very interesting since English sole exhibited a high prevalence of liver neoplasms (44, 45, 53), while carp rarely developed cancer (50). When English is sole exposed to BaP only, the major adduct which forms is are either syn- or anti-BPDE-DNA adducts. However, when the fish is exposed to a mixture of carcinogens (BaP, BF, and DBA), the major adduct is neither syn- nor anti-BPDE-DNA formed *in vitro*. Therefore, this study reveals that the formation of the major adduct resulting from exposure to BaP in humans and fish is closely associated with the interactions of the co-existing carcinogens, which plays a very important role in the metabolism of BaP in humans and fish. The results of this study indicate that these carcinogens experience the same metabolic pathways in fish and in the human body, which provides direct evidence to support the hypothesis that bottom-feeding fish species may serve as early warning indicators of carcinogenic hazards to man. Therefore, it is very significant to use fish species to study the environmental exposure of humans. Finally, this study points out that the use of a mixture of several widespread carcinogens may have general significance in carcinogenesis research.

This study shows that laser-excited fluorescence spectroscopy is a very powerful bioanalytical approach to determine macromolecular damage of the tissues of humans and animals exposed to widespread environmental pollutants.

V. LITERATURE CITED

1. Osborne, M. R. and Crosby, N. T. (1987). Benzopyrenes; Cambridge University Press: New York.
2. Dipple, A. (1985). In Polycyclic Hydrocarbons and Carcinogens; Harvey, R. G. Ed.; American Chemical Society: Washington, D.C., 1-17.
3. Doll, R. & Peto, R. (1981). J. Natl. Cancer Inst., 66: 1191-1308.
4. Baum, E. J. (1978). In "Polycyclic Hydrocarbons and Cancer"; Gelboin, H. V.and Tso, P.O.P., Eds.; Academic Press: New York, 1: 45-62.
5. "Particulate Polycyclic Organic Matter," (1972). National Academy of Sciences, Washington, D. C.
6. Huggins, G. C. B. (1979). Experimental Leukemia and Mammary Cancer; University of Chicago Press: Chicago.
7. Gräslund, A. and Jernström, B. (1989). Quarterly Reviews of Biophysics, 22: 1-37.
8. Adamson, E. D. (1987). Development, 99: 449-471.
9. Nishimura, S. and Sekiya, T. (1987). Biochem. J., 243: 313-327.
10. Vousden, K. H., Bos, J. L., Marshall, C. J. and Phillips, D. H. (1986). Proc. Natl. Acad. Sci., USA, 83: 1222-1226.
11. Marshall, C. J., Vousden, K. H. and Phillips, D. H. (1984). Nature, 310: 586-589.
12. Stevens, C. W., Manoharan, T. H., and Fahl, W. E. (1988). Proc. Natl. Acad. Sci., USA, 85: 3875-3879.
13. Miller, J. A. (1970). Cancer Res., 30: 559-576.

14. Conney, A. H. (1982). Cancer Res., 42: 4875-4917.

15. Thakker, D. R., Yagi. H., Levin, W., Wood, A. W., Conney, A. H., and Jerina, D. M. (1985). In Bioactivation of Foreign Compounds; Anders, M. W., Ed.; Academic Press: New York, 177-242.

16. Singer, B. and Grunberger, D. (1983). Molecular Biology of Mutagens and Carcinogens; Plenum: New York.

17. Harvey, R. G. and Geacintov, N. W. (1988). Accounts of Chemical Research, 21: 66-73.

18. Gelboin, H. V. (1980). Physiol. Rev. 60: 1107-1166.

19. Cooper, C. S., Crover, P. L. and Sims, P. (1983). Prog. Drug Metab., 295-390.

20. Glatt, H., Seidel, A., Bochnitschek, W., Marquardt, H., Hodgson, R. M., Grover, P. L. and Oesch, F. (1986). Cancer Res., 46: 4556-4565.

21. Lehr, R. E., Kumar, S., Levin, W., Wood, A. W., Chang, R. L., Conney, A. H., Yagi. H., Sayer, J. M. and Jerina, D. M. (1985). In Polycyclic Hydrocarbons and Carcinogenesis; Harvey, R. D. Ed.; American Chemical Society: Washington, D.C., 63-85.

22. Jerina, D. M. and Lehr, R. E. (1978). In Microsomes and Drug Oxidations, Ulrich, V. Roots, I. Hilderbrandth and Estabrook, Eds.; Pergaman Press: Elmsford, New York, 709-720.

23. Bresnick, E., Stoming, T. A., Vaught, J. B., Thakker, D. R. and Jerina, D. M. (1977). Arch. Biochem. Biophys., 183: 31-37.

24. Brooks, P. and Osborne, M. R. (1982). Carcinogensis, 3: 1223-1226.

25. Stevens, C. W., Bouek, N., Burgess, J. A., and Fahl, W. E. (1985).

Mutat. Res., 152: 514.

26. Burgess, J. A., Stevens, C. W., and Fahl, W. E. (1985). Cancer Res., 45: 4257-4262.
27. Geocintov, N. E., Yoshida, H., Ibanez, V., and Harvey, R. G. (1981). Biochem. Biophys. Res. Commun., 100: 1569-1577.
28. Geocintov, N. E., Ianez, V., Gagliano, A. G., Yoshida, H., and Harvey, R. G. (1980). Biochem. Biophys. Res. Commun., 92: 1335-1342.
29. Kootstra, A., Haas, B. L. and Slaga, T. J. (1980). Biochem. Biophys. Res. Commun., 94: 1432-1438.
30. Geocintov, N. E., Ibanez, V., Benjamin, M. J., Hibshoosh, H. and Harvey, R. G. (1983). In Polynuclear Aromatic Hydrocarbons; Cooke, M. and Dennis, A. J., Eds.; Battelle Press: Columbus, Ohio, 554-570.
31. Geocintov, N. E., Hibshoosh, H., Ibanez, V., Benjamin, M. J. and Harvey, R. G. (1984). Biophys. Biochem., 20: 121-133.
32. Geocintov, N. E. (1985). In Polycyclic Hydrocarbons and Carcinogenesis; Harvey, R. G. Ed., American Chemical Society: Washington, D.C., 107-124.
33. Geocintov, N. E. (1988). In Polycyclic Aromatic Hydrocarbon Carcinogenesis: Yang, S. and Silverman, B. D., Eds.; CRC Press: Boca Raton, FL, 181-206.
34. Kim, M., Geocintov, N. E., McQuillen, D., Pope, M. and Harvey, R. G. (1986). Carcinogenesis, 7: 41-47.
35. Kim, M., Geocintov, N. E., Pope, M. and Harvey, R. G. (1984). Biochemistry, 23: 5433-5439.

36. Osborne, M. R., Jacobs, S., Harvey, R. G. and Brooks, P. (1981). Carcinogenesis, 2: 553-558.

37. Underman, O., Sahlin, M,, Gräslund, A., Ehrenberg, A., Jernström, B., Tjerneld, F. and Norden, B. (1983). Cancer Res., 43: 1851-1860.

38. Zinger, D., Geocintov, N. E. and Harvey, R. G. (1987). Biophysical Chemistry, 27: 131-138.

39. Bigger, C. A. H., Sawicki, J. T., Blake, D. M., Raymond, L. G. and Dipple, A. (1983). Cancer Res., 43: 5647-5651.

40. Dipple, A., Sawicke, J. T., Moschel, R. C. and Bigger, C. A. H. (1983). In Extrahepatic Drug Metabolism and Chemical Carcinogenesis; Rydström, J., Montelius, J. and Bengtsson, Eds.; Amsterdam: Elsevier, 439-448.

41. DiGiovanni, J., Sawyer, T. W., and Fisher, E. P. (1986). Cancer Res., 46: 4336-4341.

42. Black, J. J. (1983). J. Great Lakes Res., 9: 326-334.

43. Fallon, M. E., and Horvath, F. J. (1985). J. Great Lakes Res., 11: 373-398.

44. Malins, D. C., McCain, B. B., Brown, D. W., Chan, S.-L., Myers, M. S., Landahl, J. T., Prohaska, P. G., Friedman, A. J., Rhodes, L. D., Burrows, D. G., Gronlund, W. D. and Hodgins, H. D. (1984). Environ. Sci. Technol., 18: 705-713.

45. Myers, M. S., Rhodes, L. D. and McCain, B. B. (1987). J. Natl. Cancer. Inst., 78: 333-363.

46. Dawe, C. J., Stanton, M. F. and Schwarts, F. J. (1964). Cancer Res., 24: 1194-1201.

47. Varanasi, U., Stein, J. E. and Hom, T. (1981). Biochem. Biophys. Res.

Commun., 103: 780-787.

48. Walton, D. G., Acton, A. B. and Stich, H. F. (1984). Cancer Res., 78: 6126-6129.
49. McCain, B. B., Myers, M. S., Varanasi, U., Brown, D. W., Rhodes, L. D., Gronlund, W. D., Elliot, D. G., Palsson, W. A., Hodgins, H. O., and Malins, D. C. (1982). In Federal Interagency Energy/Environment Research and Development Report; Environmental Protection Agency, Washington, D. C.: EPA-600/7-82-001: 1-100.
50. Dr. C. Schmidt, National Fisherry Research Laboratory, NFCRC, Missouri. Private Communication.
51. Hendricks, J. D., Meyers, T. R., Shelton, D. W., Casteel, J. L. and Bailey, G. S. (1985). J. Natl. Cancer Inst., 74: 839-852.
52. Bailey, G. S., Hendricks, J. D., Nixon, J. E. and Pawlowski, N. E. (1984). Drug Metab. Rev., 15: 725-750.
53. Varanasi, U., Reichert, W. L. and Stein, J. E. (1989). Cancer Res., 49: 1171-1177.
54. Schiewe, M. H., Landahl, J. T., Myers, M. S., Plesha, P. D., Jacques, F. J., Stein, J. E., McCain, B. B., Weber, D. D., Chan, S.-L. and Varanasi, U. (1988). In Proc. First Annual Mtg. on Puget Sound Research; Puget, 55-64.
55. Varanashi, U., Reichert, W. L., Eberhart, B-T. L., and Stein, J. E. (1989). Chemico-Biological Interaction, 69: 203-216.
56. Smolarek, T. A., Baird, W. M., Morgan, S., Ferin, M., Nishimoto, M., Stein, J. E., Varanasi, U., and Klaunig, J. (1988). Prog. Am. Assoc. Cancer Res., 94.

57. Poirier, M. C. and Beland, F. A. (1986). Carcinogenesis and Adducts in Animals and Humans; Karger: New York.

58. Everson, R. B., Randerath, E., Avitts, T. A., Schut, H. A. J. and Randerath, K. (1987). Prog. Exp. Tumor Res., 31: 86-103.

59. Welch, R. M., Harrison, Y. E., Conney, A. H., Poppers, P. J. and Finster, M. (1968). Science, 160: 541-542.

60. Nebert, D. W., Winker and J. Gelboin, M. V. (1969). Cancer Res., 29: 1763-1769.

61. Wong, T. K., Everson, R. B. and Hsu, S. T. (1985). Carcinogenesis, 721-724.

62. Tomatis, L. (1979). Perinatal Carcinogenesis, National Cancer Institute Monograph 51, DHEW Publ. No. 79, Bethesda: 1633.

63. Everson, R. B. (1980). Cancer Res., 40: 123-127.

64. Everson, R. B., Randerath, E., Santella, R. M., Cetalo, R. C., Avitts, R. C. and Randerath, K. (1986). Science, 231: 54-57.

65. Everson, R. B., Randerath, E., Santella, R. M., Avittis, T. A., Weinstein, I. B. and Randerath, K. (1988). J. Natl. Cancer Inst., 80: 6-24.

66. Santella, R. M., Gasparo, F. and Hsieh, L. L. (1987). Prog. Exp. Tumor Res., 31: 62-75.

67. Weston, A., Trivers, G., Vahakangas, K., et. al. (1987). Prog. Exp. Tumor Res., 31: 76-85.

68. Personov, R. I. (1983). In Spectroscopy and Excitation Dynamics of Condensed Molecular Systems; Agranovich, V. M. and Hochstrassev, R. M., Eds.; North-Holland Publishing Co., New York, Chapter 10.

69. Brown, J. C., Hayes, J. M., Warren, J. A. and Small, G. J. (1981). In

Lasers in Chemical Analysis; Hieftje, G. M., Travis, J. C. and Lytle, F. E. Eds.; Humana Press, Inc., Clifton, New Jersey, Chapt. 21.

70. Personov, R. J., Alshits, E. I. and Bykovskaya, L. A. (1972). Opt. Commun., 6: 169.
71. Jankowiak, R., Lu, P. and Small, T. J. (1990). J. Pharm. Biomed. Anal., (in press).
72. Jankowiak, R., Cooper, R. S., Zamzow, D., Small, G. J., Doskocil, G. and Jeffrey, A. M. (1988). Chem. Res. Toxicol., 1: 60-68.
73. Hayes, J. M., Jankowiak, R. and G. J. Small. (1987). In Topics in Current Physics, Persistent Spectral Hole Burning: Science and Applications; Moore, B. Ed.; Academic Press: New York, 4: 31-53.
74. Jankowiak, R. and Small, G. J. (1987). Science, 237: 618-625.
75. Jeffrey, A. M. (1985). In Polycyclic Hydrocarbons and Carcinogenesis; Harvey, R. G. Ed.; American Chemical Society: Washington, D.C.; Chap. 8.
76. Weinstein, I. B., Jeffrey, A. M., Jennette, K. W., Blobstein, S. H., Harvey, R. G., Harris, C., Autrup, H., Kasai, H. and Nakanishi, K. 1976). Science, 193: 592-595.
77. Maugh, T. H. (1984). Science, 226: 1183-1184.
78. Report on DNA adducts workshop measurements subgroup. (1986). Oak Ridge National Laboratory; Oak Ridge, Tennessee.
79. T. Vo-Dinh and P. R. Martinez. (1981). Anal. Chem. Acta., 125: 13-19.
80. Heisig, V., Jeffrey, A. M., McGlade, M. J. and Small, G. J. (1984). Science, 223: 289-291.
81. McGlade, M. J., Hayes, J. M., Small, G. J., Heisig, V. and Jeffrey,

A. M. (1985). Anal. Spectroscopy, 6: 31-36.

82. Sanders, M. J., Cooper, R. S., Jankowiak, R., Small, G. J., Heisig, V. and Jeffrey, A. M. (1986). Anal. Chem., 58: 816-820.
83. Zamzow, D., Jankowiak, R., Cooper, R. S., Small, G. J., Tibbels, S. R., Cremonosi, P., Devanesan, P., Rogan, E. G. and Cavalieri, E. L. (1989). Chem. Res. Toxicol., 2: 29-34.
84. Jankowiak, R., Lu, P. and Small, G. J. (1990). Chem. Res. Toxicol., 3: 39-46.
85. Sanders, M. J., Cooper, R. S. and Small, G. J. (1985). Anal. Chem., 57: 1148-1152.
86. Jankowiak, R., Day, B. W., Lu, P., Doxtader, M. M., Skipper, P. L., Tannenbaum, S. R. and Small, G. J. (1990). Submitted to J. Amer. Chem. Soc.
87. Cooper, R. S. (1987). Ph.D. Dissertation, Iowa State University, Ames, Iowa.
88. Zamzow, D. S. (1988). M. S. Thesis, Iowa State University, Ames, Iowa.
89. Geacintov, N. E., Ibanez, V., Gagliano, A. G., Jacobs, S. A. and Harvey, R. G. (1984). J. Biomol. Struct. and Dynamics, 1: 1473-1484.
90. Geacintov, N. E., Yoshida, H., Ibanez, V., Jacobs, S. A. and Harvey, R. G. (1984). Biochem. Biophys. Res. Commun., 122: 33-39.
91. Varanasi, U. and Gmur, D. J. (1980). Biochem. Pharmacol., 29: 753-761.
92. Bender, W., Spiere, P. and Hogness, D. S. (1983). J. Mol. Biol., 168: 17-34.
93. Schnell, E. H., Gruger, E. H. and Malins, D. C. (1980). Xenobiotica, 10: 229-234.
94. Wallin, H. Jeffrey, A. M. and Santella, R. M. (1987). Cancer Letter, 35: 139-146

95. Harris, J. M., Lyle, F. E. and McCain, T. E. (1976). Anal. Chem., 48: 2095-2098.

96. Bartsch, H., Hemminki, K. and O'Neill, I. K., Eds. (1988). Methods for detecting DNA damaging agents in humans: Applications in Cancer Epidemiology and Prevention; IARC Scientific Publications: No. 89, Lyon.

97. Slaga, T. J., Bracken, W. J., Gleason, G., Levin, W., Yagi, H., Jerina, D. M. and Conney, A. H. (1979). Cancer Res. 39: 67-71.

98. Alexandrov, K., Sala, M. and Rojas, M. (1988). Cancer Res., 48: 7132-7139.

99. Phillips, D. H., Hewer, A. and Grover, P. L. (1985). Cancer Res., 45: 4169-4174.

100. Ireland, C. M., Eastman, A. and Bresnick, E. (1984). Carcinogenesis, 5: 187-191.

101. Moore, C. J., Pruess-Schwartz, D., Mauthe, R. J., Gould, M. N. and Baird, W. M. (1987). Cancer Res., 47: 4402-4406.

102. Kim. S. K., Geacintov, N. E., Brenner, N. C. and Harvey, R. G. (1989). Carcinogenesis, 10: 1333-1335.

103. Kim, S. K., Brenner, N. C., Soh, B. J. and Geacintov, N. E. (1989). Photochem. Photobiol., 50: 327-337.

104. Nakajima, A. (1971). Bull. Chem. Soc., Japan, 44: 3272-3277.

105. Glushko, V., Thaler, M. S. R. and Karp, C. D. (1981). Arch. Biochem. Biophys., 210: 33-42.

106. Kano, I., Gielen, J. E., Yagi, H., Jerina, D. M. and Nebert, D. W. (1977). Mol. Pharmacol, 13: 1181-1186.

107. Geacintov, N. E. (1987). Photochem. Photobiol., 45: 547-556.

108. Haarer, D. (1977). J. Chem. Phys., 67: 4076-4085.

109. Buening, M. K., Wislocki, P. G., Levin, W., Yogi, H., Thakber, D. R., Akagi, H., Koreeda, M., Jerina, D. M. and Conney, A. H. (1978). Proc. Natl. Acad. Sci., U.S.A., 75: 5358-5-362.

110. Conney, A. H. (1982). Cancer Res., 42: 4875-4917.

111. Hingerty, B. E. and Broyde, S. (1985). Biopolymers, 24: 2279-2299.

112. Amin, S., LaVoie, E. J. and Hecht, S. S. (1982). Carcinogenesis, 3: 1171-1174.

113. Lubet, R. A., Connolly, G. M., Nebert, D. W. and Kouri, R. E. (1983). Carcinogenesis, 4: 513-517.

VI. APPENDIX A. PAPER I. LASER SPECTROSCOPIC STUDIES OF DNA ADDUCT STRUCTURE TYPES FROM ENANTIOMERIC DIOL EPOXIDES OF BENZO[a]PYRENE

A. Abstract

A methodology based on 77 K laser-excited fluorescence spectroscopy, fluorescence quenching, and fluorescence line narrowing is shown to be a highly selective and sensitive approach for the study of polycyclic aromatic carcinogen-DNA complexes. Three and five different DNA adducts derived from (+)-trans-7,8-dihydroxy-anti-9,10-epoxy-7,8,9,10-tetrahydro-benzo[a]pyrene and its (-)-enantiomer are identified, respectively. Two different methods are used to classify the adducts as type I (interior) or type II (exterior), and both yield consistent results. The first high resolution fluorescence excitation spectra are reported for DNA adducts. These spectra are suggested to be useful for characterizing the strength of the interaction between the fluorescent chromophores and the DNA bases. The above methodology has the potential for monitoring the fates of different adducts as a function of time in repair-competent cells.

B. Introduction

The characterization and determination of nucleotide, nucleoside and macromolecular DNA adducts are important for understanding the initial phases of chemical carcinogenesis. Several biochemical, biophysical, and immuno-chemical methods have been developed (1). This work will show that a methodology based on 77 K laser-excited fluorescence spectroscopy, fluorescence quenching, and fluorescence line narrowing spectroscopy (FLNS) is a powerful approach for the study of macromolecular DNA adducts. The reactive metabolites (which form

covalent adducts with DNA) selected to test this methodology are (+)-trans-7,8-dihydroxy-anti-9,10-epoxy-7,8,9,10 tetrahydro-benzo[a]pyrene ((+)-anti-BPDE), and its enantiomer (-)-anti-BPDE. While the former is highly tumorigenic, the latter is not (2), although both form stable macromolecular DNA adducts (3, 4). The differences in their mutagenic and carcinogenic activities (5-8) are likely to be due, at least in part, to differences in DNA adduct structure (3). The extent to which the above methodology can be used to probe and classify the types of adducts formed from (+)- and (-)-anti-BPDE, is the principal focus of this work.

Considerable progress on the elucidation of structurally different types of adducts has been made by Geacintov et al. (9, 10) and Kim et al. (11, 12) who have used a variety of spectroscopic techniques, including fluorescence quenching. It has also been shown that low and room temperature spectra of the adducts were qualitatively similar (12). The BPDE-DNA adducts have been classified as type I or II (11, 12). For the type I sites identified the aromatic plane of pyrene (the parent fluorescent chromophore) appears to be nearly parallel (within ~25-30°) to the planes of the unmodified DNA bases. Such adduct sites may be viewed as interior (e.g., quasi-intercalated). Type II sites are characterized by a lower degree of interaction between the pyrenyl moiety and the bases and, therefore, may be viewed as exterior. As demonstrated by Geacintov et al. (9, 10), classification according to types I and II can be made on the basis of adduct accessibility to externally added fluorescence quenchers such as acrylamide. Such studies (11-13) have thus far identified only two types of adducts from each of the (+)- and (-)-anti-BPDE enantiomers. In this paper, the aforementioned methodology is used to identify, respectively, three and five adducts from these enantiomers. Two approaches are used to classify these adducts as type I or type II and are shown to yield consistent results. The first is based on fluorescence quenching, while the

second is based on the magnitude of the ratio (R) of the intensity of the fluorescence origin (0-0) band relative to the intensity of the prominent vibronic band - 1400 cm^{-1} lower in energy. For pyrenyl chromophores this ratio has been shown to be sensitive to the polarity of the microenvironment of the chromophore (14-16). Kim et al. (12) have recently used R-values to classify BPDE-DNA adducts as type I or type II.

The improved resolution of the fluorescence spectra (77 K) reported here is due primarily to the utilization of narrow line laser excitation at wavelengths chosen for optimum selectivity. High resolution 4.2 K line narrowed spectra provide important complementary data for classification of adducts as type I and type II. In particular, it is demonstrated that the degree of interior binding (strength of coupling between the pyrenyl-chromophore and the DNA bases) is accompanied by an increase in the transition electron-phonon coupling strength. A possible mechanism for this correlation is suggested.

C. Experimental

1. Instrumentation

The underlying principles of FLNS and the associated instrumentation have been described in detail in several papers (17-20) and, thus, will not be reviewed here. Laser excited fluorescence spectra at 77 K, obtained under non-line-narrowing conditions ($S_2 \leftarrow S_0$ excitation) and excitation spectra (T = 4.2 K), were measured using a SRS Model SR280 boxcar averager equipped with two Model SR250 processor modules for channel A and B. Channel A was used to monitor the fluorescence signal, while channel B was used to monitor the pulse to pulse intensity jitter of the excimer pumped dye laser. All spectra reported were normalized for pulse jitter. The boxcar averager was interfaced through a SR245

computer interface module with a PC compatible computer for data acquisition and analysis.

2. Glasses

The glass-forming solvent used was a mixture consisting of 50% glycerol, 40% water, and 10% ethanol by volume. Quartz tubing (3 mm o.d. x 2 mm i.d. x 2 cm) sealed at one end was used to contain samples (~ 30 μl total volume). Experiments were performed with a double-nested 5 L glass liquid helium dewar equipped with quartz optical windows and designed to have no liquid nitrogen in the optical pathways (18). For 77 K studies, the same dewar was filled with liquid nitrogen. FLN and excitation spectra were obtained with the samples immersed in liquid helium, T = 4.2 K. Fluorescence spectra obtained under non-line-narrowing conditions were obtained at 77 K.

3. Materials

Calf thymus DNA was purchased from Worthington Chemicals (Freehold, NJ). The DNA was prepared and reacted with (+)-anti-BPDE or (-)-anti-BPDE as previously described by Geacintov (21). The BPDE enantiomers were purchased from the National Cancer Institute Chemical Carcinogen Reference Standard Repository.

The modification levels of the (+)- and (-)-anti-BPDE adducts studied were 0.5% bases and 1.5% bases modified, respectively. The adducts were diluted in the glass forming solvent to a concentration (pyrenyl chromophores) of ~ 10^{-5} M. To preclude the possibility of erroneous assignments of spectral features of the tetraol of BPDE (BPT, a photo-degradation product of the DNA adducts) to DNA adducts, comparison spectra for (BPT + DNA) mixture were routinely obtained (spectra not

shown). The physical mixture was employed because it was determined that the energies of the S_1 (lowest excited singlet) fluorescence origins for free BPT in the glass and the DNA mixture in the glass were slightly different. For the fluorescence quenching studies, acrylamide (ACR) was employed at a concentration of ~ 1 M, an optimal concentration in such studies (13).

D. Results and Discussion

In this section data are presented which establish that three and five DNA adducts are formed from (+)-anti-BPDE and (-)-anti-BPDE, respectively. The adducts will be designated by (+)1-3 and (-)1-5. The convention adopted is that the S_1 state energy (energy of the fluorescence origin) decreases with increasing number associated with the (+) or (-) adduct label. Since the order in which the adducts are identified does not correlate with these numbers, the reader may find it useful to refer to Table I before proceeding. This table lists the fluorescence origin wavelengths for the different DNA adducts as determined from the 77 K fluorescence spectra obtained with $S_2 \leftarrow S_0$ laser excitation. Each adduct is classified as type I or type II in the table.

1. Absorption spectra

The absorption spectra of (+)-anti-BPDE-DNA adducts and benzo(a)pyrene-tetraol (BPT) are presented in Figure 1. The absorption spectrum of (+) adducts is red shifted (~ 2-3 nm) with respect to the absorption peak of BPT and exhibits a broad tail beyond 350 nm which is not observed for BPT. For the (-)-anti-BPDE-DNA adducts, the absorption spectrum is more diffuse and considerably red shifted, indicating that the (-) adducts may be more heterogeneous.

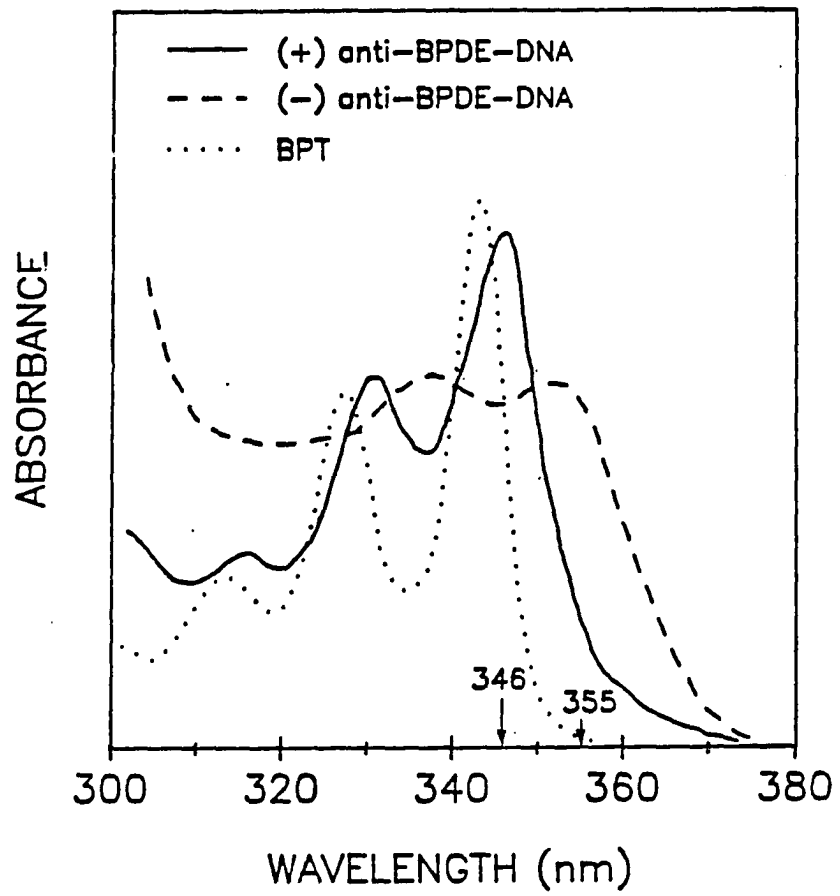

Figure 1. Typical absorption spectra at room temperature. —— : (+)anti-BPDE-DNA adducts, 1.3 μM of bound chromophores, 0.26 mM DNA base concentration. ---: (-)anti-BPDE-DNA adducts, 0.8 μM bound chromophores and 0.26 mM DNA base concentration. ····: BPT (2.4 μM), in buffer. Excitation wavelengths of 346 and 355 nm are indicated

2. Laser-exited fluorescence spectra at 77 K

In this subsection, we explore the utility of 77 K fluorescence spectra obtained with $S_2 \leftarrow S_0$ excitation for the distinction between macromolecular adducts derived from (+)-anti-BPDE and (-)-anti-BPDE, and the different binding configurations associated with a given enantiomer. In this regard, it will become apparent that the origin or (0,0) transitions of the $S_1 \rightarrow S_0$ fluorescence spectra are particularly useful. Although $S_2 \leftarrow S_0$ excitation precludes line narrowing, and thermal broadening at 77 K is significant, the relatively broad fluorescence spectra still provide very useful information. In the following subsection, fluorescence quenching and FLN data are used to provide additional insights on the heterogeneity associated with BPDE-DNA adducts.

Figure 2 shows the fluorescence spectra at 77 K for (-)-anti-BPDE-DNA (A), and (+)-anti-BPDE-DNA (B) obtained with λ_{ex} = 346.0 nm. At 77 K, the fluorescence origin of BPT + DNA is located at 376.8 nm (spectrum not shown). The BPT fluorescence spectrum is readily distinguishable from those of the two adducts and no contamination of the adduct spectra by BPT could be discerned for λ_{ex} = 346.0 nm. The (+)-anti-BPDE-DNA spectrum is dominated by a single adduct whose (0,0) band occurs at 378.0 nm (solid arrow). This adduct will be referred to as (+)1 in what follows, *cf.* Table I. The shoulder in spectrum C located at 380.6 nm (dashed arrow) will be assigned shortly to the origin band of another adduct (+)3, Table I. Inspection of spectrum A reveals that the adduct distribution from (-)-anti-BPDE is more heterogeneous with the highest energy origin at 378 nm (solid arrow). The corresponding adduct is denoted by (-)1. The dashed and dotted arrows indicate the possible existence of additional

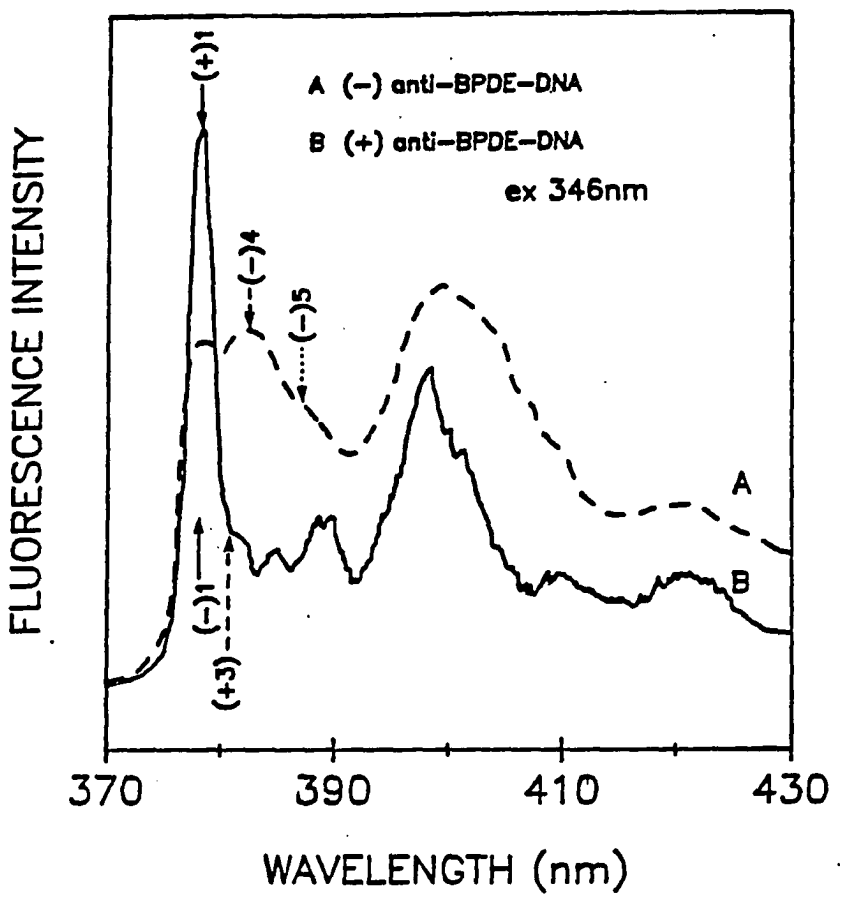

Figure 2. Laser-excited fluorescence spectra. (-)anti-BPDE-DNA (A) and (+)anti-BPDE-DNA (B). Gate delay (GD) = 30 nsec, gate width (GW) = 70 nsec; λ_{ex} = 346 nm, T = 77 K

adduct origins in the ~ 380-387 nm region.

The wavelengths of the adduct fluorescence origins serve as good approximations for the energies or wavelengths of the $S_1 \leftarrow S_0$ absorption origins, Table I. Since the S_1 energies are different, the relative intensities of different adducts derived from a specific enantiomer should depend on λ_{ex}. Figure 3, through comparison with Figure 2, illustrates this point. Spectrum B in Figure 3 reveals that λ_{ex} = 355 nm excitation leads to a marked increase in the intensity of the 380.6 nm origin fluorescence spectrum (dashed arrow, Figure 3B), thus confirming its assignment to a unique adduct, (+)3. At the same time, the origin intensity of (+)1 (solid arrow in Figure 2) is greatly diminished. The weak shoulder in spectrum B of Figure 3 indicated also by a solid arrow may be due to a trace of BPT and/or (+)1. Comparison of spectra A in Figures 2 and 3 also shows that λ_{ex} = 355 nm leads to a significant decrease in the fluorescence origin intensity of the (-)1 adduct. As a result, an adduct with a fluorescence origin at ~ 380.6 nm is revealed. This adduct is denoted as (-)3. Furthermore, spectrum A of Figure 3 reveals that a third (-)-type DNA adduct does exist with an origin located at ~ 385-386 nm (dotted arrow). It is designated as (-)5. Its possible existence is also suggested in spectrum A of Figure 2 (dotted arrow). A more exact determination of the location of the (-)5 origin will be made in the following subsection. Our gated detection studies revealed no significant differences in the fluorescence lifetimes of the adducts identified from Figures 2 and 3.

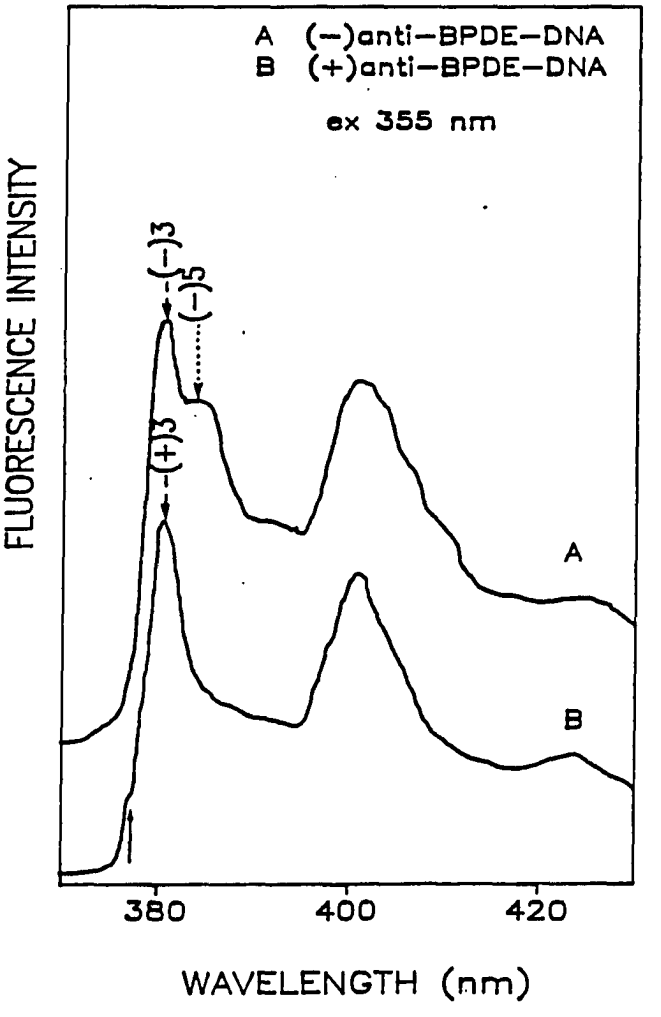

Figure 3. Laser-excited fluorescence spectra. (-)anti-BPDE-DNA (A) and (+)anti-BPDE-DNA (B). GD = 30 nsec, GW = 70 nsec, λ_{ex} = 355 nm, T = 77 K. The solid arrow indicates possible contribution due to a trace of BPT and/or (+)1

3. FLN spectra and fluorescence quenching DNA adducts formed from (+)-anti-BPDE

Geacintov et al. (9, 10) have utilized fluorescence, linear dichroism, and fluorescence quenching to classify DNA binding sites as type I (interior) or type II (exterior). Quasi-intercalated or pyrene-DNA base stacking sites are of the former type, and are expected to be significantly less accessible to solvent or fluorescence quenchers (such as acrylamide) than type II sites for which the pyrenyl moieties are located at exterior regions of the DNA double helix.

From the results of Ref. 12, it would appear that the 378 nm (+)1 adduct, *vide supra*, corresponds to a type II site with binding at N^2-dG. Figure 4 provides support for this assignment. Spectrum A for (+)-anti-BPDE-DNA + ACR (acrylamide) was obtained with λ_{ex} = 346 nm which, in the absence of quencher, yields (+)1 as the dominant contributor to the fluorescence, see spectrum B of Figure 2. Comparison of the latter spectrum with spectrum A of Figure 4 reveals that (+)1 is significantly quenched by ACR (although its fluorescence origin is still observable, see dotted arrow). The fluorescence origin in spectrum A (solid arrow) at 379.3 nm is assigned to a minor adduct, (+)2, which is apparently significantly less quenched than the (+)1 adduct. Spectrum B of Figure 4 for (+)-anti-BPDE-DNA was obtained with λ_{ex} = 355 nm in the presence of the quencher. In the previous subsection, it was shown that this excitation is selective for the (+)3 adduct at 380.6 nm. Spectra B of Figures 3 and 4 are very similar and our intensity measurements indicate that (+)3 is not significantly quenched by ACR. It is assigned as a type I site.

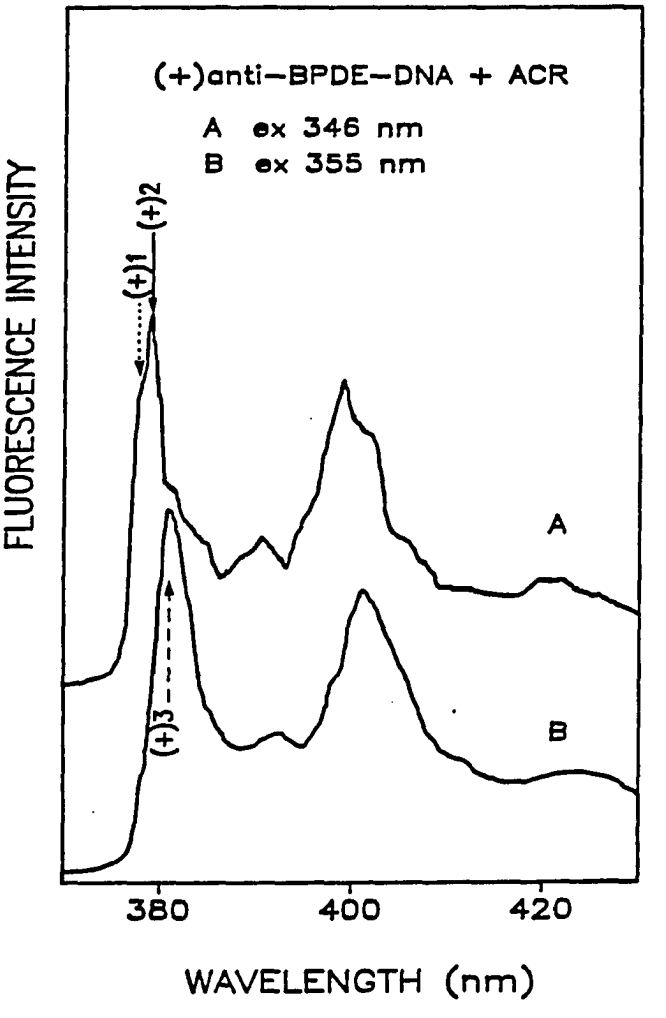

Figure 4. Laser-excited fluorescence spectra of (+)anti-BPDE-DNA in the presence of 1 M acrylamide. Spectra A and B were obtained for λ_{ex} = 346 nm and λ_{ex} = 355 nm, respectively. GD = 30 nsec, GW = 20 nsec, T = 77 K

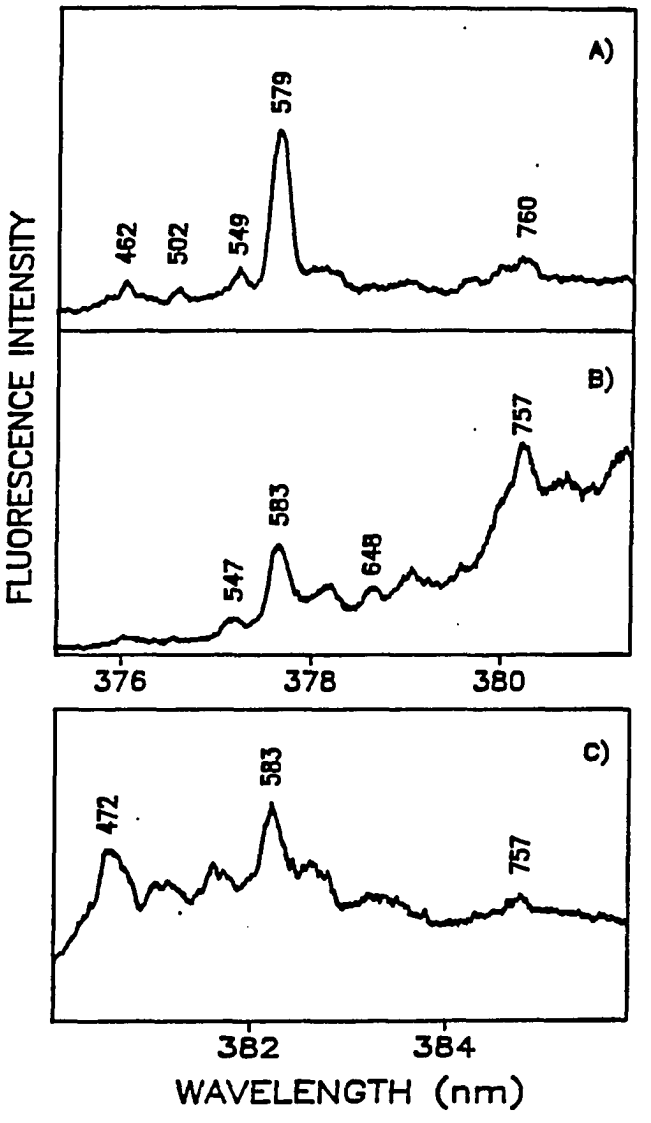

Figure 5. FLN spectra of BPDE-DNA adducts for vibronic excitation: (A) and (B) obtained with λ_{ex} = 369.6 nm for (+)anti-BPDE-DNA and (-)anti-BPDE-DNA, respectively; spectrum (C) for (-)anti-BPDE-DNA, λ_{ex} = 373.9 nm. Bands are labeled according to excited-state vibrational frequencies (cm^{-1}), T = 4.2 K

Frame A of Figure 5 is a portion of the FLN spectrum of (+)-anti-BPDE-DNA obtained with λex = 369.6 nm and in the absence of quencher. The sharp zero-phonon lines (ZPL) are labeled with excited state (S_1) mode frequencies (in cm^{-1}). This vibronically-excited FLN spectrum is identical to that of the major (+) adduct (N^2-dG) reported earlier (18). The excitation wavelength of 369.6 nm is located about 600 cm^{-1} higher in energy than the zero-point level of S_1 for (+)1 and, therefore, yields the excited state mode frequencies in the vicinity of 600 cm^{-1} (18). Frames B and C, for (-)-anti-BPDE-DNA, are shown for comparison and will be discussed in the following subsection.

We next explore the utility of combining quenching with FLNS. Figure 6 shows the FLN spectra for (+)-anti-BPDE-DNA with (A) and without (B) quencher. Comparison of A with BPT spectra shows that released BPT does not contribute to spectrum A for λ_{ex} = 371.6 nm. Although for this excitation wavelength the major (+)1 adduct makes a significant contribution to the ZPL of spectrum A, a comparison of this spectrum with spectrum B indicates that a second adduct also contributes. This follows, since the relative intensities of the ZPLs in spectrum A are changed by the addition of the quencher. For example, compare the relative intensities of the bands near 463 and 580 cm^{-1} (the experimental uncertainty in our frequency measurements is ± 3 cm^{-1}) in A and B. With reference to Table I, we conclude that the (+)2 adduct contributes to the ZPLs of spectrum A and more significantly to the 579 cm^{-1} band than the lower frequency bands, since the frequency difference between λ_{ex} and the S_1 state of (+)2 is ~ 560 cm^{-1}. In the same way, it follows that the (+)1 adduct makes a greater contribution to the bands in the vicinity of 462 cm^{-1} since the pertinent λ_{ex} - S_1 state energy gap is ~ 470

cm^{-1}. Since (+)1 undergoes significant quenching while (+)2 does not (*vide infra*), the bands in the vicinity of 462 cm^{-1} should undergo a greater degree of quenching than the 579 cm^{-1} band. This is consistent with the results of Figure 6. We do not believe that the (+)3 makes a significant contribution to the ZPLs in Figure 6, since its fluorescence excitation spectrum does not predict sharp fluorescence ZPLs, *vide infra*.

Thus far, three (+)-anti-BPDE-DNA adducts have been identified, (+)1 - (+)3, and (+)1 and (+)3 classified as sites II and I, respectively. Based on our available data, a firm classification cannot be made. However, because (+)2 is intermediate in energy between (+)1 and (+)3, one might postulate that the (+)2 site is located more in the interior than (+)1 but not to the same degree as (+)3. Figure 7 provides some support for this. Spectra 1-3 are high resolution fluorescence excitation scans obtained for fluorescence detection (5 cm^{-1} detection band pass) at 381.0, 379.5, and 378.5 nm, respectively. Notice from Table I that these λ_{obs}-values should be selective for the (+)3, (+)2, and (+)1 adducts of (+)-anti-BPDE-DNA, respectively. Spectrum 3 (no ACR) reveals that the (+)1 excitation spectrum is dominated by sharp ZPLs and, therefore, that its linear electron-phonon coupling is weak. The spectrum is contaminated by a few BPT bands which are likely the result of photo-degradation of the DNA adducts. The fluorescence excitation spectrum of the BPT + DNA standard mixture is also characterized by pronounced ZPL and weak coupling (spectrum not shown). Spectra 1 and 2 of Figure 7 were obtained in the presence of ACR. Spectrum 1 for (+)3 with its weak ZPL structure and intense and broad envelope provides a sharp contrast to spectrum 3 for (+)1.

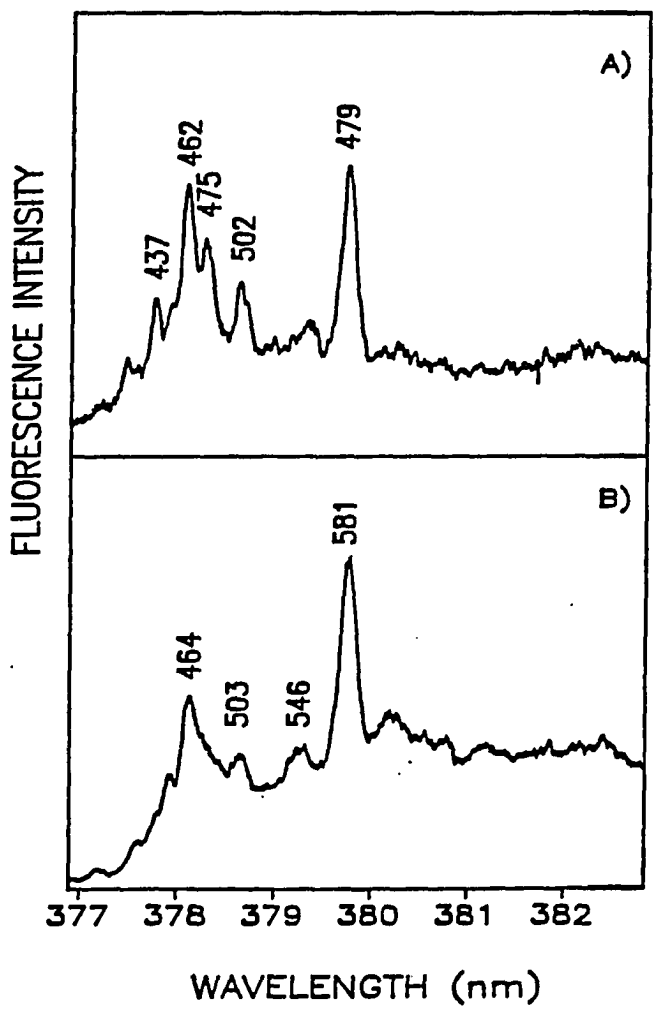

Figure 6. Comparison of FLN spectra. (+)anti-BPDE-DNA (A) and (+)anti-BPDE-DNA in the presence of ~ 1 M acrylamide (B). λ_{ex} = 371.6 nm, vibronic excitation, T = 4.2 K

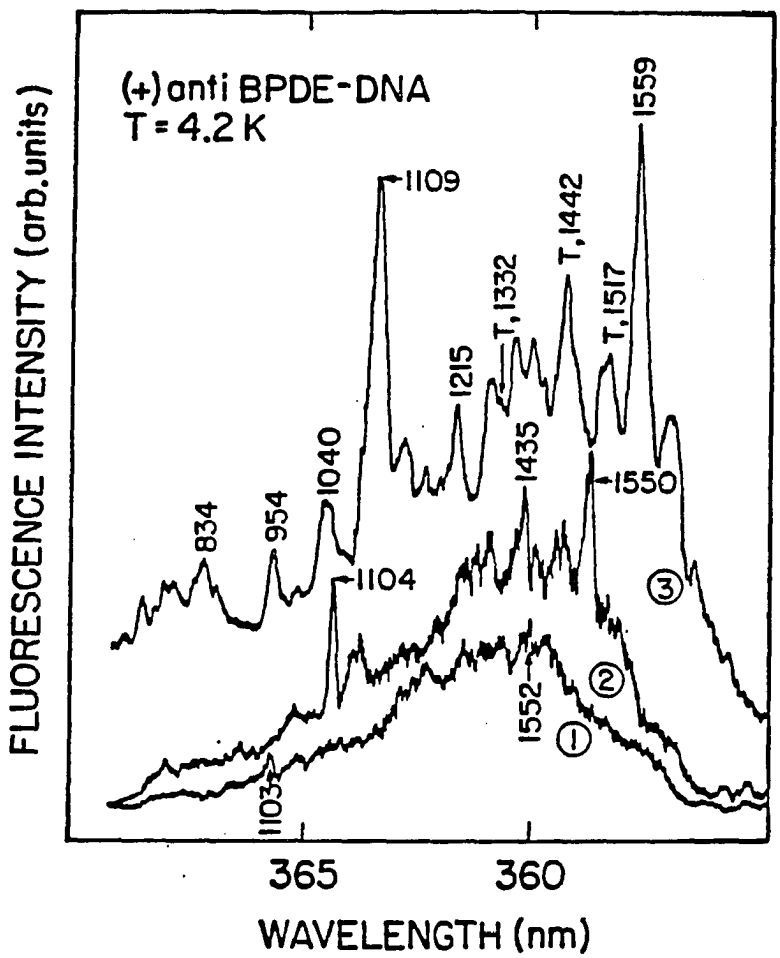

Figure 7. Fluorescence excitation spectra of (+)anti-BPDE-DNA. Spectra 1 and 2 obtained with 1 M acrylamide; spectrum 3 obtained in absence of quencher. Spectra 1-3, obtained with λ_{obs} = 381 nm, 379.5 nm and 378.5 nm (bandpass ~ 5 cm^{-1}) , respectively (see text). Spectra are arbitrarily shifted for clarity. Peaks are labeled with excited-state vibrational frequencies Bands labeled by T are due to BPT. T = 4.2 K

We interpret the difference in terms of stronger electron-phonon coupling for the (+)3 adduct and suggest that this increase in coupling strength may be due to an increase in the charge-transfer (CT) character of the S_1 state resulting from a stronger interaction between the pyrenyl moiety and the DNA bases for the type I site. We have studied this effect for pyrene with FLN (unpublished data) and shown that the red shift for the S_1 state of pyrene produced by intercalation into DNA is accompanied by an increase in the electron-phonon coupling strength. Furthermore, it is firmly established that the CT states of 1:1 π-molecular charge-transfer complexes are characterized by very strong coupling (22). With the observation that spectrum 2 of Figure 7 for (+)2 is intermediate in nature between spectra 1 and 3, the following conjecture emerges: the decrease in solvent or quencher accessibility which reflects the degree of interior binding is accompanied by a decrease in the S_1 state energy and a concomitant increase in the electron-phonon coupling strength (CT character). We proceed to further test this notion with the results for the (-)-anti-BPDE-DNA adducts and, in the following subsection, through consideration of the R-values for all the adducts.

4. DNA adducts formed from (-)-anti-BPDE

Before considering the fluorescence quenching results for (-)-anti-BPDE-DNA, we compare its FLN spectrum for λ_{ex} = 369.6 nm, spectrum B in Figure 5, with the corresponding FLN spectrum for (+)-anti-BPDE-DNA, spectrum A, which is mainly due to the (+)1, N^2-dG adduct. The ZPLs such as 547, 583, 648, and 757 cm^{-1} in spectrum B are most reasonably assigned to (-)1 and (-)2, since their fluorescence origins lie close in energy to that of (+)1, Table I. It will become apparent that the

onset of the broad underlying fluorescence in spectrum B, upon which the 757 cm^{-1} ZPL is superimposed, is due to the (-)3 adduct. The spectrum in the bottom frame of Figure 5 is that of (-)-anti-BPDE-DNA obtained with λ_{ex} = 373.9 nm and, as expected, its ZPL intensity distribution is different than the distribution in spectrum B obtained with λ_{ex} = 369.6 nm. The contribution of (-)1 adduct to spectrum C is negligible, since the center of the observation window at ~ 383 nm was chosen to be selective for the (-)4 adduct (identified in the following subsection, *cf.* Table I). A similar FLN spectrum was observed for the observation window at ~ 385 nm, selective for (-)5. We believe, therefore, that (-)4/5 are the major contributors to the ZPLs of spectrum C.

Figure 8 shows three laser excited 77 K fluorescence spectra for (-)-anti-BPDE-DNA in the presence of quencher. Comparing the origin region of spectrum A (λ_{ex} = 346 nm) with the same for spectrum A of Figure 2 (the same λ_{ex}, no quencher) reveals that the origin in the latter spectrum at 378 nm (solid arrow) due to (-)1 is markedly suppressed by ACR. Thus (-)1, like (+)1, can be assigned as a type II site. Spectrum C of Figure 8 for λ_{ex} = 355 nm is very similar to spectrum B of Figure 4 and is due to the (-)3 adduct at 380.6 nm (solid arrow), which is not subject to quenching. Therefore, it is assigned as a type I (interior) site. Note that the contribution from (-)1 to spectrum C of Figure 8 is rendered negligible because of ACR quenching and the value of λ_{ex} = 355 nm (see preceding subsection). All spectra presented thus far were obtained with a 30 ns gate delay. The adducts determined thus far have similar lifetimes (~ 120 ns, based on comparisons of spectra obtained with 0, 30, and 100 ns gate delays). We have encountered only one instance where this is not the case.

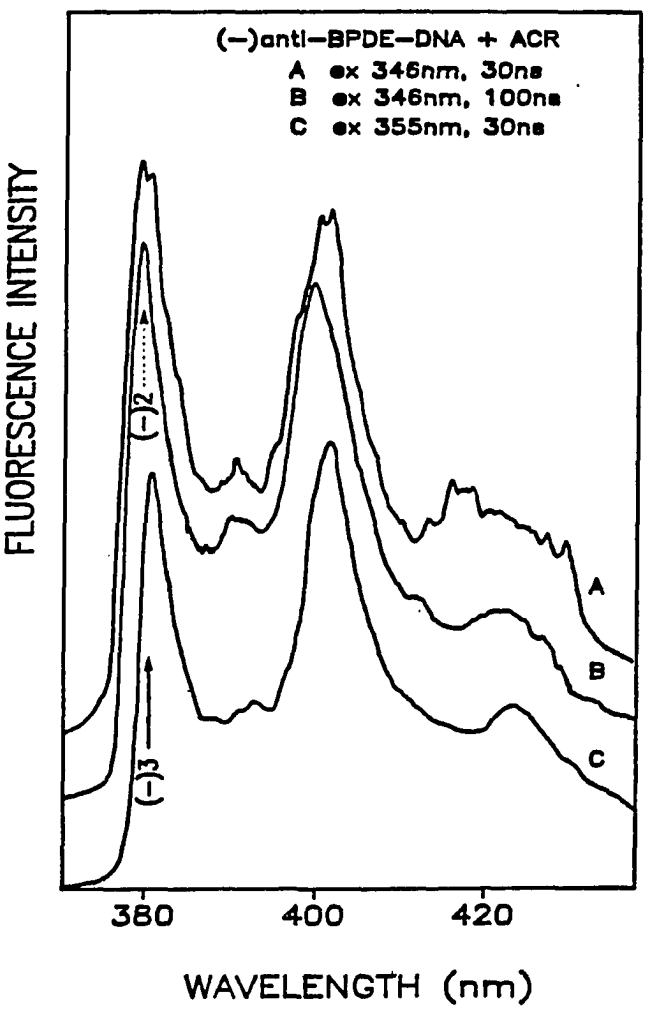

Figure 8. Laser-excited fluorescence spectra of (-)-anti-BPDE-DNA in the presence of 1 M acrylamide. Spectra A and B were obtained with λ_{ex} = 346 nm and GD times of 30 nsec and 100 nsec, respectively. Spectrum C was obtained for λ_{ex} = 355 nm and a GD of 30 nsec (see text). T = 77 K

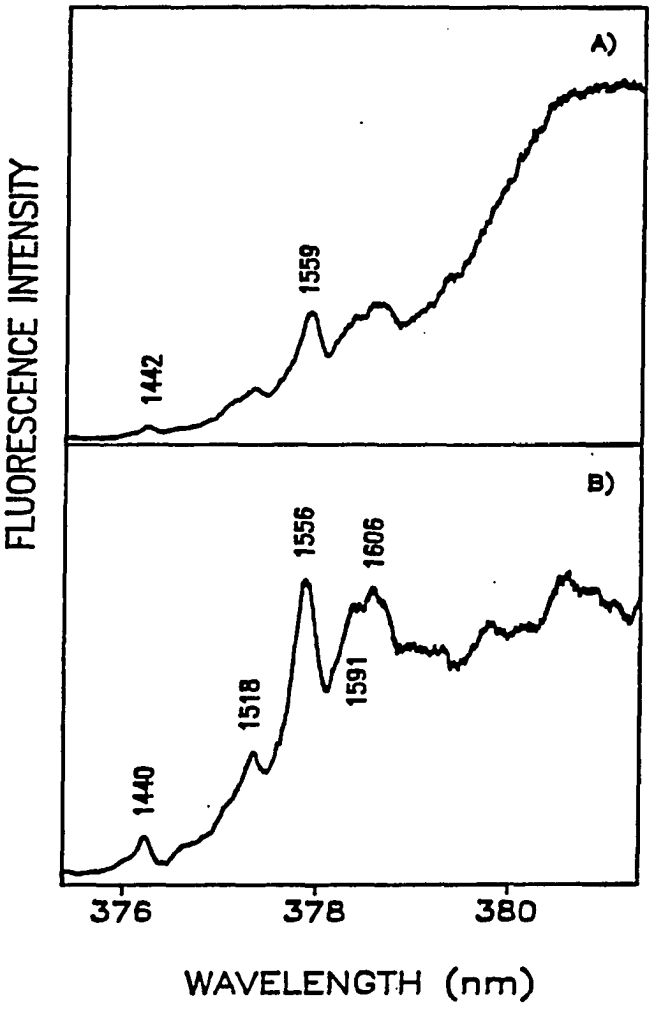

Figure 9. FLN spectra of the (-)-anti-BPDE-DNA. Absence (A) and presence (B) of quencher; T = 4.2 K, λ_{ex} = 356.9 nm, GD = 30 nsec, GW = 20 nsec. FLN peaks are labeled with their excited-state vibrational frequencies (cm^{-1})

Spectrum B of Figure 8 was obtained with λ_{ex} = 346 nm for a gate delay of 100 ns and should be compared with spectrum A of the same figure. It is apparent that the contribution from (-)3 to the origin region of spectrum A has been effectively eliminated in spectrum B which reveals, however, the existence of another longer lived (-) adduct whose origin band (dotted arrow) lies at 379.3 nm. It is denoted by (-)2 and has an energy which is approximately equal to that of (+)2, Table I.

Figure 9 shows the FLN spectra for a relatively high S_1 excitation energy (λ_{ex} = 356.9 nm) in the absence (A) and presence (B) of quencher. It should be noted that (18) the active mode frequency range (width of 200-300 cm^{-1}) probed for each adduct is approximately centered at a frequency determined by the difference in frequency associated with λ_{ex} and the frequency of the adduct absorption (fluorescence) origin, Table I. This central frequency for (-)5 is ~ 2100 cm^{-1}. At such a high excess vibrational energy above the zero-point level of S_1, vibrational congestion for active modes is quite severe and, as a result, FLN is largely precluded. It is reasonable to suggest that the broad unstructured fluorescence in spectrum A, which has an onset near 383 nm, is due to (-)5 as well as (-)4 and (-)3. This is consistent with the marked reduction of the broad fluorescence produced by the addition of quencher (spectrum B). Except for the 1440 cm^{-1} band, which we have confirmed is due to BPT, the labeled ZPLs in spectrum B are believed to be predominantly due to (-)2 since the (-)1 adduct is to a large extent quenched (along with (-)4/5). The (-)3 type I adduct is likely to make its major contribution to the underlying broad fluorescence of spectrum B.

Fluorescence excitation spectra for the (-) 1, 2, and 3 adducts were obtained

under high resolution conditions. The excitation spectra in Figure 7 and those for the above (-) adducts (not shown) are quite similar. Thus, the discussion presented earlier for Figure 7 need not be repeated. Suffice it to say that the linear electron-phonon coupling strength increases in the order (-)1, (-)2, and (-)3 and in parallel to the degree of interior binding.

5. Binding site classification based on the fluorescence intensity ratio R

In this subsection, we exploit the fact that the ratio R of the intensity of the origin band relative to the prominent vibronic band at ~ 1400 cm^{-1} (near 400 nm in our spectra) of the pyrenyl moiety in the DNA adducts (and BPT) is very sensitive to the solvent-cage polarity (11, 12), thus mimicking the well-known behavior of pyrene itself (14-16). This solvent-chromophore induced effect is expected for weakly allowed electronic transitions, such as $S_1 \leftarrow S_0$ for pyrene; the low molar extinction coefficient is due to the near cancellation of two transition dipoles associated with the two single-electron excited electronic configurations whose interaction determines the S_1 state wavefunction. To our knowledge, however, an adequate theoretical treatment of the polarity dependence of the factor R for pyrene does not exist. In what follows, we are guided by earlier work which indicates that R increases with increasing solvent-cage polarity. For DNA adducts dissolved in the glycerol/H_2O based glass, one expects that R should increase with increasing solvent accessibility. Therefore, type II sites should exhibit higher R-values than type I sites.

Since the adducts from (+)-anti-BPDE are the less heterogeneous, with (+)1 being the dominant adduct, we consider these adducts first. That the (+) adducts

exhibit a relatively small heterogeneity, and that the major adduct is type II, have been previously established (12, 13). The R-values of 1.75, 1.25, and 1.15 given in Table II for (+)1, (+)2 and (+)3 were measured directly from spectrum B of Figure 2, spectrum A of Figure 4, and spectrum B of Figure 3, respectively. The last spectrum for (+)3 appears to be "pure" and was used to correct the R-value for (+)1 whose spectrum in Figure 2 is contaminated by a small contribution from (+)3 (see dashed arrow of spectrum B in Figure 2). The corrected value is 1.9 and is given in parenthesis in Table II. Also included in Table II is the R-value for the (BPT + DNA) mixture. The relative magnitudes of R for (+)1 and (+)3 are consistent with our earlier conclusion that they are type II and I, respectively. The value of 1.25 for (+)2 is only slightly higher than for (+)3, suggesting that it may also be a type I site.

Analysis of the R-factors for the adducts from (-)-anti-BPDE is more difficult because of the presence of 5 adducts, (-)j (j = 1-5). Nevertheless, the improved resolution of the laser excited 77 K fluorescence spectra (with and without a quencher) has enabled us to determine the values given in Table II.. Some discussion of the analysis procedure is appropriate. From spectra A of Figures 2 and 3, one estimates that $R_{346} = 0.85 < R_{355} = 1.15$, where the subscript on R denotes the laser excitation wavelength. This would appear to be in contradiction to our earlier conclusion, *vide supra*, that $\lambda_{ex} = 355$ nm is quite highly selective for quasi-intercalated or pyrene-base stacking type adducts. However, this contradiction does not exist when appropriate deconvolution of overlapping spectral features from different adducts is taken into account. Our own, and previous results (12-13), indicate that type I sites are important for the (-)-anti-BPDE-DNA adducts.

The value of R ~ 1.1 in Table II for (-)2 was obtained directly from spectrum B of Figure 8, but it may be higher since spectrum B contains a contribution from (-) 3 adduct. The (-)2 adduct is a minor adduct which is observable only in the presence of the quencher and for a longer fluorescence gate delay (100 ns). Thus, to a first approximation, its contribution to the spectrum of (-)1 in Figure 2(A) is taken to be negligible. The R-value of 0.9 for (-)3 was measured from spectrum C of Figure 8 (λ_{ex} = 355 nm with quencher). This spectrum was then appropriately weighted and subtracted from spectrum A of Figure 3 to yield the spectrum for (-)5 (not shown) which was used to determine R 1.8, Table II. To determine the R-value for (-)1, the (-)3 and (-)5 spectra were appropriately scaled and subtracted from spectrum A of Figure 2. This procedure yielded the spectrum shown in Figure 10. Spectra A of Figures 2 and 8 had led to a tentative assignment of a fifth adduct (-)4, *cf.* Table I, with a fluorescence origin near 382 nm. The appearance in Figure 10 of a fluorescence origin at 382.7 nm makes this assignment firmer. Taking into account the minor overlap between the (-)1 and (-)4 spectra, Figure 10 provides R-values of 1.6 and 1.7 for (-)1 and (-)4, respectively. The uncertainty for these values is estimated at ± 0.1.

The results discussed in the two previous subsections showed that both (+)1 and (-)1 are readily quenched while (+)3 and (-)3 are not subject to quenching. Although not specifically discussed, the spectra (77 K) indicate that (-)2 and (+)2 are not subject to significant quenching (note, for example, that (+)2 was identified by spectrum A of Figure 4 obtained with quencher) but that (-)4 and (-)5 are. The R-values in Table II are in accord with the quenching behaviors of the adducts; namely, adducts (type II) which are quenchable are characterized by high

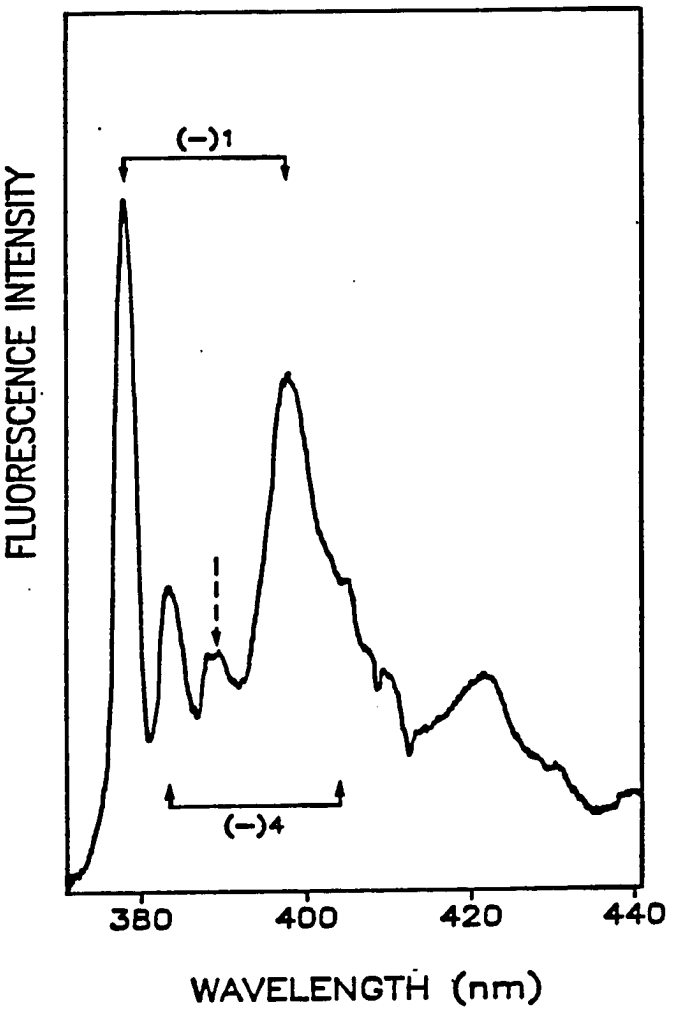

Figure 10. Deconvolved fluorescence spectrum for (-)1 and (-)4 adducts. Dashed arow indicates the ~ 750 cm^{-1} vibronic band corresponding to the (-)1 adduct

R-values (~ 1.6-1.8) while those which are not have low values (0.9-1.25). On the other hand, the earlier mentioned hypothesis that solvent (quencher) accessibility decreases as the S_1 state energy decreases is not in accord with the data for (-)4, and decreases as the S_1 state energy decreases is not in accord with the data for (-)4 and (-)5 (both of which possess a high A-value). Spectrum C of Figure 5 (and other spectra, not shown) suggest that the (-)4/5 type adducts are characterized by quite prominent ZPLs, consistent with weak electron-phonon coupling.

E. Concluding Remarks

Our results are in agreement with those of earlier studies which showed that the DNA adducts derived from (-)-anti-BPDE are significantly more heterogeneous than those derived from (+)-anti-BPDE (23, 24), and that the (+)-adducts are dominated by type II binding sites, while the (-)-adducts also are characterized by significant contributions from type I binding sites (12, 13). However, contrary to the conclusion of Ref. 12, our studies indicate that the (-)5 adduct (with fluorescence origin at ~ 385 nm) is type II. Since the fluorescence lifetimes of the (+)-adducts at cryogenic temperatures are similar, we estimate from the spectral data that the (+)1-N^2-dG type II (exterior) adduct constitutes about 85% of the stable macromolecular adducts formed at the damage levels employed. The remaining two adducts, (+)2 and (+)3, are type I and are presumably of the quasi-intercalated and intercalated type. For the high DNA damage levels employed, the (+)2 and (+)3 adducts contribute only 15% of the total binding. However, when the damage level is very low (~ $1:10^6$ modified bases), the relative contribution of (+)3 adduct significantly increases (*cf.* Chapter 4C). That is, the

adduct distribution may depend on the damage level. Since *in vivo* DNA damage levels are very low and it is difficult to determine the relative efficiencies for repair of adduct sites from a given stereoisomer of a metabolite, it is important to develop macromolecular analysis techniques of appropriately high selectivity and sensitivity.

The results presented do not permit further structural characterization of the (+)j (j = 1-3) adducts. However, very recent results obtained for synthetic (+)-anti-BPDE-polynucleotide adducts indicate that (+)j (j = 1-3) are due to binding at a nucleophilic center of guanine (*cf.* Appendix B).

The similarity between the S_1 state energies and fluorescence spectra of the (-)1-3 and (+)1-3 adducts is very striking and suggests a correspondence between the nature of the base modified and the site of binding on that base. Thus, for example, (-)1 may be the N^2-dG analogue of (+)1. However, the adduct distributions from (+)- and (-)-anti-BPDE are very different. We conclude that the major adducts for the latter are (-)1 and (-)3 with a relative weight of ~ 70-80%. The (-)3 adduct is type I which to a large extent, dominates the absorbance and linear dichroism spectra of the (-)-BPDE-DNA adducts (13). In contrast, the adducts from the (+) enantiomers are predominantly type II. It is interesting to note that both enantiomers are reasonably mutagenic in the repair-deficient *salmonella typhimurium* tester strains, while the (+)-enantiomer is markedly more mutagenic in repair-competent mammalian v79 cells, as well as being the only tumorigenic isomer in mice (23-26). For these reasons it has been speculated that the intercalated or quasi-intercalated type I adducts possibly are more readily repaired due to their marked increase in the distances between adjacent base pairs in the double helix (27). The methodology presented here has the potential for

distinguishing between adduct conformations in DNA and for monitoring the fates of different adducts as a function of time in repair-competent cells.

Finally, we remark that the nature of the (-)4 and (-)5 adducts poses an interesting problem, since they are type II (exterior) and yet possess S_1 state energies lower than those of the type I adducts. One possible explanation is that the former adducts are associated with a base other than guanine, for example, adenine. Another is that they are associated with binding to a nucleophilic center of guanine other than N^2. Still, another would emerge were the S_1 state energies of chemical adducts to be dependent on DNA base composition and sequence. We are currently investigating the latter possibility through studies on (+)- and (-)-anti-BPDE adducts formed from synthetic polynucleotides of specific base composition and sequence. Thus far these studies have shown, for example, that the (-)5 adduct exhibits base pair selectivity for alternating (dG-dC). We are encouraged to think that the study of adducts formed from synthesized polynucleotides will lead to further insights on the structures of the macromolecular adducts.

F. References

1. Bartsch, H., Hemminki, K. and O'Neill, I. K., Eds. (1988). Methods for detecting DNA damaging agents in humans: Applications in Cancer Epidemiology and Prevention, IARC Scientific Publications: No. 89, Lyon
2. Slaga, T. J., Bracken, W. J., Gleason, G., Levin, W., Yagi, H., Jerina, D. M. and Conney, A. H. (1979). "Marked differences in the skin tumor initiating activities of the optical enantiomers of the diastereomeric benzo[a]pyrene

7,8-diol-9,10-epoxides," Cancer Res., 39, 67-71.

3. Brookes, P. and Osborne, M. R. (1982). "Mutation in mammalian cells by stereoisomers of anti-benzo[a]pyrene-diol-epoxide in relation to the extent and nature of the DNA reaction products," Carcinogenesis, 3, 1223-1226.
4. Geacintov, N. E. (1988). "Mechanisms of reaction of polycyclic aromatic epoxide derivatives with nucleic acids," In: Polycyclic Aromatic Hydrocarbon Carcinogenesis: Structure-Activity Relationships, Vol. 2, Yang, S. K. and Silverman, B. D., Eds., CRC Press, Inc.: Boca Raton, FL, 181-205.
5. Alexandrov, K., Sala, M. and Rojas, M. (1988). "Differences in the DNA adducts formed in cultured rabbit and rat dermal fibroblasts by benzo[a]pyrene and (-) benzo[a]pyrene-7,8-diol," Cancer Res.. 48, 7132-7139.
6. Phillips, D. H., Hewer, A. and Grover, P. L. (1985). "Aberrant activation of benzo[a]pyrene in cultured rat mammary cells *in vitro* and following direct application to rat mammary glands *in vivo*," Cancer Res., 45, 4169-4174.
7. Ireland, C. M., Eastman, A. and Bresnick, E. (1984). "The influence of inhibitors on the repair of benzo[a]pyrene-damaged DNA in hamster tracheal epithelial cells," Carcinogenesis, 5, 187-191.
8. Moore, C. J., Pruess-Schwartz, D., Mauthe, R. J., Gould, M. N. and Baird, W. M. (1987). "Interspecies differences in the major DNA adducts formed from benzo[a]pyrene but not 7,12-dimethylbenz[a]anthracene in rat and human mammary cell cultures," Cancer Res., 47, 4402-4406.
9. Geacintov, N. E., Ibanez, V., Gagliano, A. G., Jacobs, S. A. and Harvey, R. G. (1984). "Stereoselective covalent binding of anti-benzo[a]pyrene diol epoxide to DNA. Conformation of enantiomer adducts," J. Biomol. Struct. &

Dynamics 1, 1473-1484.

10. Geacintov, N. E., Yoshida, H., Ibanez, V., Jacobs, S. A. and Harvey, R. G. (1984). "Conformations of adducts and kinetics of binding to DNA of the optically pure enantiomers of anti-benzo[a]pyrene diol epoxide," Biochem. Biophys. Res. Commun., 122, 33-39.
11. Kim. S. K., Geacintov, N. E., Brenner, N. C. and Harvey, R. G. (1989). "Identification of conformationally different binding sites in benzo[a]pyrene diol epoxide-DNA adducts by low temperature fluorescence spectroscopy," Carcinogenesis, (in press)
12. Kim, S.K., Brenner, N.C., Soh, B.J. and Geacintov, N.E. (1989). "Fluorescence spectroscopy of benzo[a]pyrene diol epoxide-DNA adducts. Conformation-specific emission spectra," Photochem. Photobiol., 50, 327-337.
13. Zinger, D., Geacintov, N. E. and Harvey, R. G. (1987). " Conformations and selective photodissociation of heterogeneous benzo[a]pyrene diol epoxide enantiomer-DNA adducts," Biophysical Chem., 27, 131-138.
14. Nakajima, A. (1971). "Solvent effect of the vibrational structures of the fluorescence and absorption spectra of pyrene," Bull. Chem. Soc., Japan, 44, 3272-3277.
15. Glushko, V., Thaler, M. S. R. and Karp, C. D. (1981). "Pyrene fluorescence fine structure as a polarity probe of hydrophobic regions: behavior in model solvents," Arch. Biochem. Biophys., 210, 33-42.
16. Kalyanasundaram, K. and Thomas, J. K. (1977). "Environmental effects of vibronic band intensities in pyrene monomer fluorescence and their application in studies of micellar systems," J. Amer. Chem. Soc., 99, 2039-2044.

17. Chiang, I., Hayes, J. M. and Small, G. J. (1982). "Fluorescence line narrowing spectrometry of amino polycyclic aromatic hydrocarbons in an acidified organic glass," Anal. Chem., 54, 315-318.

18. Jankowiak, R., Cooper, R. S., Zamzow, D., Small, G. J., Doscocil, G. and Jeffrey, A. M. (1988). "Fluorescence line narrowing-nonphotochemical hole burning spectrometry: femtomole detection and high selectivity for intact DNA-PAH adducts," Chem. Res. Toxicol., 1, 60-68.

19. Zamzow, D., Jankowiak, R., Cooper, R. S., Small, G. J., Tibbels, S. R., Cremonosi, P., Devanesan, P., Rogan, E. G. and Cavalieri, E.L. (1989). "Fluorescence line narrowing spectrometric analysis of benzo[a]pyrene-DNA adducts formed by one-electron oxidation," Chem. Res. Toxicol., 2, 29-34.

20. Cooper, R. S., Jankowiak, R., Hayes, J. M., Lu, P. and Small, G. J. (1988). "Fluorescence line narrowing spectrometry of nucleoside-polycyclic aromatic hydrocarbon adducts on thin-layer chromatographic plates," Anal. Chem., 60, 2692-2694.

21. Geacintov, N. E. (1987). "Principles and applications of fluorescence techniques in biophysical chemistry," Photochem. Photobiol., 45, 547-556.

22. Haarer, D. (1977). "Zero-phonon lines in the singlet spectrum of the charge transfer crystal anthracene-PM0A: experimental evidence and model calculations," J. Chem. Phys., 67, 4076-4085.

23. Brookes, P. and Osborne, M. R. (1982). "Mutation in mammalian cells by stereoisomers of anti-benzo[a]pyrene-diolepoxide in relation to the extent and nature of the DNA reaction products," Carcinogenesis, 3, 1223-1226.

24. Osborne, M. E., Jacobs, S., Harvey, R. G. and Brookes, P. (1981). "Minor

products from the reaction of (+) and (-) benzo[a]pyrene-anti-diol epoxide with DNA," Carcinogenesis, 2, 553-558.

25. Buening, M. K., Wislocki, P. G., Levin, W., Yogi, H., Thakber, D. R., Akagi, H., Koreeda, M., Jerina, D. M. and Conney, A. H. (1978). "Tumorigenicity of the optical enantiomers of the diastereomeric benzo[a]pyrene-7,8-diol-9,10-epoxides in newborn mice: exceptional activity on (+)7β,8α-dihydroxy-9α,10α-epoxy-7,8,9,10-tetrahydrobenzo[a]pyrene," Proc. Natl. Acad. Sci., USA, 75, 5358-5362.
26. Conney, A. H. (1982). "Induction of microsomal enzymes by foreign chemicals and carcinogenesis by polycyclic aromatic hydrocarbons: G. H. A. Clowes Memorial Lecture," Cancer Res., 42, 4875-4917.
27. Hingerty, B. E. and Broyde, S. (1985). "Carcinogen-base stacking and base-base stacking in dCpdG modified by (+) and (-) anti-BPDE," Biopolymers, 24, 2279-2299.

Table I. Spectral characteristic of (+) and (-) BPDE-DNA adducts at T = 77 K

(+) adducts			(-) adducts		
	fluorescence band max. (nm)	site type		fluorescence band max. (nm)	site type
(+)1	378.0	II	(-)1	378.0	II
(+)2	379.3	I[a]	(-)2	379.3	I[a]
(+)3	380.6	I	(-)3	380.6	I
			(-)4	382.7	II
			(-)5	385.2	II

[a] We assign (+)2 and (-)2 as site I type adducts with a "degree" of interior binding that is less than that for (+)3 and (-)3.

Table II. Summary of R ratios

	λ_{ex} (nm)	R		λ_{ex} (nm)	R
(BPT+ DNA)	345	1.8[a]	(-)1	346	1.60
			(-)2	346	~1.1[b]
(+)1	346	1.75 (~1.9)	(-)3	355	0.90
(+)2	346	~ 1.25	(-)4	346	1.7
(+)3	355	1.15[c]	(-)5	355	1.8

[a] For λ_{ex} = 355 nm, the spectrum of BPT-DNA complex consists of two bands at ~ 376.8 and 381 nm with R ratio 1.8 and 1.36, respectively. The physical nature of BPT-DNA complex will be discussed elsewhere (*cf.* Appendix B).

[b] This value could be slightly higher since spectrum B in Figure 14 may contain a contribution from (-)3 adduct.

[c] This value could be smaller if corrected for possible contribution due to a trace of BPT and/or (+)1 (see Figure 8, curve B).

VII. APPENDIX B: PAPER II. A COMPARATIVE LASER SPECTROSCOPIC STUDY OF DNA AND POLYNUCLEOTIDE ADDUCTS FROM (+)-ANTI-DIOL EPOXIDE OF BENZO[a]PYRENE

A. Abstract

Fluorescence line narrowing spectroscopy in combination with fluorescence quenching and 77 K laser excited fluorescence spectroscopy is shown to be a powerful approach for characterization of chemically and/or structurally different adducts of (+)-anti-BPDE formed from DNA and the synthetic polynucleotides. Three polynucleotide duplexes ((poly(dG-dC)·poly(dG-dC), poly(dG)·poly(dC), poly(dA-dT)·poly(dA-dT)) and single strand poly(dG) were used in this study, and the spectral characteristics and the quenchability of each corresponding adduct were elucidated. Of these it is the alternating poly(dG-dC)·poly(dG-dC) that yields (+)-1 and -2 adducts which are most similar to the trans N^2-dG adducts of DNA. Fluorescence experiments with *trans* and *cis* standards of N^2-dG from (+)-anti-BPDE and guanine monophosphate were the bases for this stereochemical assignment. The model (+)-anti-BPDE adducts of the oligonucleotide d(ATATGTATA) were studied spectroscopically, and the results further confirm our previous conformation assignment of (+)-1 as a type II adduct and (+)-2 as a quasi-intercalated adduct, and indirectly supports (+)-3 as an intercalated adduct. In addition, the FLN spectra of (+)-anti-BPDE-DNA reveal a new minor adduct, (+)-4, which is assigned as N^6-dA on the base of the spectra of standard (+)-anti-BPDE-poly(dA-dT)·poly(dA-dT). Finally, the 77 K fluorescence spectroscopy revealed three different species of racemic anti-BP tetraol which has been physically mixed

with DNA and poly(dG), and their spectral characteristics and the quenchability are also presented, which will be greatly conducive to the spectral analysis of "real adducts".

B. Introduction

The mutagenic and tumorigenic properties of polycyclic aromatic hydrocarbons (PAH) have been the subjects of numerous studies (1-3). Benzo[a]pyrene (BP) has been most extensively studied and provides an important testing ground for models of DNA-metabolite physical and chemical interactions, mutagenesis and tumorigenesis. The physico-chemical properties of DNA adducts from and the biological effects of BaP have been recently reviewed by Geacintov (4, 5) and Gräslund and Jernström (6). The metabolic pathways (diol epoxide and one-electron oxidation or radical cation (7, 8)) of BaP and base-nucleophilic center specificity of its electrophilic metabolites are rather well understood. However, the relationships between base-metabolite chemical structure, site structure and genetic mutation (e.g., of proto-oncogenes) or error-free and -prone DNA repair are not (4-6, 9-12). Thus, the problem of base sequence specificity for metabolites should receive greater attention. This also pertains to the relevance for intact mammalian cells of the structural and dynamical properties of the adducts observed *in vitro* with pure DNA.

Solution of such problems will depend, in part, on the availability of highly selective and sensitive bioanalytical methodologies for the characterization of both stable and labile covalent DNA-PAH adducts. The required selectivity is well-illustrated by noting that the primary diol epoxides of BaP which react with DNA

are (+)-trans-7,8-dihydroxy-anti-9,10-epoxy-7,8,9,10-tetrahydro-BP ((+)-anti-BPDE), (-)-anti-BPDE and their syn-diastereomers, Figure 1. Moreover, each stereoisomer yields a distribution of adducts, *vide infra*. For studies of DNA from mammalian cells exposed to ambient concentrations of PAH the required detection limit for adducts is about 1 femtomole. Techniques that allow for the analysis of intact macromolecular DNA are particularly attractive for a number of obvious reasons.

At present, the highest resolution frequency domain technique available for the analysis of DNA-PAH adducts is laser-excited fluorescence line narrowing spectroscopy (FLNS) (13-21). FLNS is also applicable to nucleotide and nucleoside adducts (7, 21). Most recently, this technique has been used for analysis of macromolecular DNA and globin damage from *in vivo* exposure to PAH (20, 22). For example, it was shown that the major stable DNA adduct from the liver of fish exposed to high dosage levels of BaP is derived from syn-BPDE (20), in agreement with previous work (23). At low dosage levels the major adduct was found to originate from (+)-anti-BPDE (23, 24). FLNS was used to prove that (22) the major human globin adduct from BaP is a carboxylic ester and that this adduct is of the interior type (i.e., undetectable by monoclonal anti-body approaches). Analyses by FLNS of the urine and feces of rats treated with BaP has proven, for the first time, that the cytochrome P-450 catalyzed one-electron oxidation of BaP is a major pathway for DNA damage in mammalian cells (25). The nucleotide adduct identified was BaP bound at its C^6 position to N^7 of guanine. Distinction by FLNS between this adduct and that formed at C^8 of guanine had been demonstrated earlier (17).

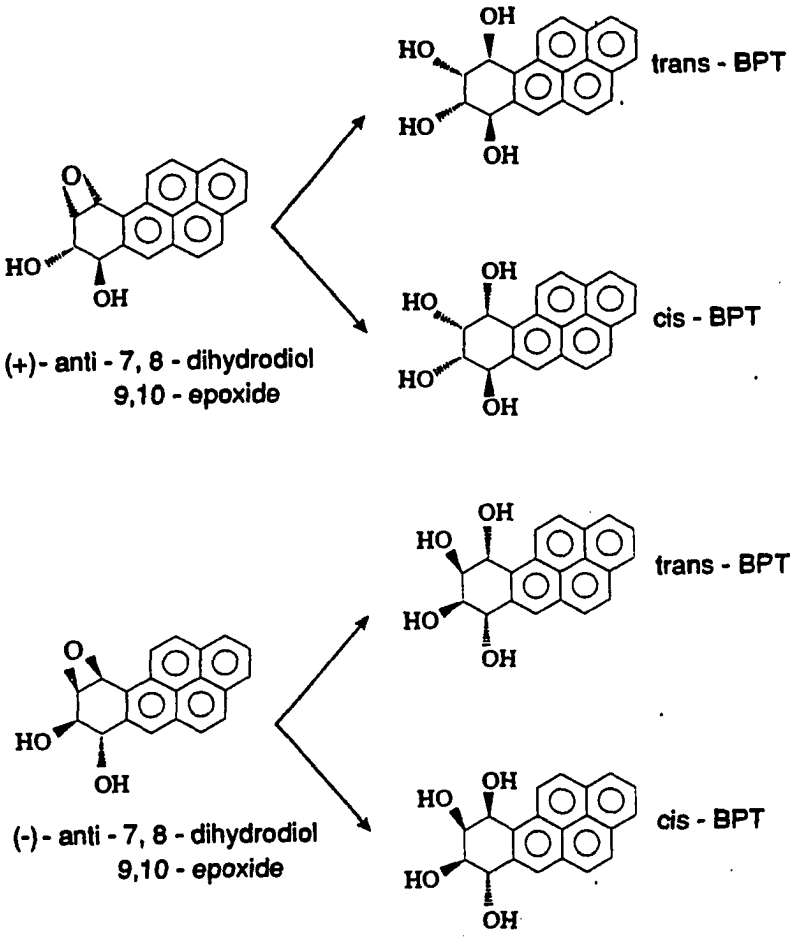

Figure 1. Structures of anti-BPDE stereoisomers and associated *cis* and *trans* tetraols

However, we recently reported that FLNS in combination with fluorescence quenching and 77 K selectively excited ($S_2 \leftarrow S_0$) fluorescence spectroscopy is a more powerful methodology for DNA adduct analysis (19). In this work five ((-)-j, j = 1-5) adducts from the reaction of (-)-anti-BPDE with purified DNA were identified and classified as type I (interior or quasi-intercalated) or type II (exterior, solvent accessible). The (+)-anti-BPDE enantiomer yielded three adducts with (+)-1 dominant at ~ 85%, Table I. That the (-)-enantiomer yields the more heterogeneous distribution of adducts was known from earlier work (26, 27). It is important for the present paper to note also that type II adducts are characterized by a higher value for the ratio (R) of the intensity of the fluorescence origin to that of the prominent vibronic band at ~ 1400 cm^{-1}. That is, the more hydrophobic the environment of the pyrenyl chromophore the lower the R-value. With increasing hydrophobicity the linear electron-phonon coupling increases; for example, line narrowing in fluorescence or fluorescence excitation was not observed for the quasi-intercalated and solvent inaccessible (+)-3 and (-)-3 adducts (19). The strong coupling is presumably the result of a strong interaction between the pyrenyl chromophore and the bases, which imparts significant charge-transfer character to the S_1 state. On the basis of FLN spectra both (+)-1 and (-)-1 were assigned as N^2-dG-BPDE adducts. The (-)-4 and -5 species were suggested to be due to adducts of BPDE with a base(s) other than guanine, for example, adenine. Unavailability of appropriate standard adducts prevented more definitive assignments.

The results of Ref. (19) suggest that the above methodology should prove useful for the study of DNA repair and base sequence specificity of covalent

binding. It is the latter application that the present paper deals with. Specifically, we report the results of studies on adducts formed from (+)-anti-BPDE with the alternating co-polymers poly(dG-dC)·poly(dG-dC) and poly(dA-dT)·poly(dA-dT) and non-alternating poly(dG)·poly(dC) as well as single strand poly(dG) and the oligonucleotide d(ATATGTATA). Detailed comparisons of their fluorescence spectra, fluorescence quenching and other properties with those of (+)-anti-BPDE-DNA adducts are given in order to gain some insight about base sequence specificity. In addition, the fluorescence spectra of the *trans* and *cis* isomers of the adduct formed from guanine-monophosphate and (+)-anti-BPDE are used to assign the stereosymmetry of the (+)-1 and -2 DNA adducts. A fourth minor DNA adduct from (+)-anti-BPDE, (+)-4-DNA, is identified and assigned as N^6-dA (type II).

C. Experimental

1. Instrumentation

The underlying principles of the low temperature (4.2 K) FLNS and the associated instrumentation have been described in detail (13). The excitation source was a Lambda Physik FL-2002 dye laser pumped by a Lambda Physik EMG 102 MSC excimer laser. Typical intensities used for the FLNS (4.2 K) and $S_2 \leftarrow S_0$ (77 K) laser excited experiments were ~ 3 and ~ 30 mW/cm^2, respectively. Fluorescence was detected with a Princeton Instruments IRY-1024 intensified blue-enhanced gateable photodiode array. Gated detection was accomplished using a Lambda Physik EMG-97 zero-drift controller to trigger a FG-100 high voltage gate pulse generator which provides adjustable delay and width of the detector's

temporal observation window.

Laser excited fluorescence spectra at 77 K, obtained under non-line-narrowing conditions ($S_2 \leftarrow S_0$ excitation) were measured using a SRS Model SR280 boxcar averager (Stanford Research) equipped with two Model SR250 processor modules for channel A and B. Channel A was used to monitor the fluorescence signal, while channel B was used to monitor the pulse to pulse intensity jitter of the excimer pumped dye laser. All spectra reported were normalized for pulse jitter. The boxcar averager was interfaced through a SR245 computer interface module with a PC compatible computer for data acquisition and analysis.

The delay time for fluorescence measurements was 25 ns and the width of the observation window wa 60 nsec. Samples were dissolved in 30 μL of 5:4:1 glycerol-H_2O-EtOH in quartz tubes, taken through several freeze-pump-thaw degassing cycles, sealed, cooled to 4.2 K.

2. Materials

Calf thymus DNA was purchased from Worthington Chemicals (Freehold, NJ). The DNA was prepared and reacted with (+)-anti-BPDE or (-)-anti-BPDE as described previously (28, 29). The BPDE enantiomers were purchased from the NCI Chemical Carcinogen Reference Repository. The synthesis and purification of the polynucleotides poly(dG-dC)·poly(dG-dC), poly(dA-dT)·poly(dA-T), poly(dG)·poly(dG) and d(ATATGTATA) is described elsewhere (30, 31). For all adducts studied (incl. DNA) the % modification levels fell in the range 0.2-1.5, except for poly(dG) for which the level was 0.03. The synthesis of the adducts from (+)-anti-BPDE and guanine monophosphate and the isolation procedure for the

trans and *cis* isomers is given in Ref. (32). For all reaction products extreme care was taken to remove physically bound tetraols (33). The adducts were diluted in the glass forming solvent to a pyrenyl chromophore concentration of ~ 10^{-5} M.

For formation of physical adducts BPT (50 µl, 4 x 10^{-5} M) was mixed with DNA or poly(dG) (50 µl, 1 mg/ml). The mixture was sonicated for 5 min at 20 °C twice. Then, 150 µl of glycerol:ethanol solvent (5:1 by volume) was added to the mixture, followed by sonication for another 5 min.

For the fluorescence quenching studies, acrylamide (ACR) was employed at a concentration of 1 M, an optimal concentration for such studies (33).

D. Results and Discussion

Spectrofluorimetric analysis of native DNA and polynucleotide samples for covalent adducts formed with BPDE is complicated by the presence of BP tetraols or, more generally, non-covalently linked species which possess pyrene as the parent fluorescent chromophore. For the present work it is the tetraol of BPDE (referred to hereafter as BPT) that is of concern since it can be produced by hydrolysis or photodecomposition of the adducts. To identify interferences from BPT it is not sufficient to have only determined the fluorescence spectra of BPT in the solvent (glass) of interest. Although a considerable fraction of the BPT in a solution containing DNA is isolated by the solvent cage ("free" BPT), BPT also forms physical adducts with DNA (34). The differences in the intermolecular interactions between BPT and its environment for these two situations are sufficient to produce spectral shifts of several nm and differences in vibronic intensity distributions. Thus, it is essential to generate standard BPT fluorescence spectra

from samples for which BPT has been physically mixed with DNA (or poly-dG) in the solvent.

We have performed such experiments for tetraols from anti-BPDE mixed with DNA and poly(dG). Both 77 K laser excited ($S_2 \leftarrow S_0$) and 4.2 K FLN spectra for several excitation wavelengths were obtained and analyzed. In addition, fluorescence quenching studies (with ACR) were conducted in order to determine the degree of solvent accessibility for different BPT configurations. The results, although interesting from physico-chemical and spectroscopic points of view, are not central to the present paper and, therefore, are given in the Appendix. That is, the spectral features of BPT species shall be viewed here as potential interferences in the spectra of covalent adducts. Thus, for what follows, we need only summarize the essential findings: there are three BPT species with fluorescence origin bands at ~ 376, 377 and 381 nm; the first two bands are assigned to trans- or cis-BPT which are "free" or externally bound to a DNA base while the latter is due, at least in part, to quasi-intercalated BPT. All three types of BPT are subject to quenching by ACR; the degrees of quenching are discussed in the Appendix. The BPT species emitting at 376 and 377 nm are distinguishable from covalent BPDE adducts because their origins are significantly blue-shifted relative to those of the latter. In addition, these BPT species exhibit relatively narrow fluorescence bands in the 77 K spectra. This is not the case for the 381 nm emitting species, which is referred to as BPT-381 in what follows. BPT-381 represents a potentially serious interference for adducts since it can be easily misassigned to an intercalated covalent DNA adduct from (+)-anti-BPDE which exhibits an origin at 381 nm (19). This covalent adduct, however, can be differentiated from BPT-381 since its

fluorescence is not significantly quenched by ACR.

1. Preliminary remarks

The importance of establishing correlations between the moderate and high resolution fluorescence spectra of DNA and poly(oligo)nucleotide adducts is discussed in the Introduction. To this end, the analyses of laser excited ($S_2 \leftarrow S_0$) 77 K and FLN spectra as well as fluorescence quenching data are essential. Table II lists the polynucleotides and oligonucleotides whose adducts from (+)-anti-BPDE have been studied along with their abbreviations. For example, the alternating duplex poly(dG-dC)·poly(dG-dC) is denoted by $(dG\text{-}dC)_2$ and the non-alternating duplex poly(dG)·poly(dC) by (dG)·(dC). It proved important to study the (+)-anti-BPDE adducts of guanine-monophosphate monomer (GMP) since they are of the N^2-dG type.

Table III summarizes the spectral characteristics of the DNA and polynucleotide adducts from (+)-anti-BPDE. The results for the first three entries, (+)-1 DNA, (+)-2 DNA and (+)-3 DNA, are based primarily on our previous work (19), *cf.* Introduction. The peak position of the fluorescence origin band ($\lambda_{fl(0,0)}$) and its FWHM provide a good approximation to the energy and width of the $S_1 \leftarrow S_0$ absorption origin for each adduct listed in Table III. The band positions and widths were determined by analysis of the $S_2 \leftarrow S_0$ excited fluorescence spectra, as described elsewhere (19). Following the convention of this reference we label the adducts formed from each biomolecular species as (+)-j (j = 1,2, ...) with $\lambda_{fl,(0,0)}$ increasing with increasing j. For adduct assignments based on 77 K spectra, only two λ_{ex}-values, 346 and 355 nm, were required. The former and latter are

quite selective for BPDE-adducts whose $\lambda_{fl,(0,0)}$-values are lower or higher than ~ 379.0 nm, respectively (19). For example, although the major (+)-1 DNA adduct from (+)-anti-BPDE (an N^2-dG adduct) dominates the fluorescence spectrum for λ_{ex} = 346 nm, it is a minor contributor to the spectrum obtained with λ_{ex} = 355 nm (19). The latter spectrum is dominated by the (+)-3 adduct. We hasten to add, however, that a complete disentanglement of the spectra from a mixture will often require utilization of a fluorescence quencher such as ACR. For example, the fluorescence from the minor (+)-2 DNA adduct excited with λ_{ex} = 346 nm could only be resolved from that of the (+)-1 adduct when ACR was used to markedly suppress the emission from the latter (19) ((+)-1 is an exterior (type II) adduct and is readily accessible to ACR, whereas adducts of type I, such as (+)-2-DNA, are relatively less accessible).

Fluorescence line narrowing spectroscopy provides the ultimate spectral resolution for fluorescence-based characterization of biomolecular samples. Vibronic linewidths of only a few cm^{-1} are attainable, meaning that detailed analysis of both the ground and excited state vibrational modes of the fluorescent chromophore is possible. The principles of FLNS for analysis of DNA- and globin-PAH adducts have been recently reviewed (13). Briefly, the phenomenon of FLN is generally observable for narrow line laser excitation of the inhomogeneously broadened vibronic absorption bands of the $S_1 \leftarrow S_0$ absorption system. A reduction in the inhomogeneous broadening contribution to the vibronic fluorescence bands of up to two orders of magnitude can be achieved. Either origin- or vibronic, (1,0), excitation may be employed. The former yields a spectrum which contains only information pertaining to the ground state vibrational

modes. In contrast, vibronic excitation at different frequencies yields a series of spectra which provide the excited state mode frequencies and their relative absorption cross-sections. Because the excited state modes are more sensitive than ground state modes to substituent and environmental perturbations, vibronically excited FLNS is the more selective approach. The reader, who is not familiar with vibronically excited FLNS, may find the following discussion helpful. Let $\omega_{(0,0)}$ and Γ_{inh} be the center frequency and inhomogeneous width of the $S_1 \leftarrow S_0$ absorption origin. To generate a spectrum characterized by excited state vibrational modes in the frequency range $\approx \Omega \pm \Gamma_{inh}/2$ requires excitation at $\omega_{ex} \approx \omega_{(0,0)} + \Omega$. This frequency will generally excite several inhomogeneously broadened and overlapping vibronic absorption bands, α, β, ... The "isochromats" of bands α, β, ... selected by ω_{ex} undergo rapid vibrational relaxation ($\approx$ 1 picosecond) to their respective and energetically distinct positions in the overall distribution (inhomogeneous) of the zero-point vibrational level of the S_1 state. Subsequently, (0,0) fluorescence of the α, β, ... isochromats occurs to produce a <u>multiplet origin structure</u> in the $\approx \omega_{(0,0)} \pm \Gamma_{inh}/2$ spectral region, with as many (0,0)-components as vibrations excited by ω_{ex}. The differences between the frequencies of these components and ω_{ex} yield the excited state mode frequencies (13, 35, 36). For example, to generate excited state modes in the vicinity of 600 cm^{-1} for the (+)-1 DNA adduct, *cf.* Table III, one would employ a laser excitation wavelength of ~ 370 nm. An important point is that the multiplet origin structure is located in the region of the inhomogeneously broadened fluorescence origin produced under non-line narrowing conditions (i.e., $S_2 \leftarrow S_0$ excitation).

2. Synthetic polynucleotide adducts from (+)-anti-BPDE

The synthetic polynucleotides studied (Table II) are alternating or non-alternating purine-pyrimidine copolymers with backbone conformational parameters which place them in the B-DNA class. Since we have found that the alternating $(dG\text{-}dC)_2$ duplex adducts are most similar to those of DNA we focus on their $S_2 \leftarrow S_0$ excited 77 K and FLN spectra. Although it has been established that the excitation and emission spectra of (±)-anti-BPDE-$(dG\text{-}dC)_2$ are heterogeneous in nature (30, 37), the improved resolution of the spectra reported here are required for definitive distinction between different adduct types.

2a. Laser excited ($S_2 \leftarrow S_0$) fluorescence spectra at 77 K

Figure 2 shows the 77 K fluorescence spectra for (+)-anti-BPDE-$(dG\text{-}dC)_2$ obtained with λ_{ex} = 346 nm (A) and 355 nm (B). The "free" BPT bands at 376.1 and 376.8 nm bands are absent in spectrum A (*cf.* Appendix), which exhibits a dominant origin at ~ 377.6 nm (solid arrow) and a shoulder at 381 nm (dashed arrow). The shoulder is assigned first. The lower energy excitation at 355 nm results in a spectrum (B) for which the shoulder is resolved into the dominant origin, i.e., λ_{ex} = 355 nm discriminates against the 377.6 nm emitting species. Spectrum B is similar to that of BPT-381 (*cf.* Appendix), for example, the R-ratios are 1.34 and 1.36. (The R-ratio is defined as the intensity of the origin band to that of the most intense vibronic feature near 400 nm (19), *cf.* Introduction.) Furthermore, the 381 nm emitting species of spectrum B (Figure 2) and BPT-381 are both subject to significant and comparable quenching by ACR. There are other similarities, *cf.* Appendix. Thus, we conclude that the 381 nm emitting species

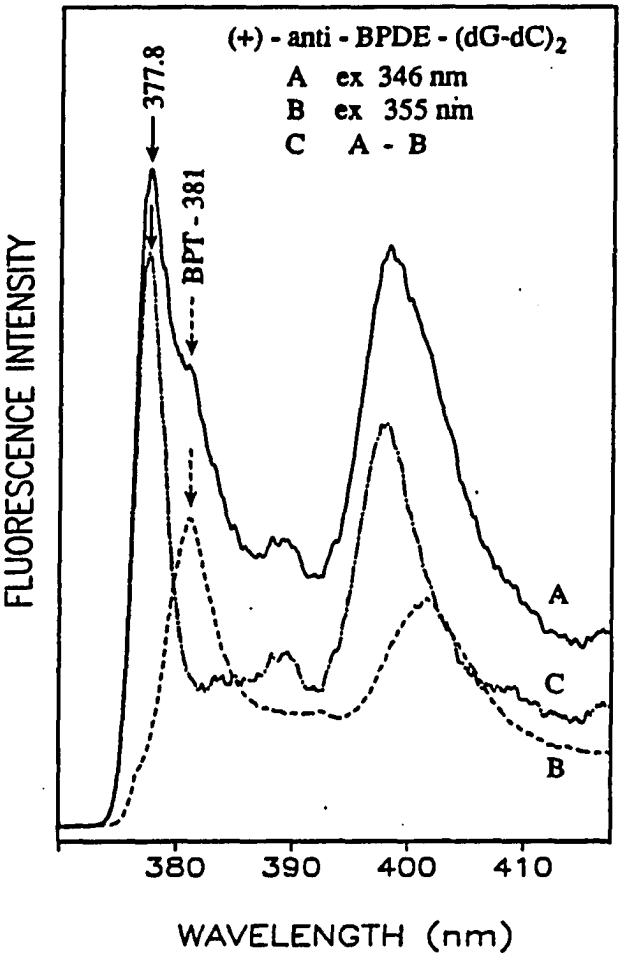

Figure 2. Laser-excited fluorescence spectra of (+)-anti-BPDE-$(dG\text{-}dC)_2$ for λ_{ex} = 346 nm (A) and λ_{ex} = 355 nm (B), respectively. The band at 381.1 nm corresponds to quasi-intercalated tetraol. Spectrum C is mainly due to the (+)1$(dG\text{-}dC)_2$ N^2-dG adduct

of (+)-anti-BPDE-(dG-dC)$_2$ is BPT-381 and not the (+)-3 adduct formed with DNA, *vide supra*. The latter is not subject to significant quenching and has an R-ratio of 1.15 (19), Table III. Furthermore, the (+)-3 adduct, unlike BPT-381 does not exhibit fluorescence line narrowing due to strong electron-phonon coupling produced by intercalation (19).

We turn next to the 377.6 nm origin band of Figure 2. Spectrum C of this figure is the A-B difference spectrum to which BPT-381 makes a negligible contribution. The difference spectrum is due primarily to the covalent adduct (+)-1-(dG-dC)$_2$, *cf.* Table III. There is also a weak contribution to the spectrum from a second adduct, (+)-2-(dG-dC)$_2$. Evidence for this is provided by Figure 3 which shows the origin-region for (+)-anti-BPDE-(dG-dC)$_2$ in the presence of ACR obtained with λ_{ex} = 346 nm (A) and 355 nm (B). Comparison of spectrum A with spectrum A of Figure 2 (no quencher) shows that ACR significantly quenches fluorescence from (+)-1-(dG-dC)$_2$, resulting in the dominance of the former by a band at ≈ 379 nm (due mainly to (+)-2-(dG-dC)$_2$). Nevertheless, (+)-1-(dG-dC)$_2$ is not completely quenched and is responsible for the shoulder at ≈ 377.5 nm (solid arrow). Utilization of λ_{ex} = 355 nm leads to essentially complete suppression of (+)-1-(dG-dC)$_2$ emission and a spectrum (B) from the (+)-2-(dG-dC)$_2$ adduct (BPT-381 makes, at most, a weak contribution). Spectrum C is that which when added to B, yields A. It is very similar to the origin band at 377.6 nm in Figure 2 and, therefore, is assigned to (+)-1-(dG-dC)$_2$. The S_1 origins for (+)-1- and (+)-2-(dG-dC)$_2$ are at 377.8 and 379.4 nm. These wavelengths are, within experimental uncertainty, the same as those for the (+)-1- and (+)-2-DNA adducts,

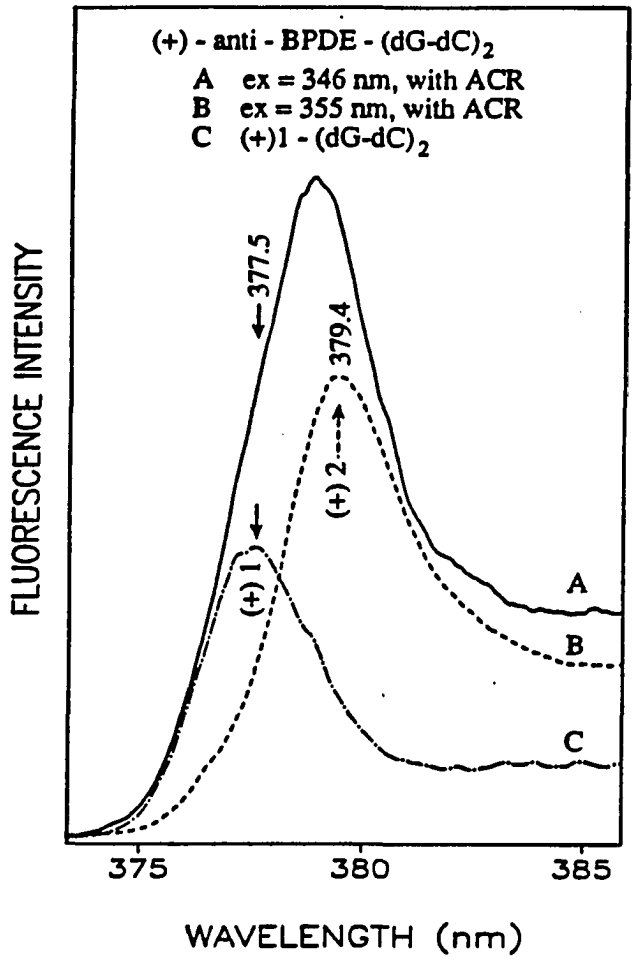

Figure 3. Origin bands of the 77 K laser-excited fluorescence spectra of (+)-anti-BPDE-$(dG\text{-}dC)_2$ in the presence of 1 M ACR, obtained with λ_{ex} = 346 nm (A) and λ_{ex} = 355 nm (B), respectively

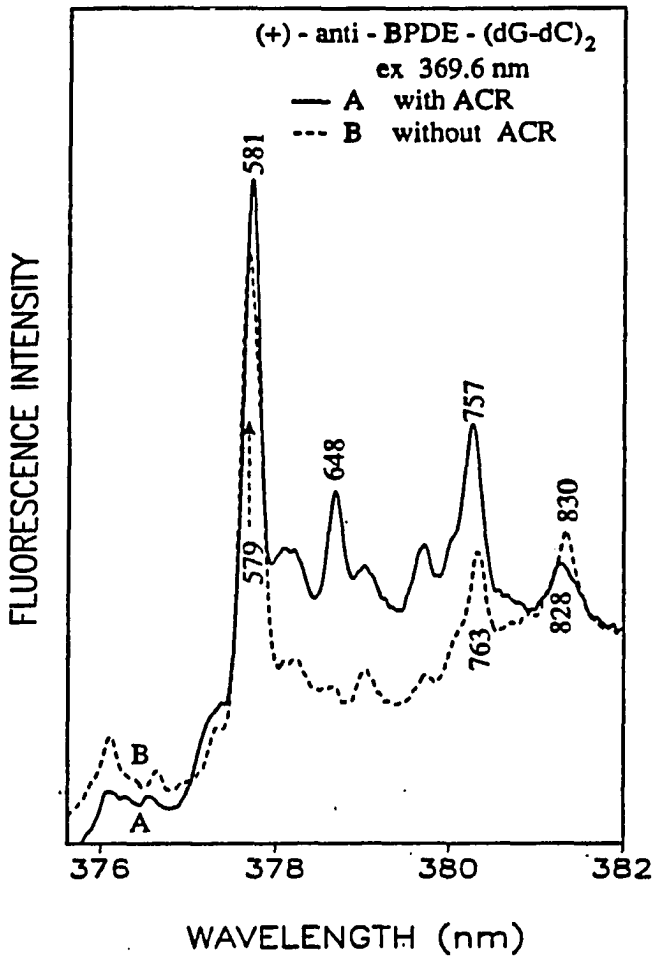

Figure 4. Comparison of FLN spectra of (+)-anti-BPDE-(dG-dC)$_2$ for experimental conditions which provide as the major adduct, (+)-1 (B) and (+)-2 (A), respectively (see also Figure 2). λ_{ex} = 369.6 nm, T = 4.2 K. Zero-phonon lines are labeled with excited-state vibrational frequencies

cf. Table III. Furthermore, the (+)-2-DNA adduct was also found to be significantly less quenchable by ACR than the (+)-1-DNA adduct.

2b. Laser-excited FLN spectra

The 4.2 K FLN spectra provide additional support for the above assignments of the (+)-1- and (+)-2-(dG-dC)$_2$ adducts. Figure 4 presents spectra obtained with λ_{ex} = 369.6 nm for (+)-anti-BPDE-(dG-dC)$_2$ in the presence (A) and absence (B) of ACR. This wavelength is that which was used to obtain multiplet origin structure for (+)-1-DNA in the ~ 600 cm^{-1} region (19). Spectrum B is dominated by the vibronic line at 579 cm^{-1}. This is also the case for (+)-1-DNA (19). However, the higher energy vibrations at 763 and 828 cm^{-1} are more prominent in spectrum B of Figure 4. The reason is that the (+)-2-(dG-dC)$_2$ adduct makes a greater contribution to the FLN spectrum. This follows from spectrum A of Figure 4, which shows that ACR produces an enhancement in modes at 648, 757 and 830 cm^{-1} relative to the mode near 579 cm^{-1} (now 581 cm^{-1}). Because the (+)-1-(dG-dC)$_2$ adduct is more efficiently quenched than (+)-2-(dG-dC)$_2$ and their S_1 origins are located at 377.8 and 379.4 nm, respectively, we conclude that spectrum A is due predominantly to the (+)-2-(dG-dC)$_2$ adduct. In the Appendix, it is shown that BPT-381 cannot be contributing appreciably to the 757 and 830 cm^{-1} bands of spectrum A. It is noteworthy that the modes for (+)-1- and (+)-2-(dG-dC)$_2$ are identical to those measured for (+)-1- and (+)-2-DNA (19). The possibility that the (+)-1-(dG-dC)$_2$ adduct contributes to the 581 cm^{-1} band of spectrum A in Figure 4 cannot be excluded since ACR does not completely quench its fluorescence.

In our studies of BPDE-DNA and BPDE-$(dG\text{-}dC)_2$ we have observed what are apparently irreversible changes in the fluorescence spectra of samples stored in the dark at - 5 °C over a period of several months. Although we have not studied this effect in detail, it is clear that aging results in a diminution of fluorescence from the (+)-1 adducts relative to that from (+)-2 adducts. For example, the R-value for (+)-anti-BPDE-DNA obtained with λ_{ex} = 346 nm was observed to decrease from 1.75, Table III, to 1.3 (with an accompanying red shift of the fluorescence spectrum) for one particular sample. Similar behavior was observed for an aged (+)-anti-BPDE-$(dG\text{-}dC)_2$ sample. These changes might be due to slow decomposition of the (+)-1 adduct into BPT, which then quasi-intercalates to form BPT-381 or, possibly, to conversion of (+)-1 into (+)-2 (in the following subsection both (+)-1 and (+)-2 adducts are assigned to an N^2-dG species). An example of the effect of aging on a FLN spectrum of (+)-anti-BPDE-$(dG\text{-}dC)_2$ is given in Figure 5. Spectra A and B were obtained in the absence and presence of ACR (0.5 M) with λ_{ex} = 356.9 nm. ACR is seen to preferentially quench the 1388, 1442 and 1522 cm^{-1} bands. In fact, spectrum B is identical to that of a fresh adducted $(dG\text{-}dC)_2$ sample (not shown) and is due primarily to the (+)-1-$(dG\text{-}dC)_2$ adduct. The A-B difference spectrum (C) represents the quenched fluorescence spectrum and is similar to that of "free" BPT. Thus, decomposition of (+)-anti-BPDE-$(dG\text{-}dC)_2$ to tetraols has occurred.

In Figure 5 the broad feature in spectra A and B near 381 nm is due to BPT-381 which is subject to quenching, *vide supra*. Increasing the ACR concentration to 1 M led to a further decrease in the intensity of the 381 nm band, *vide infra*.

3. Comparison of (+)-anti-BPDE adducts of DNA and polynucleotides

In this subsection Table III is used for a discussion of the similarities and differences between the fluorescence characteristics of the (+)-1-, (+)-2-, and (+)-3-DNA adducts and those of adducts formed with $(dG\text{-}dC)_2$, (dG)·(dC) and (dG). For the sake of brevity, spectra for the latter two polynucleotides have not been presented and only a portion of the FLN spectra obtained for $(dG\text{-}dC)_2$ are shown. The first column of Table III lists the adducts; when more than one adduct from the precursor is observed the major adduct is so labeled. Thus, for example, (+)-1-DNA and (+)-1-$(dG\text{-}dC)_2$ are major adducts. The second and third columns provide the wavelength and width of the inhomogeneously broadened fluorescence origin, while the fourth column gives the R-value. These parameter values, together with the degree of quenchability by ACR, are most important for the above comparison.

From Table III one observes that all polynucleotides, except $(dA\text{-}dT)_2$, yield an adduct with a fluorescence origin at ~ 378 nm, a (+)-1 adduct. We emphasize again, however, that the adducts for each polynucleotide are labeled as (+)-j, with increasing j corresponding to increasing $\lambda_{fl(0,0)}$. That is, adducts from different polynucleotides with the same j-value need not necessarily be the same (chemically and/or structurally). Figure 6 gives the FLN spectra for the standard *trans* isomer of the (+)-anti-BPDE-N^2-GMP adduct (spectrum C), (+)-1-DNA (spectrum A), (+)-anti-BPDE-$(dG\text{-}dC)_2$ (spectrum B), (+)-anti-BPDE-(dG)·(dC) (spectrum D) and (+)-anti-BPDE-(dG) (spectrum E). All spectra were obtained with λ_{ex} = 369.6 nm, which is quite highly selective for (+)-1 adducts whose S_1 state is located at

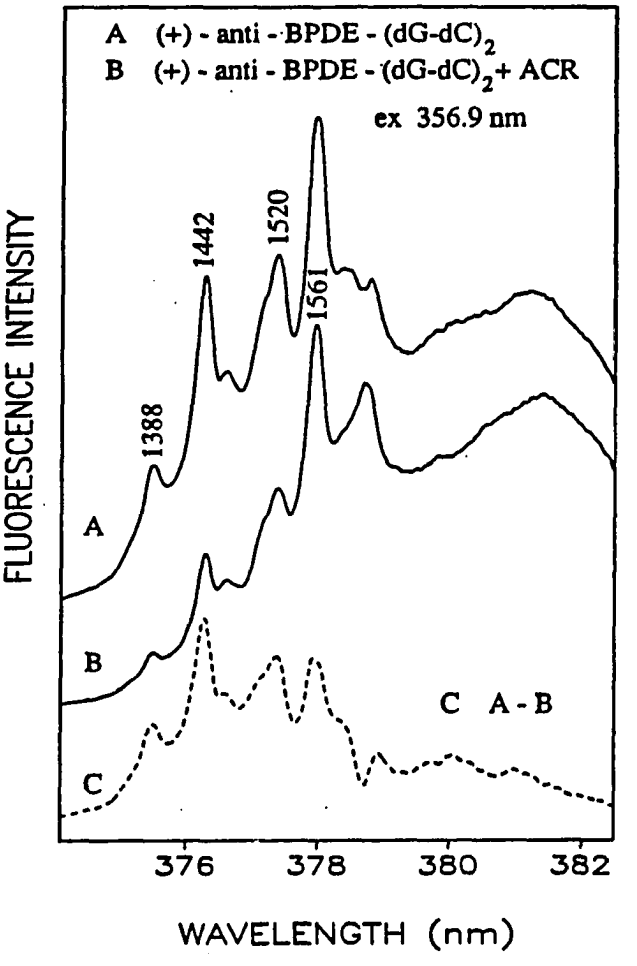

Figure 5. FLN spectra of (+)-anti-BPDE-$(dG\text{-}dC)_2$ contaminated with BPT obtained without (A) and with quencher (0.5 M ACR) (B). λ_{ex} = 356.9 nm, T = 4.2 K. Spectrum C represents the quenched contribution originating mostly from "free" BPT

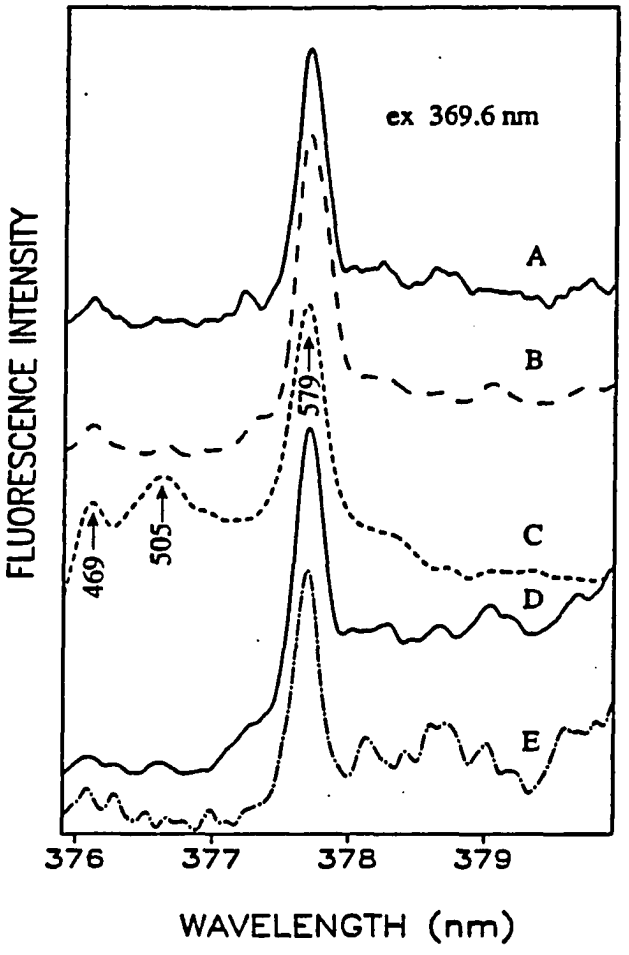

Figure 6. Comparison of FLN spectra: (+)-anti-BPDE-DNA, (+)-1 adduct (A); (+)-anti-BPDE-(dG-dC)$_2$ (B); *trans* isomer of (+)-anti-BPDE-N2-GMP (C); (+)-anti-BPDE-(dG)-(dC) (D); (+)-anti-BPDE-poly(dG) (E). λ_{ex} = 369.6 nm, T = 4.2 K

~ 378 nm. That the spectrum for (+)-1-DNA is dominated by the 579 cm^{-1} mode was established earlier (19). The close similarity of the spectra in Figure 6 establishes that all adducts are of the N^2-dG type. Furthermore, the standard spectrum of the cis isomer of (+)-anti-BPDE-N^2-GMP is distinctly different from that of the *trans* isomer (spectrum C) (38). Thus, we may conclude that the (+)-1 adducts are *trans* isomers, a conclusion consistent with that of earlier work (39). We note that the (+)-2 adduct from (dG)·(dC) probably contributes to spectrum D since its S_1 state is almost degenerate with that of the (+)-1 adduct.

The (+)-1-DNA adduct and the *trans* isomer of (+)-anti-BPDE-GMP exhibit the same R-value of 1.75, Tables III and IV. This result, together with spectra A and C of Figure 6, support our earlier assignment (19) for (+)-1-DNA to a type II (external) adduct with high quenching efficiency. Inspection of Table III reveals that it is the (+)-1 adduct of $(dG\text{-}dC)_2$ whose R-value (1.55) and other fluorescence characteristics are most similar to those of (+)-1-DNA. For example, the R-values for the (+)-1 adducts of (dG)·(dC) and (dG) are considerably smaller (1.20 and 1.15), indicating that they correspond to a type I (interior) site (19). Consideration of the values given in Table III for the widths of the fluorescence origin bands due to inhomogeneous broadening (the linear electron-phonon coupling is weak for all (+)-1 adducts, as judged by the FLN spectra, and makes only a negligible contribution to the bandwidth reveals that the structure of (dG) is highly irregular, thereby providing a relatively less ordered environment for the *trans* (+)-1-N^2-dG adduct. Coiling of (dG) probably contributes to the heterogeneity. It should also be noted that the adducts from (dG)·(dC) are distinct from those of DNA and $(dG\text{-}dC)_2$ in that the (dG)·(dC) (+)-1 adduct is less quenchable by ACR than the

(+)-2 adduct. Table III also reveals that it is the (+)-2 adduct of $(dG\text{-}dC)_2$ which is most similar to (+)-2-DNA.

Thus, the alternating $(dG\text{-}dC)_2$ copolymer affords a structure conducive to the formation of two adducts with spectral and other properties which are very similar to the (+)-1 (type II) and (+)-2 (type I) adducts identified in previous work (19). However, this copolymer does not yield an adduct of the intercalated and non-quenchable (+)-3-DNA type with a fluorescence origin at ~ 381 nm. This adduct does not exhibit line narrowing in its fluorescence or excitation spectra due to strong electron-phonon coupling (19). In the Appendix it is shown that BPT-381, which can be easily mistaken for a covalent adduct of the (+)-3 type, does exhibit line narrowing and is quenchable by ACR. Figure 7 compares the 4.2 K fluorescence spectra of (+)-anti-BPDE-DNA and -$(dG\text{-}dC)_2$ obtained with λ_{ex} = 356.9 nm ($S_1 \leftarrow S_0$ vibronic excitation) and in the presence of 1 M ACR. Although fluorescence from the (+)-1 adduct is significantly quenched, (+)-1 is still the major contributor to the sharp vibronic features at 1442, 1519, 1560 and 1606 cm^{-1} ((+)-2 is a minor adduct for DNA (19) and $(dG\text{-}dC)_2$). The close similarity between these features for DNA and $(dG\text{-}dC)_2$ further confirms that $(dG\text{-}dC)_2$ yields an exterior type II adduct of the (+)-1-DNA type. It is, however, the broad feature at ~ 381 nm for (+)-anti-BPDE-DNA that is of primary interest, spectrum A. It is the fluorescence origin of (+)-3-DNA (19). Spectra obtained without ACR (not shown) show that this fluorescence is not quenchable. In contrast, $(dG\text{-}dC)_2$ emission at 381 nm is quenchable. (The degree of quenching for 1 M ACR is higher than for 0.5 M ACR, see Figure 5). Figure 7 and other results

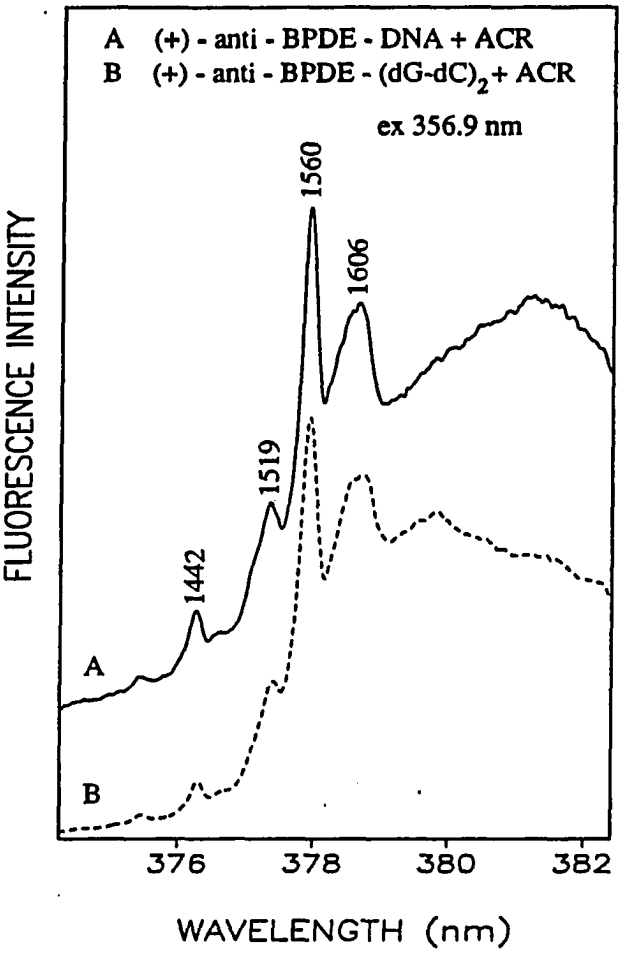

Figure 7. FLN spectra of (+)-anti-BPDE-DNA (A), and (+)-anti-BPDE-$(dG\text{-}dC)_2$ (B) in the presence of 1 M ACR. λ_{ex} = 356.9 nm, T = 4.2 K

establish that $(dG\text{-}dC)_2$ does not yield an appreciable amount of an intercalated adduct. This is consistent with the finding that the intercalation association constant for this duplex is small relative to that of DNA (37, 40). The explanation may lie in the fact that DNA has many intercalation binding sites, 10 when strand polarity is taken into account. In addition, the reactivities of guanines with (+)-anti-BPDE are distinctly non-statistical with respect to sequence (11, 12, 41).

In summary, all polynucleotides studied yield a (+)-1 adduct of the trans-N^2-dG type whose special characteristics are very similar to those of (+)-1-DNA. However, it is the alternating $(dG\text{-}dC)_2$ that provides the best model for the (+)-1 and (+)-2-DNA adducts. The FLN spectra of the (+)-1 and -2 adducts, when compared with those of the standard *trans* isomer of (+)-anti-BPDE-GMP, reveal that both are the *trans* isomer of the N^2-dG covalent adduct. As noted earlier, the FLN spectra of the *cis* isomer of (+)-anti-BPDE-GMP are distinct from those of the *trans* isomer. Furthermore, HPLC analysis of the nucleotide adducts from $(dG\text{-}dC)_2$ and (+)-anti-BPDE has shown that only the *trans* isomer is formed (32). Of course, with this analysis procedure all information pertaining to different DNA sites for the same chemical adduct is lost. The present and earlier work (19) establishes that the (+)-1 adduct for DNA and $(dG\text{-}dC)_2$ is of type II or exterior (solvent accessible) with a relatively weak interaction between the pyrene chromophore and bases. The (+)-2 adduct is characterized by a stronger interaction (with concomitant red shift of the S_1 state) and has a more interior (hydrophobic) configuration, albeit not an intercalated configuration as is the case for (+)-3-DNA. The chemical structure of the latter is considered later.

4. Anti-BPDE adducts of an oligodeoxynucleotide with specific base composition

According to the above analysis, the (+)-1 and (+)-2 adducts of trans-N^2-dG for DNA and $(dG\text{-}dC)_2$ are not of the intercalated type. If this is correct then one might expect to observe both adducts for an oligodeoxynucleotide such as d(ATATGTATA). On the other hand, an intercalated adduct of the (+)-3-DNA type should not be observed. The single strand d(··TGT··) provides for high yields of N^2-dG adducts (31). For (+)-anti-BPDE and (-)-BPDE the trans:cis ratios are 7:1 and 2:1, respectively, as determined by HPLC analysis following enzymatic digestion (31). Table IV summarizes the spectral characteristics of the *trans* and *cis* standard isomers of the N^2-dG adduct from GMP and the *trans* and *cis* isomers from d(··TGT··). Only spectra for the *trans* isomers from d(··TGT··) are shown.

Figure 8 presents 77 K fluorescence spectra for a (+)-anti-BPDE-deoxynucleotide sample containing only the *trans* N^2-dG adduct (as determined by HPLC analysis). Spectra A and B were obtained with λ_{ex} = 355 and 346 nm, respectively. Only the origin regions are shown. Spectrum A is dominated by an origin near 379 nm but exhibits a distinct shoulder at ~ 377 nm. The latter origin dominates the spectrum (B) for λ_{ex} = 346 nm (recall that this wavelength is optimum for a (+)-1 adduct while λ_{ex} = 355 nm discriminates against the (+)-1 adduct (in favor of (+)-2)). Thus, the picture which emerges is very similar to that seen earlier for DNA and $(dG\text{-}dC)_2$. Straightforward deconvolution leads to the assignment of two covalent adducts with fluorescence origins at 377.6 and

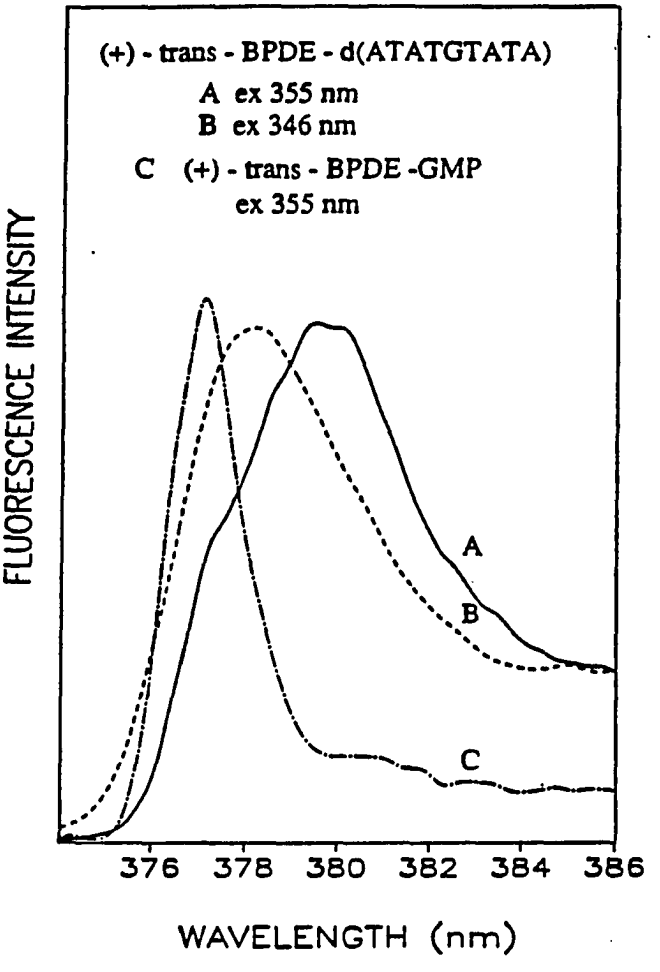

Figure 8. A comparison of 77 K laser-excited fluorescence spectra of (+)-anti-*trans*-BPDE-d(ATATGTATA) for λ_{ex} = 355 nm (A) and 346 nm (B) with spectrum of trans isomer (+)-anti-BPDE-GMP (C), obtained with λ_{ex} = 355 nm

379.6 nm, Table IV. These wavelengths are essentially identical to those for the (+)-1 and (+)-2 adducts of DNA and $(dG\text{-}dC)_2$, Table II. Only one *trans* N^2-dG adduct is observed from GMP, spectrum C of Figure 8. Its origin is slightly blue shifted relative to 377.6 nm and is slightly contaminated by BPT, which gives rise to a barely discernible low energy shoulder.

The covalent adducts from d(··TGT··) are prone to very slow decomposition into tetraols. Figure 9 presents FLN spectra obtained with λ_{ex} = 356.9 nm for a fresh sample (A) and partly decomposed (B) sample. These spectra should be compared with those of Figure 7, from which it may be concluded that spectrum A of Figure 9 exhibits narrow vibronic features (1388-1603 cm^{-1}) which are essentially identical to those of (+)-anti-BPDE-DNA and -$(dG\text{-}dC)_2$ due primarily to the dominant (+)-1 adduct. A striking difference between the spectra of Figures 7 and 9 is the absence of the broad ~ 381 nm emission in the latter. Thus the (+)-3 adduct or BPT-381, as the case may be, are absent for the deoxyoligonucleotide. Returning to the tetraol contaminated spectrum (B) of Figure 9, we note that our standard FLN spectra establish that the increased intensities of the lower frequency modes (e.g., 1443 cm^{-1}) relative to the 1560 cm^{-1} mode is entirely consistent with fluorescence from "free" BPT.

Comparison of the R-values of 1.55 and 1.3 for the 377.6 and 379.6 nm *trans* adducts of d(··TGT··) (referred to hereafter as A and B) with those of the (+)-1 and (+)-2 adducts of DNA and $(dG\text{-}dC)_2$, Table III, provides additional support for strong correlations. The A and B conformations are actually quite stable. Heating to 80 °C or prolonged laser irradiation at 355 nm did not lead to significant

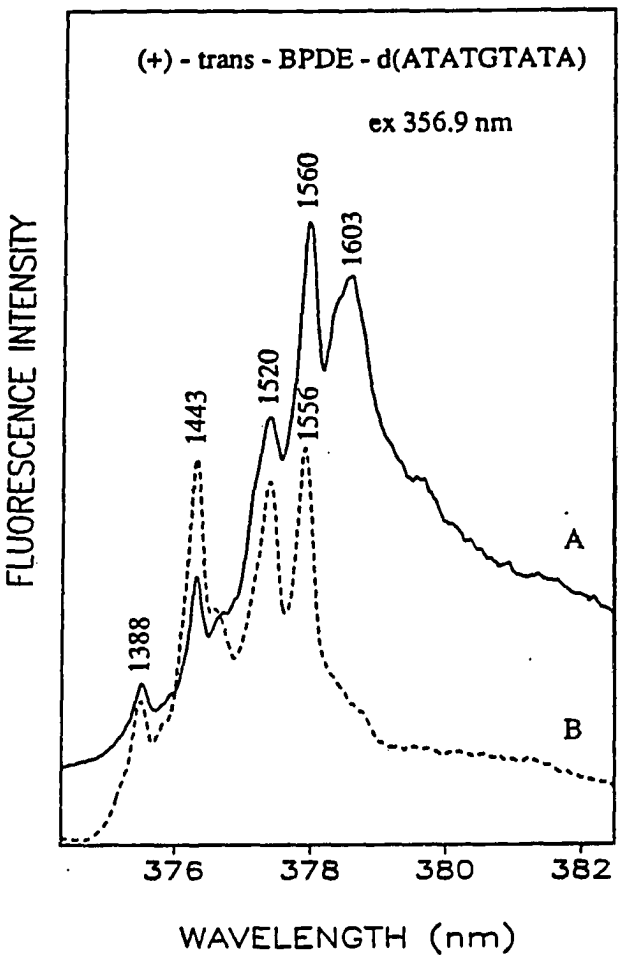

Figure 9. Comparison of FLN spectrum of (+)-anti-trans-BPDE-d(ATATGTATA) adducts (A) with that from a decomposed sample (B), λ_{ex} = 356.9 nm, T = 4.2 K

changes in the low temperature fluorescence spectra. However, heating to 80 °C produced a significant blue shift of the $S_2 \leftarrow S_0$ absorption. Upon subsequent cooling to room temperature the original absorption spectrum was recovered. This suggests that the A and B conformations of the *trans* N^2-dG adduct may be of the base-base stacking type since stacking interactions can be disrupted at higher temperatures.

The results of this sub-section indicate that the A and B conformations of the *trans* N^2-dG adduct from d(··TGT··) are very similar to those for the (+)-1 and -2 adducts of DNA and $(dG\text{-}dC)_2$ and provide strong support for the analysis procedure utilized in the earlier sub-sections and work (19).

5. Assignment of a (+)-anti-BPDE-deoxyadenosine adduct of DNA

As discussed in the Introduction, (-)-anti-BPDE yields a more heterogeneous distribution of DNA adducts than (+)-anti-BPDE which consists of 5 covalent adducts, (-)-j (j = 1-5). Although the relative levels of (-)-j (j = 1-3) differ significantly from those of (+)-j (j = 1-3), the spectral and quenching characteristics of the adducts with the same j-level are identical. It was suggested that (19) the (-)-4 adduct could be associated with a base other than guanine, for example, adenine, since its $\lambda_{fl,(0,0)}$ of 382.7 nm is higher than those of (-)-j (j = 1-3) and, yet, the adduct is of type II. Osborne et al. (26) and Brookes and Osborne (27) have reported that (+)- and (-)-BPDE-DNA consists of 2% and 18% of N^6-dA adducts, respectively, which could explain why the (+)-4 adduct could not be detected (19). In an attempt to identify this minor adduct studies of (+)-anti-BPDE-$(dA\text{-}dT)_2$ were undertaken. First, the results from 77 K fluorescence studies summarized in Table

III show, as expected, that the (+)-1 and (+)-2 from dG are absent. Only one adduct with a fluorescence origin at 382.5-383.0 nm was identified and is of type II. These characteristics are identical to those of (-)-4-DNA.

Figure 10 compares the FLN spectra of (+)-anti-BPDE-DNA (A) and (+)-anti-BPDE-(dA-dT) (B) obtained with λ_{ex} = 374.2 nm. This wavelength was chosen to reveal mode structure in the 600 cm^{-1} region for adducts with a fluorescence origin near 382 nm. The spectra exhibit the same modes, for example, 472 and 585 cm^{-1}. The latter is the counterpart of the 579 cm^{-1} mode of the (+)-1 and -2 adducts. The frequency shift of 6 cm^{-1} is large and, by itself, could be used to distinguish between N^2-dG and N^6-dA adducts of BPDE. However, the vibronic intensity distributions of spectra A and B in Figure 10 are different. Two possible explanations for this are that (+)-2-DNA makes a significant contribution to the 472 cm^{-1} band of spectrum A and that the *trans* to *cis* distributions for DNA and $(dA\text{-}dT)_2$ are different. The FLN spectrum for (-)-4-DNA is similar to those of Figure 10. The FLN data indicate that the (+)-4 and (-)-4 adducts possess the same chemical structure and, furthermore, that they are not N^2-dG adducts. Consistent with the results of Osborne et al. (26), we have observed a much higher relative signal strength from (-)-4-DNA than from (+)-4-DNA. On the basis of their work it is not reasonable to assign both adducts as N^6-dA. The structures of the *trans* isomer of this adduct and N^2-dG are shown in Figure 11.

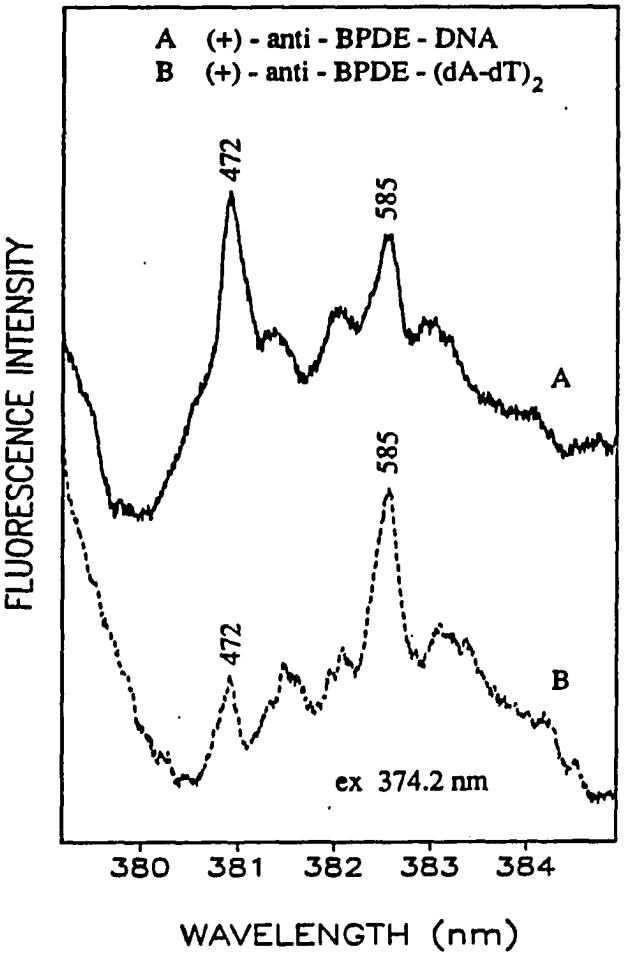

Figure 10. Comparison of FLN spectra: (+)-anti-BPDE-DNA (A) and (+)-anti-BPDE-$(dA\text{-}dT)_2$. λ_{ex} = 374.2 nm, T = 4.2 K.

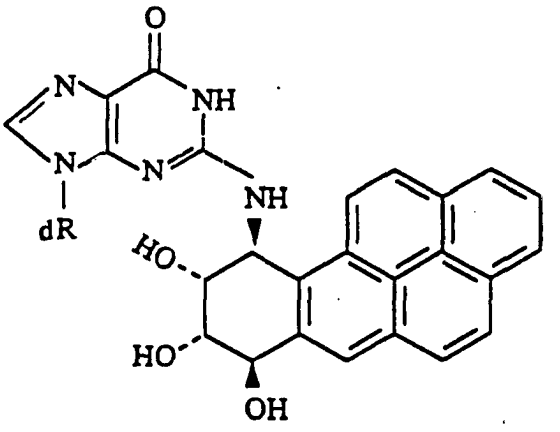

A) 2 - NH_2 - dG

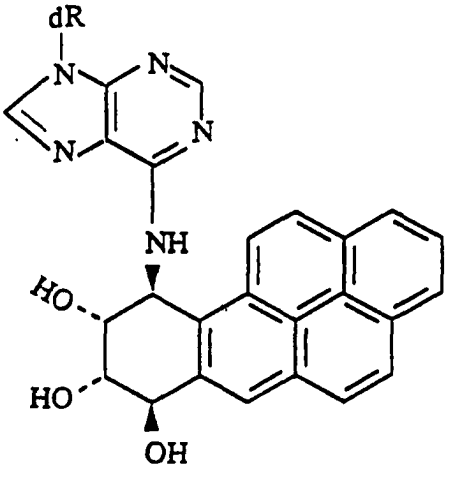

B) 6 - NH_2 - dA

Figure 11. Structures of the N^2-dG (2-NH_2) (A), and N^6-dA (6-NH_2) (B) adducts formed from (+)-anti-BPDE

E. Conclusions and Further Discussion

This work shows that FLNS in combination with fluorescence quenching and laser excited $S_2 \leftarrow S_0$ fluorescence spectroscopy can distinguish between chemically and/or structurally (site) different adducts of BPDE in the distribution of adducts from a polynucleotide. Furthermore, differences in the type and heterogeneity of distributions from different polynucleotides and single strand oligonucleotides can be detected. By themselves the results establish that the major DNA adduct from the stereoselective reaction with (+)-anti-BPDE (~ 85%) is the *trans* isomer of N^2-dG, which is in accord with previous work (39). The (+)-2-DNA is also an N^2-dG adduct which is suggested to be the same stereoisomer in a different site configuration. The (+)-3-DNA adduct also involves binding to dG and this, together with the results of other workers (26, 27), indicate that it is probably intercalated O^6-dG. A fourth, very minor adduct ((+)-4-DNA) was observed and assigned as N^6-dA. It should be noted that the major (+)-1-DNA adduct does not appear to be responsible for the high mutagenic activity of (+)-anti-BPDE (27, 42). It has been shown, for example, that 36% of the activation of the ras protoncogene *in vitro* by (+)-anti-BPDE occurs at the adenine residue (43), despite the latter's low reactivity. Therefore, the characterization and determination of minor stable adducts and labile adducts which undergo elimination (e.g., the alkali labile N^7-dG adduct (11, 12, 41)) is very important (26, 27, 42, 43).

In this work only three polynucleotide duplexes ($(dG\text{-}dC)_2$, (dG)·(dC), $(dA\text{-}dT)_2$) were studied and of these it is the alternating $(dG\text{-}dC)_2$ that yields (+)-1 and -2 adducts which are most similar to the *trans* N^2-dG adducts of DNA. However, the R-ratio for (+)-1-$(dG\text{-}dC)_2$ of 1.55 is somewhat lower than the value

of 1.75 for (+)-1-DNA. Since (dG)·(dC) and d(ATATGTATA) yield an N^2-dG adduct with spectral properties similar to those of (+)-1-DNA and dG tracts have been found to be particularly conducive to reactions of (+)-anti-BPDE with dG (11, 12, 31, 41) it is most likely that in native DNA more than one type of base-triplet involving dG contributes to the (+)-1-DNA fluorescence. This is probably also the case for (+)-2 and -3-DNA. The $(dG\text{-}dC)_2$ duplex, however, does not yield an adduct with the spectral properties of (+)-3-DNA. The only duplex that does is (dG)·(dC) and so it is possible that a dG tract is important for the formation of the (+)-3 intercalated adduct.

Although our results for the adducts from (-)-anti-BPDE with the above polynucleotides have not been presented, they support our finding that the laser excited $S_2 \leftarrow S_0$ fluorescence spectra, FLN spectra and quenching properties of the (+)-j-DNA and (-)-j-DNA adducts with the same j-value (j = 1-4) are exceedingly similar (only the distributions differ). Since we have shown that the *trans* and *cis* isomers of the N^2-dG adduct with GMP are readily distinguishable by FLNS, the above close similarity suggests that (+)-j-DNA and (-)-j-DNA are enantiomeric pairs, *cf.* Figure 2. Distinction between the two enantiomers would depend, in part, on interactions with chiral centers of neighboring bases which, if weak, would not allow for distinction by FLNS. We note that we have shown that the (+)- and (-)-anti-BPDE-DNA adducts can be distinguished from those from racemic syn-BPDE by FLNS (20).

Although (+)- and (-)- anti-BPDE form stable adducts, the former is significantly more mutagenic for the same total adduction (stable) level in repair-competent cells (1, 27). Both are comparably mutagenic in the repair deficient

Salmonella typhimurium strain (44). Our results provide a more detailed picture of the differences in the adduct distributions from (+)- and (-)-anti-BPDE but the different mutagenic activities of the two enantiomeric forms cannot be understood in terms of the adduct (stable) distributions without invoking unique site structural properties of the (+)-j and (-)-j adducts (6, 42, 43). However, if one is to hold to the assumption that it is the diol epoxide metabolic pathways of BaP which, *in vivo*, lead to mutagenesis and tumorigenesis than the roles of labile adducts and (+) and (-)-syn-BPDE must be more carefully assessed. In addition, the possibility that the radical cation (one-electron oxidation) metabolic pathway may be important for mutagenesis and carcinogenesis is now distinct (8, 25).

F. References

1. Thakker, D. R., Yagi, H., Levin, W., Wood, A. W., Conney, A. H. and Jerina, D. M. (1985). Polycyclic aromatic hydrocarbons: metabolic activation to ultimate carcinogens. In Bioactivation of Foreign Compounds, Anders, M. W., Ed., Academic Press, New York, pp 177-242.
2. Stevens, C. W., Bouck, N., Burgess, J. A. and Fahl, W. E. (1985). Benzo(a)pyrene diol epoxides: different mutagenic efficiency in human and bacterial cells. Mut. Res. 152, 5-14.
3. Pelling, J. C., Neades, R. and Strawhecker, J. (1988). Epidermal papillomas and carcinonmas induced in uninitiated mouse skin by tumor promoters along contain a point mutation in 61st codon of the Ha-ras oncogene. Carcinogenesis, 9, 665-667.
4. Geacintov, N. E. (1988). Mechanisms of reaction of polycyclic aromatic

epoxide derivatives with nucleic acids. In Polycyclic Aromatic Hydrocarbon Carcinogenesis: Structure-Activity Relationships, Yang, S. K., and Silverman, B. D., eds., Vol. 2, CRC Press, Boca Raton, FL, pp 181-206.

5. Geacintov, N. E. (1985). Mechanisms of interaction of polycyclic aromatic diol epoxides with DNA and structures of the adducts. In Polycyclic Hydrocarbons and Carcinogenesis, Harvey, R. G., Ed., ACS Press, Washington, D.C., pp 107-124.
6. Gräslund, A. and Jernström, B. (1989). DNA-carcinogen interaction: covalent DNA-adducts of benzo(a)pyrene 7,8-dihydrodiol 9,10-epoxides studied by biochemical and biophysical techniques. Quart. Revs. Biophys. 22, 1-37.
7. Lehr, R. E., Kumar, S., Levin, W., Wood, A. W., Chang, R. L., Conney, A. H., Yagi, H., Sayer, J. M. and Jerina, D. M. (1985). The bay region theory of polycyclic aromatic hydrocarbon carcinogenesis. In Polycyclic Hydrocarbons and Carcinogenesis, Harvey, R. G., Ed., ACS Press, Washington, D.C., pp 63-84.
8. Cavalieri, E. and Rogan, E. (1985). Role of radical cations in aromatic hydrocarbon carcinogenesis. Environ. Health Perspect., 64, 69-84.
9. Glatt, H. and Oesch, F. (1986). Structural and metabolic parameters governing the mutagenicity of polycyclic aromatic hydrocarbons. Chem. Mut., 10, 73-127.
10. Stevens, C. W., Manoharan, T. H. and Fahl, W. E. (1988). Characterization of mutagen-activated cellular oncogenes that coner anchorage independence to human fibroblasts and tumorigenicity to NIH 3T3 cells: sequence analysis of

an enzymatically amplified mutant HRAS alkele. Proc. Natl. Acad. Sci., USA, 85, 3875-3879.

11. Boles, T. C. and Hogan, M. E. (1986). High-resolution mapping of carcinogen binding sites on DNA. Biochemistry, 25, 3039-3043.
12. Lobanenkov, V. V., Plumb, M., Goodwin, G. M. and Grover, P. L. (1986). The effect of neighboring bases on G-specific DNA cleavage mediated by treatment with the anti-diol epoxide of benzo(a)pyrene *in vivo*. Carcinogenesis, 7, 1689-1695.
13. Jankowiak, R. and Small, G. J. (1989). Fluorescence line-narrowing spectrometry in the study of chemical carcinogenesis. Anal. Chem., 61, 1023-1032.
14. Heisig, V., Jeffrey, A. M., McGlade, M. J. and Small, G. J. (1984). Fluorescence-line-narraowed spectra of polycyclic aromatic carcinogen-DNA adducts. Science, 223, 289-291.
15. Sanders, M. J., Cooper, R. S., Small, G. J., Heisig, V. and Jeffrey, A. M. (1985). Identification of polycyclic aromatic hydrocarbon metabolite sin mixtures using fluorescence line narrowing spectrometry. Anal. Chem., 57, 1148-1152.
16. Sanders, M. J., Cooper, R. S., Jankowiak, R., Small, G. J., Heisig, V. and Jeffrey, A. M. (1986). Identification of polycyclic aromatic hydrocarbon metabolites and DNA adducts in mixtures using fluorescence line narrowing spectrometry. Anal. Chem., 58, 816-820.
17. Zamzow, D., Jankowiak, R., Cooper, R. S. and Small, G. J. (1989). Fluorescence line narrowing spectrometric analysis of benzo[a]pyrene-DNA

adducts formed by one-electron oxidation. Chem. Res. Toxicol. 2, 29-34.

18. Jankowiak, R., Cooper, R. S., Zamzow, D., Small, G. J., Heisig, V. and Jeffrey, A. M. (1988). Fluorescence line narrowing-nonphotochemical hole burning spectrometry: Femtomole detection and high selectivity for intact DNA-PAH adducts. Chem. Res. Toxicol., 1, 60-68.
19. Jankowiak, R., Lu, P. and Small, G. J. (1990). Laser spectroscopic studies of DNA adduct structure types from enantiomeric diol epoxides of benzo[a]pyrene. Chem. Res. Toxicol., 3, 39-46.
20. Jankowiak, R., Lu, P. and Small, G. J. (1990). Fluorescence line narrowing spectrometry: A versatile tool for the study of chemically initiated carcinogenesis. J. Pharm. Biomed. Anal. (in press).
21. Cooper, R. S., Jankowiak, R., Hayes, J. M., Lu, P. and Small, G. J. (1988). Fluorescence line narrowing spectrometry of nucleoside-polycyclic aromatic hydrocarbon adducts on thin-layer chromatographic plates. Anal. Chem., 60-2692-2694.
22. Jankowiak, R., Day, B. W., Lu, P., Doxtader, M. M., Skipper, P. L., Tannenbaum, S. R. and Small, G. J. (1990). Fluorescence line-narrowing spectral analysis of *in vivo* human hemoglobin-benzo[a]pyrene adducts: Comparison to synthetic analogues. J. Am. Chem. Soc. (accepted publication).
23. Varanashi, U., Reichert, W. L., Eberhart, B. T. L. and Stein, J. E. (1989). Formation and persistence of benzo[a]pyrene-diolepoxide-DNA adducts in liver of English sole (Parophrys vetulus). Chem. Biol. Interaction, 69, 203-216.
24. Lu, P. (1990). Laser excited fluorescence studies of cellular macromolecular damage from chemical carcinogens. Ph.D. Dissertation, Iowa State University,

Ames, Iowa (in preparation).

25. Rogan, E. G., Ramakrishna, N. V. S., Higginbothan, S., Cavalieri, E. L., Jeong, H., Jankowiak, R. and Small, G. J. (1990). Identification and quantitation of 7-(benzo[a]pyrene]6]yl)guanine in the urine and feces of rats treated with benzo[a]pyrene, submitted to Chem. Res. Toxicol.

26. Osborne, M. E., Jacobs, S., Harvey, R. G. and Brooks, P. (1980). Minor products from the reaction of (+) and (-) benzo[a]pyrene-anti-diol-epoxide with DNA. Carcinogenesis, 2, 553-558.

27. Brookes, P. and Osborne, M. R. (1982). Mutation in mammalian cells by stereoisomers of anti-benzo[a]pyrene-diolepoxide in relation to the extent and nature of the DNA reaction products. Carcinogenesis, 3, 1223-1226.

28. Geacintov, N. E., Ibanez, V., Gagliano, A. G., Jacobs, S. A. and Harvey, R. G. (1984). Stereoselective covalent binding of anti-benzo[a]pyrene diol epoxide to DNA. Conformation of enantiomer adducts. J. Biomol. Struct. Dynamics, 1, 1473.

29. Geacintov, N. E., Yoshida, H., Ibanez, V., Jacobs, S. A. and Harvey, R. G. (1984). Conformations of adducts and kinetics of binding of the optically pure enantiomers of anti-benzo[a]pyrene diol epoxide. Biochem. Biophys. Res. Commun., 122, 33.

30. Kim, S. K., Geacintov, N. E., Zinger, D. and Sutherland, J. C. (1990). Fluorescence spectral characteristics and fluorescence decay profiles of covalent polycyclic aromatic carcinogen-DNA adducts, Synchrotrom Radiation in Structural Biology, Brookhaven Symposium in Biology No. 35 (in press).

31. Cosman, M., Ibanez, V., Geacintov, N. E. and Harvey, R. G. (1990).

Preparation and isolation of adducts in high yield derived from the binding of two benzo[a]pyrene-7,8-dihydroxy-9,10-oxide stereoisomers to the oligonucleotide d(ATATGTATA). Biochemistry, submitted.

32. Kim, S. K. and Geacintov, N. E. (1990). in preparation.
33. Zinger, D., Geacintov, N. E. and Harvey, R. G. (1987). Conformations and selective photodissociation of heterogeneous benzo[a]pyrene diol epoxide enantiomer-DNA adducts. Biophys. Biochem., 27, 131-138.
34. Geacintov, N. E. (1986). Is intercalation a critical factor in the covalent binding of mutagenic and tumorigenic polycyclic aromatic diol epoxides to DNA? Carcinogenesis, 7, 759-766.
35. Brown, J. C., Hayes, J. M., Warren, J. A. and Small, G. J. (1981). In Lasers in Chemical Analysis, Hiefje, G. M., Travis, J. C. and Lyfle, F. E., Eds., Humana Press, Inc., Clifton, New Jersey, Chap. 12.
36. Personov, R. I. (1983). Site selection molecular spectroscopy. In Spectroscopy and Excitation of Condensed Molecular Systems, Agranovich, V. M. and Hochstrasser, R. M., Eds., North-Holland Press, New York, pp 555-619.
37. Moussaoui, K., Geacintov, N. E. and Harvey, R. G. (1985). Reactivity and binding of benzo[a]pyrene diol epoxide to poly(dG)(dC)·(dG-dC) and poly(dG-m^5dC)·(dG-m^5dC) in the B and Z forms. Biophys. Biochem., 22, 285-297.
38. unpublished data in this group.
39. Meehan, T. and Straub, K. (1979). The covalent binding of enantiomeric BaPDE's to double stranded DNA is stereoselective. Nature, 227, 410-412.

40. Yang, N-C. C., Hrinyo, T. P., Petrich, J. W. and Yang, D-D. H. (1983). Base sequence selectivity in binding of aromatic hydrocarbons with synthetic polynucleotides. Biochem. Biophys. Res. Commun., 114, 8-13.

41. Rill, R. L. and Marsh, G. A. (1990). The sequence preference of covalent DNA binding by anti-(+)- and anti-(-)-benzo[a]pyrene diol epoxide. Biochemistry, accepted.

42. Di Giovanni, J., Sawyer, T. W. and Fisher, E. P. (1986). Correlation between formation of a specific hydrocarbon-deoxyribonucleoside adduct and tumor initiating activity of 7,12-dimethylbenz[a]anthracene and its 9- and 10-monofluoro derivatives in mice. Cancer Res., 46, 4336-4341.

43. Vousden, K. H., Bos, J. L., Marshall, C. J. and Phillips, P. H. (1986). Mutations activating human C-Haras 1 proto-oncogene ($HRAS_1$) induced by chemical carcinogens and epurination. Proc. Natl. Acad. Sci., USA, 83, 1222-1226.

44. Burgess, J. A., Stevens, C. W. and Fahl, W. E. (1985). Mutation at separate gene loci in Salmonella typhimurium TA_{100} related to DNA nucleotide modification by stereoisomeric benzo[a]pyrene 7,8-diol 9,10-epoxides. Cancer Res., 45, 4257-4262.

G. Appendix: Physical Mixtures of Anti-BPT with Native DNA and (dG)

Figure A1 shows 77 K laser-excited ($S_2 \leftarrow S_0$) spectra of racemic anti-BPT (6×10^{-6} M) which has been physically mixed with DNA (10^{-3} M). Spectrum A and B were obtained in the absence and presence of the fluorescence quencher (ACR, 1 M) with λ_{ex} = 355 nm. The former is characterized by three origins at

~ 376.1, 376.8, and 381.1 nm. Utilization of λ_{ex} = 346 nm yielded a spectrum (not shown) that is dominated by the BPT responsible for the 376.1 and 376.8 nm bands. These two bands are assigned to "free" and/or weakly physically bound (to DNA) BPT. Spectrum C (dashed) in Figure A1 is the A-B difference spectrum which illustrates (as does a comparison of spectra A and B) that with 1 M ACR the 381.1 nm fluorescence is almost entirely quenched (considerably more so than the "free" BPT bands; the 376.1 nm band is more efficiently quenched than the 376.8 nm band). Since these are low temperature glass spectra, it is clear that the observed quenchings are of the static type dictated by frozen in configurations of ACR-BPT-DNA which exist at room temperature. The 381.1 nm band is referred to as BPT-381. BPT-381 and "free" BPT was also observed for a physical mixture of poly (dG) and DNA. The significant red shift of the S_1 state energy of BPT for the BPT-381 entity indicates that in the latter the pyrenyl chromophore is strongly interacting with nucleic acid bases, for example, base-base stacking interaction. Yet the structure of the physically bound BPT is sufficiently open to permit solvent accessibility, i.e., ACR quenching. At sufficiently high laser intensity (~ 30 mW/cm^2) it was observed that the fluorescence intensity of BPT-381 relative to that of the "free" BPT bands increased, suggesting the possibility that BPT-381 could be contributed to by a photoproduct or that interconversion in the excited state between the "free" BPT and BPT-381 is occurring.

FLN spectra of BPT-DNA and BPT-(dG) were also obtained. As an example, Figure A2 shows spectra for the BPT-DNA mixture obtained with λ_{ex} = 369.6 nm in the absence (A) and presence (B) of ACR. The sharp zero-phonon lines (ZPL) are labeled with the S_1 state vibrational frequencies since the ZPL for "free" BPT

and BPT-381 should be centered near 376-377 nm and 381 nm, respectively, comparison of FLN spectra A and B and the results of Figure A1 establish that the 763 and 830 cm^{-1} ZPL are due to BPT-381 while the lower frequency modes, for example, 469 and 579 cm^{-1}, are due to "free" BPT.

As discussed in the main body of the text, BPT-381 can be easily misassigned to the (+)-3-DNA type I adduct. However, the latter is distinct in that its strong linear electron-phonon coupling precludes the observation of line narrowing (of the type observed for BPT-381) and its fluorescence is not significantly quenched by ACR.

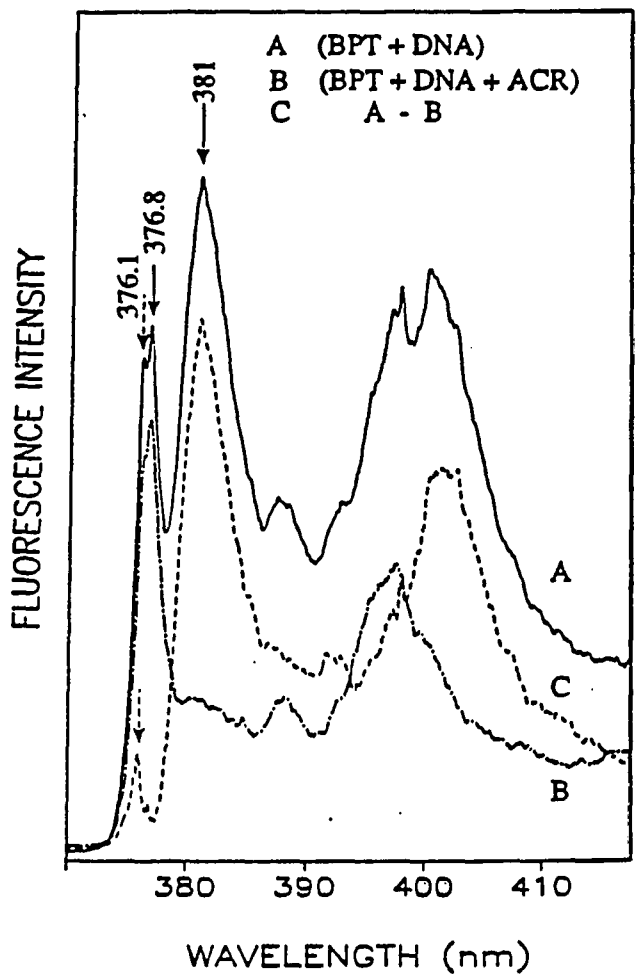

Figure A1. Laser-excited fluorescence spectra: racemic BPT-DNA (A) and racemic BPT-DNA + 1 M ACR (B). λ_{ex} = 355 nm and T = 77 K. Spectrum C is the difference between A and B which identifies the ACR-quenched bands

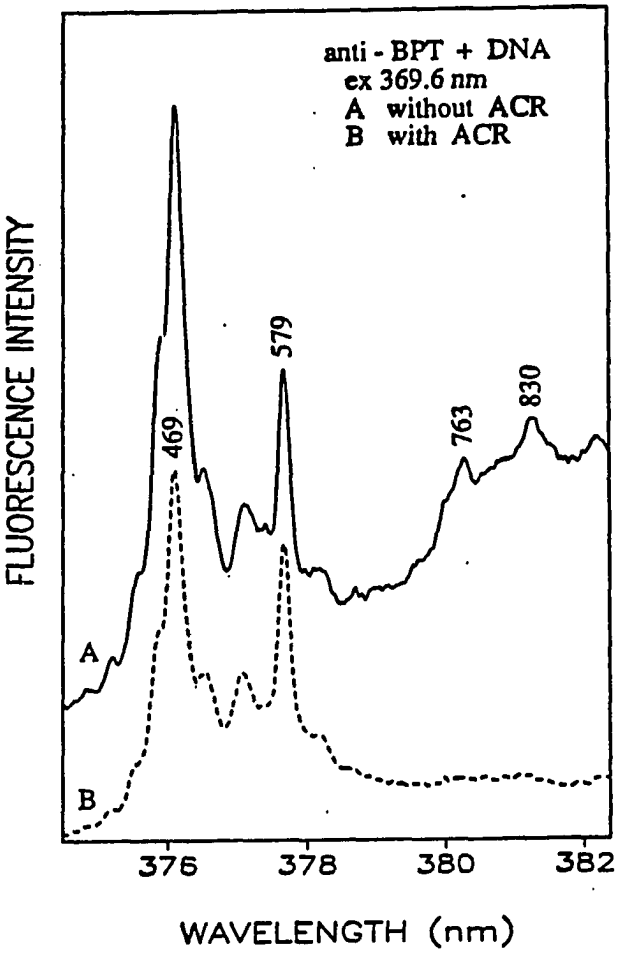

Figure A2. FLN spectra of (+)-anti-BPT+DNA obtained for vibronic excitation: without (A) and with quencher (1 M ACR) (B). λ_{ex} = 369.6 nm, T = 4.2 K

Table I. Spectral characteristic of (+)- and (-)-BPDE-DNA adducts at T = 77 K

	(+) adducts			(-) adducts	
	fluorescence band max, nm	site type		fluorescence band max, nm	site type
(+)-1	378.0	II	(-)-1	378.0	II
(+)-2	379.3	I[a]	(-)-2	379.3	I[a]
(+)-3	380.6	I	(-)-3	380.6	I
			(-)-4	382.7	II
			(-)-5	385.2	II

[a] We assign (+)-2 and (-)-2 as site I type adducts with a "degree" of interior binding that is less than that for (+)-3 and (-)-3.

Table II. Biomolecules used in adduction experiments with (+)-anti-BPDE

Biomolecule	Abbreviation	Adduct concentration[a] (M)
poly (dG-dC)·poly (dG-dC) poly (dA-dT)·poly (dA-dT) poly (dG)·poly (dC) poly (dG)	$(dG\text{-}dC)_2$ $(dA\text{-}dT)_2$ (dG)·(dC) (dG)	~ 10^{-6}
guanine-monophosphate	GMP	*trans* ~ 10^{-6} *cis* ~ 10^{-7}
d(ATATGTATA) oligonucleotide	(..TGT..)	*trans* ~ 10^{-6} *cis* ~ 2 x 10^{-7}
calf thymus DNA	DNA	~ 10^{-6}

[a] At 20 mM sodium cacodylate buffer, 20 mM NaCl, pH 7.0.

Table III. Spectral characteristic of (+)anti-BPDE covalent adducts

Adducts	$\lambda_{fl(0,0)}$ (nm)	FWHM (0,0) (cm^{-1})	R	Site type	Quenchable by ACR
(+)-1DNA[a]	378.0	190	1.75	II	yes
(+)-2DNA	379.3	180	1.25	I[b]	yes[c]
(+)-3DNA	380.6	340	1.15	I	no
(+)-4DNA	382.7	~200	----	II	yes
(+)-1(dG-dC)[a]	377.6	180	1.55	II	yes
(+)-2(dG-dC)	379.4	200	1.25	I[b]	yes[c]
(+)-1(dG)·(dC)	377.9 with ACR	210	1.2	I	yes, less than (+)2
(+)-2(dG)·(dC)[a]	378.3	230	1.35	I[c]	yes, more than (+)1
(+)-3(dG)·(dC)	380.5	~250	1.1	I	no
(+)-4(dA-dT)	~382.5	~200	----	II	yes
(+)-1poly(dG)	378.5	270	1.15	I	yes
(+)-2poly(dG)[a]	379.3	300	1.0	I[b]	yes
(+)-3poly(dG)	380.5	340	1.1	I	slightly

[a] Major adduct.

[b] We assign (+)2 as site I type adducts with a "degree" of interior binding (and/or stacking interactions between the DNA bases and the pyrenyl residues) that is less than that for (+)3.

[c] But less than (+)1.

Table IV. Spectral characteristics of (+)anti-BPDE-GMP and (+)anti-BPDE d(ATATGTATA) adducts

Adducts of (+)-anti BPDE	(0,0) band max (nm) ± 0.1 nm	FWHM[b] (0,0)(cm^{-1})	R (± 0.05)	Site type
N^2-dG *trans*-GMP	377.3[a]	130	1.75	--
N^2-dG *cis*-GMP	377.4[a]	150	1.75	--
N^2-dG	379.6[a]	250	1.3	I
trans-d(..TGT..)	377.6[a]	200	1.55	II
N^2-dG	379.4	190	1.25	I
cis-d(..TGT..)	377.4[a]	200	1.6	II
	377.2	140	-1.85	II

[a] Band maxima and width of (0,0) fluorescence bands were obtained after deconvolution.

[b] FWHM was calculated as a twice the half-width on the high energy side.

VIII. ACKNOWLEDGMENTS

I would like to express my sincere gratitude to a number of people for their guidance and support throughout this research and during my stay in Ames.

First of all, I would like to deeply thank my research advisor, Dr. Gerald J. Small, for his expert guidance, great care, and patience on my path towards a Ph.D. The work described in this thesis could not have been completed without his vigorous support. I also sincerely appreciate his advice and help in the non-research aspects.

Dr. R. Jankowiak was invaluable in my research, and deserves much credit for this work and also my appreciation. I acknowledge and thank Dr. S. R. Cooper for providing me with wonderful training at the beginning of my research. A special thanks to Mr. D. S. Zamzow for teaching me some basic experimental skills and spending a lot of invaluable time to correct parts of this thesis. This was one instance where good help was not hard to find.

I would like to acknowledge my collaborators: Dr. N. E. Geacintov (Department of Chemistry, New York University, NY); Dr. U. Varanasi (National Marine Fisheries, Seattle, WA); Dr. A. Maccubbin (Grace Cancer Drug Center, Roswell Park Memorial Institute, New York State Department of Health, NY); and Dr. A. Jeffrey (Institute for Cancer Research, Columbia University, NY), for providing the model compounds, standards, and the DNA samples.

I would like to thank all my committee professors, Dr. K.-M. Ho, Dr. R. S. Houk, Dr. K. Ruedenberg, and Dr. W. S. Struve, for their precious evaluation of this work. I would like to thank Dr. Houk, in particular, for first introducing me to

study here, and later providing tremendous help in my research, morale, and life.

To the members of Dr. Small's research group and all the other friends at Iowa State that I have come to know in these past four years, thanks for all the non-chemistry-related fun, entertainment, and valuable friendship.

Finally, I would like to thank my parents, Dexing-Lu and Yiaohua-Shao, my parents-in-law, Pei-Wang and Yinkun-Zhang, and my wife, Junying-Wang, for their endless support, understanding, and encouragement, and most of all, their love.